Cheongmi Stream Hydraulic Modeling Analysis

Final Report Prepared for:

Korea Institute of Construction Technology, Republic of Korea

by:

Pierre Y. Julien

Seema C. Shah-Fairbank

Jaehoon Kim

Hyeyun Ku

Colorado State University

Engineering Research Center

Department of Civil and Environmental Engineering

Fort Collins, Colorado, 80523

May, 2009

ABSTRACT

KICT is assuming a leadership role in stream restoration in South Korea. Cheongmi Stream has been selected as a potential site for the restoration of an abandoned channel. Cheongmi Stream is one of the main tributaries on the South Han River. Stream channelization from 1970 to 2002 formed an abandoned channel within the study reach. There is an interest to restore this abandoned channel to increase flow interaction, improve water quality, and enhance wildlife habitat. This hydraulic modeling study will be used to aid in reconnecting the abandoned channel to the main flow.

This report provides a detailed study of 1.6 km of Cheongmi Stream from station 17+000 to Sulsung Stream at station 15+400. The hydraulic modeling analysis has been performed to determine changes in channel morphology and other important hydraulic and sediment parameters. Spatial and temporal trends in channel geometry, discharge, and sediment have been analyzed.

The hydraulic analysis was performed using HEC-RAS. Hydraulic parameters were examined for various discharges and reach-averaged spatial trends were examined. At a reference discharge of 980 cms, the results showed that the hydraulic parameters are relatively constant upstream of the confluence with Sulsung Stream. The reach average values are 251 m for channel width, 2.58 m for flow depth, 4.4 m for the maximum flow depth, 98 for the width/depth ratio, and 1.56 m/s for the mean flow velocity. The reach average slope and Froude number are 0.00058 and 0.3 respectively. The Manning n value for the reach was set at 0.03.

In terms of width, depth and slope, two methods were used: the SAM program and the equilibrium channel width analysis. The SAM program was used to determine the stable channel slope, width and depth which are

compared to the HEC-RAS hydraulic modeling results. The results suggested that the stable channel slopes at discharges with period of return ranging from 1.58 to 5 years are slightly less than the measured slope. However, the stable channel width is less than the measured width. This may explain why alternate bars have formed along Cheongmi Stream. In addition, the stable channel is deeper than the measured depth. In the equilibrium channel width analysis, the methods of Julien-Wargadalam, and Simons and Albertson gave an equilibrium width of 201 m and 225 m respectively, at the reference discharge of 980 cms. The actual measured channel width using HEC-RAS was 251 m.

The changes in channel planform geometry are analyzed using aerial photographs from 1930 and 2006. Based on aerial photographs the channel geometry changed from meandering to straight. This occurred because of the channelization and levee construction on the stream banks. The observations were compared to several methods. The methods of Leopold and Wolman, and Schumm and Khan are the best methods for identifying the planform geometry for Cheongmi Stream. The thalweg and mean bed elevation profile were analyzed using field measurement from 1983, 1994, and 2004. Both measured profiles indicated that the channel has degraded about 2 m over the 20 year period from 1983 to 2004.

In terms of sediment transport, the particle size distribution of the bed material was investigated. The study reach is composed of sand with a median particle diameter of 1.48 mm. The sediment transport capacity was calculated with different sediment transport equations. The methods of Engelund-Hansen and Yang predicted reasonable results of total bed material discharge. Both methods predicted a total sediment load around 95,000 tons/day at a reference discharge of 980 cms. Under flood conditions, the sediment concentration is expected to be high, such that flow diversion into the abandoned channel may cause sedimentation problems during floods.

The following additional considerations are recommended for the restoration of the abandoned channel at Cheongmi Stream: (1) based on the flow duration analysis a discharge of 565 cms corresponds to the best estimate of flow discharge with a period of return of 1.58 years upstream of the confluence with Sulsung Stream (the corresponding discharge is 635 cms downstream of the confluence); (2) the stream had a tendency to degrade an average of 10 cm/year from 1983 to 2004; and (3) the downstream migration rate of alternate bars is roughly estimated to be about 8 m/year from 2000-2006. The alternate bars could affect the operations of the intake structure. A sill, such as a drop structure or weir, could be constructed to prevent further degradation and ensure sufficient hydraulic head to deliver water to the abandoned channel at low flows.

ACKNOWLEDGMENT

This work was completed with data and support provided by the Korea Institute of Construction Technology (KICT), Republic of Korea. The authors would like to thank Dr. Hyoseop Woo at his dedication and insight on restoration of the abandoned channel at Cheongmi Stream. Many other scientists contributed to this study and we are thankful to Dr. Honggu Yeo, Dr. Jungu Kang, and Il Hong at KICT. Dongbu Engineering was responsible for field data collection at Cheongmi Stream. Finally, we are particularly grateful to Dr. Un Ji at Myongji University for the direct collaboration and joint hydraulic and sediment transport analysis for this project.

TABLE OF CONTENTS

LIST OF FIGURES

LIST OF TABLES

Chapter 1 INTRODUCTION

1.1 BACKGROUND

In Korea, all rivers and streams are classified by three categories: national rivers, local rivers of first grade, and local rivers of second grade. They are divided with respect to conservation and economic management. Korean rivers are divided into six watersheds: Han River, Kum River, Youngsan River, Nakdong River, Sumjin River and Jeju Island watershed. The Han River watershed is located in northern west part of South Korea and consists of North Han River and South Han River. Cheongmi Stream, which is the location for this study, is part of the Han River watershed. Figure 1-1 shows the six watersheds in South Korea.

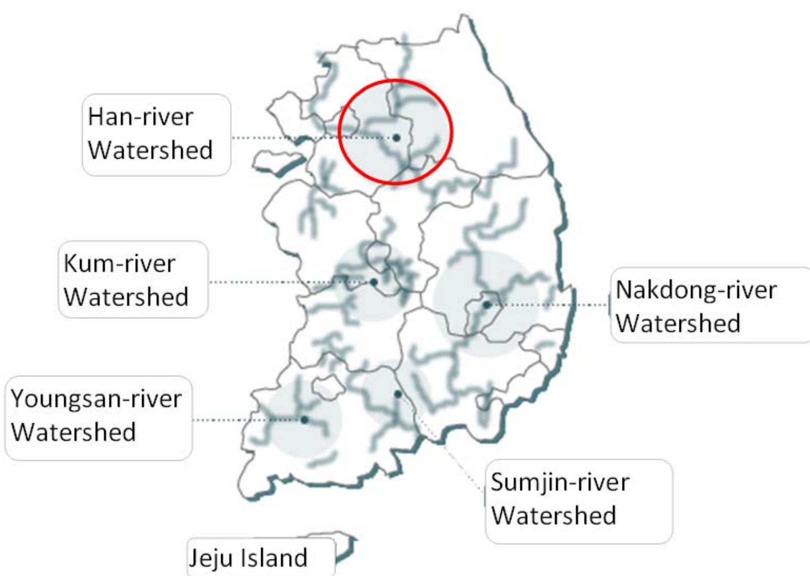

Figure 1-1: Watershed in Korea (KRA 2008)

Cheongmi Stream is located in the middle of South Han River. This watershed contains mountains and hills, it is located at the following latitude and longitude: E127˚20' ~ 127˚44' and N36˚56 ~ 37˚ 13'. Cheongmi Stream is 59.5 km long and is located in the following provinces: Yeoju-gun, Icheon-si, Anseong-si, Yongin-si in Gyeonggi-do and Eumseong-gun in Chungcheongbuk-do.

The study site is located in the town of Janghowon in the province of Icheon-si. The upper reach of Cheongmi Stream is classified as a local second grade river; however, the downstream reach from South Han River to 25.5 km upstream is classified as a national river. By definition, the national river needs to be maintained every 10 year. The study reach is located within the national river classification and extends from Sulsung Steam (15+523) to station 17+000. Figure 1-2 provides a location map of the site.

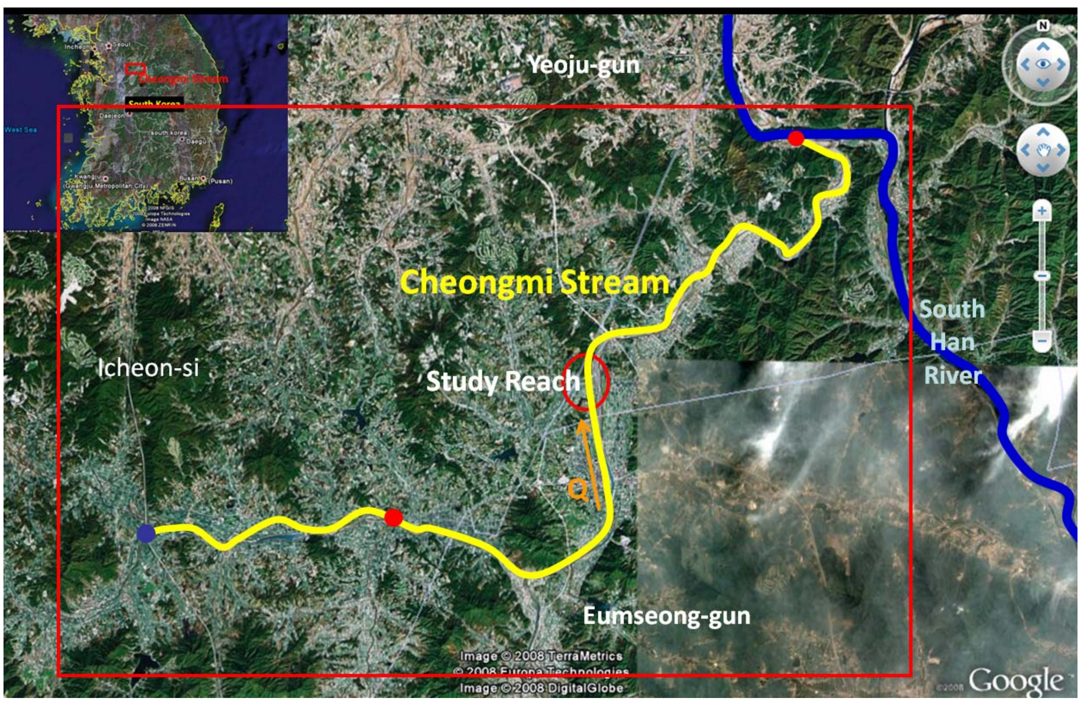

Figure 1-2: Location of Cheongmi Stream

Within the study site area over 82% of the land is devoted to farmland. In May of 2005 the estimated population within this region was 8,297 people. The population density of this region is approximately 91.62 people per 1 km^2.

1.2 STUDY REACH

From 1970 to 2002, Cheongmi Stream was straightened and levees were constructed to control flow and prevent flooding. Figure 1-3 is an aerial photo image from 2006. An abandoned channel is located within the study reach from station 16+800 to 15+600. Thus, for analysis purposed, the study reach was extended from 17+000 to 15+400. Sulsung Stream, which is a tributary to Cheongmi Stream, is located at station 15+523.

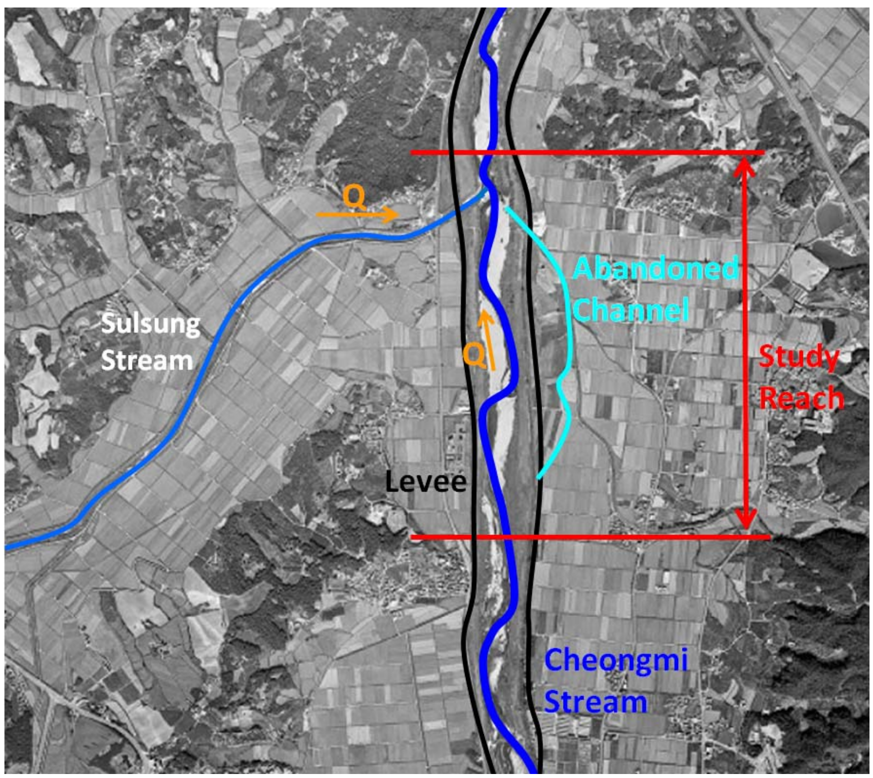

Figure 1-3: Study Reach on Cheongmi Stream

Alternate bars are located along the study reach of Cheongmi Stream. Alternate bars are defined as regularly-spaced depositional features positioned on opposite sides of a straight or slightly sinuous stream and it may be a precursor to meander initiation or braiding (Watson et al. 2007). Since levees have been constructed on either side of the stream the channel will not meander. The presence of vegetation on some alternate bars suggests that they are old. Yellow circles have been drawn on Figure 1-4 to clearly identify the alternate bars along Cheongmi Stream.

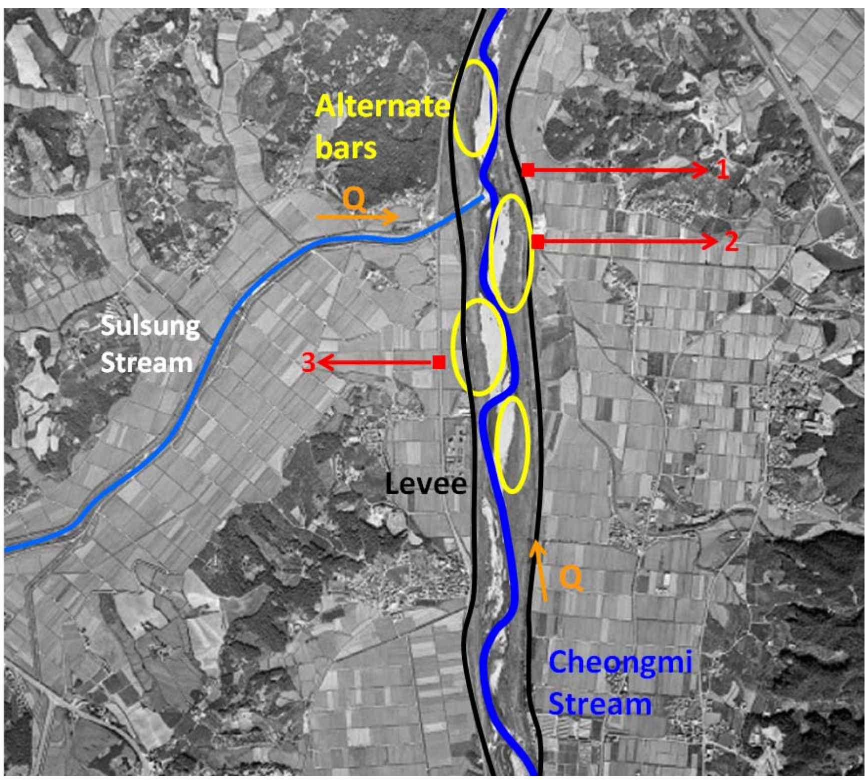

Figure 1-4: Shape of Bars in Cheongmi Stream

Figure 1-5 shows the field site photos numbering 1 to 3 from Figure 1-4. No. 1 is the levee reconstruction downstream of a pumping station near the tributary of Sulsung Stream. No. 2 is a pond upstream of the pumping station. No. 3 is the view of the alternate bar. No. 3 also shows the stream during low flow condition.

Figure 1-5: Field Site Photos

1.3 OBJECTIVES

The objectives of this project are to analyze the morphological changes and equilibrium conditions along Cheongmi Stream for future abandoned channel restoration. To accomplish this study, the following analyses will be performed:

- Hydrologic analysis using available information.
- Hydraulic analysis based on survey data from 2004.
- Bed material classification and sediment transport capacity analysis.
- Equilibrium analysis using downstream hydraulic geometry.
- Geomorphic characterizations of the study reach using survey data and aerial photos.

The results of this study will be used to analyze existing and future channel changes.

Chapter 2 AVAILABLE DATA

The data used in this project was provided by the Ministry of Construction and Transport (MOCT) and Korea Institute of Construction Technology (KICT). All analysis has been performed and reported in SI units.

2.1 HYDROLOGY DATA

Stream flow is available along Cheongmi Stream; however, daily and peak yearly stream flow was not available on Cheongmi Stream. Thus, (MOCT 2007) performed a hydrologic study that determined the discharge at various locations along the stream. The Hydrologic Modeling System (HEC-HMS) was used to determine the discharge at various return intervals along Cheongmi Stream. These locations are summarized in Table 2-1 and shown in Figure 2-1.

Table 2-1: Flood Estimating Locations

Location Code	Locations
CM-1	Downstream end of Cheongmi Stream (No. 0)
CM-2	Downstream of Geumgok Stream (No.8 + 600)
CM-3	Upstream of Geumgok Stream (No.8 + 600)
CM-4	Downstream of Sulsung Stream (No.15+600)
CM-5	Upstream of Sulsung Stream (No.15+600)
CM-6	Downstream of Ogab Stream (No.19+400)
CM-7	Upstream of Ogab Stream (No.19 +400)
CM-8	Downstream of Eung Stream (No.24+628)
CM-9	Upstream of Eung Stream (No.24+628)

Figure 2-1: Watershed Map

The flow rate are determined at locations where the discharge changes due to tributary inflow and irrigation, where river improvements are necessary and sites where previously measured data can be compared. For this study the location of interest is from Ogab Stream (CM-6) to Sulsung Stream (CM-4). Table 2-2 summarizes the discharge at the upstream and downstream extents of the study reach.

Table 2-2: Summary of Flow Rates

Return Interval (year)	Discharge (cms)	
	CM 6	CM 4
1.58	610	670
5	1180	1290
10	1480	1610
20	1770	1930
30	1940	2110
50	2150	2330
70	2290	2480
80	2340	2540
100	2440	2650

150	2600	2820
200	2710	2940

2.2 SEDIMENT

2.2.1 Suspended Sediment Measurements

Sediment measurements were taken in 2008 at Wonbu Bridge (Ji 2008). Total load was determined by Bureau of Reclamation Automated Modified Einstein Procedure, referred to as BORAMEP (USBR 2006). The measured load was determined using a depth-integrated sampler. Table 2-3 summarizes the calculated total sediment load based on BORAMEP at Wonbu Bridge.

Table 2-3: Sediment Measurement (Ji 2008)

Station	Q (cms)	Qs (tons / day)
Cheongmi Station at Wonbu Bridge	11	153
	72	9,118
	809	413,840

No measurements were taken during high flows.

2.2.2 Bed Material

Bed material was measured during 2005 along Cheongmi Stream (KICT 2008). Samples were collected for 25.2 km of Cheongmi Stream (classified as a national river). The measured particles were analyzed in a laboratory and the particle size distribution of the bed was constructed at each location. In general, the samples indicated that the bed is composed of sand. Figure 2-2 shows the sample particle size distribution at the cross section 17+000. This cross section is located at the upstream extent of the study site.

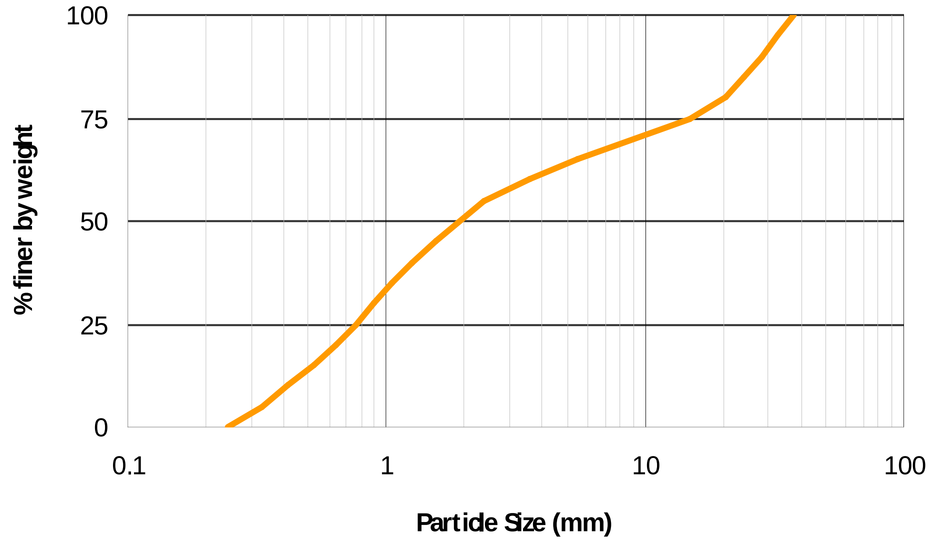

Figure 2-2: Particle Size Distribution at the Cross Section 17+000

2.3 HYDRAULIC DATA

Hydraulic data was provided by MOCT and KICT for 25.2 km of Cheongmi Stream. The study reach extends from station 17+000 (downstream of Ogab Stream) to station 15+400 (downstream of Sulsung Stream). Figure 2-3 provides a cross section location map of the study reach.

Detailed survey files from 2004 were provided by KICT. The files included cross section survey, longitudinal survey, topography, and digitized map. In addition, thalweg profile and mean bed elevation were measured in 1983 and 1994 by Han River Restoration Master Plan and Cheongmi Stream Restoration Master Plan, which are summarized by MOCT (2007).

The hydraulic roughness coefficient was estimated based on the classification developed by (Chow 1959). For natural streams the Manning's n value ranges from 0.025 to 0.06. Based on the judgment of survey team, the n value of Cheongmi Stream was determined to be 0.03.

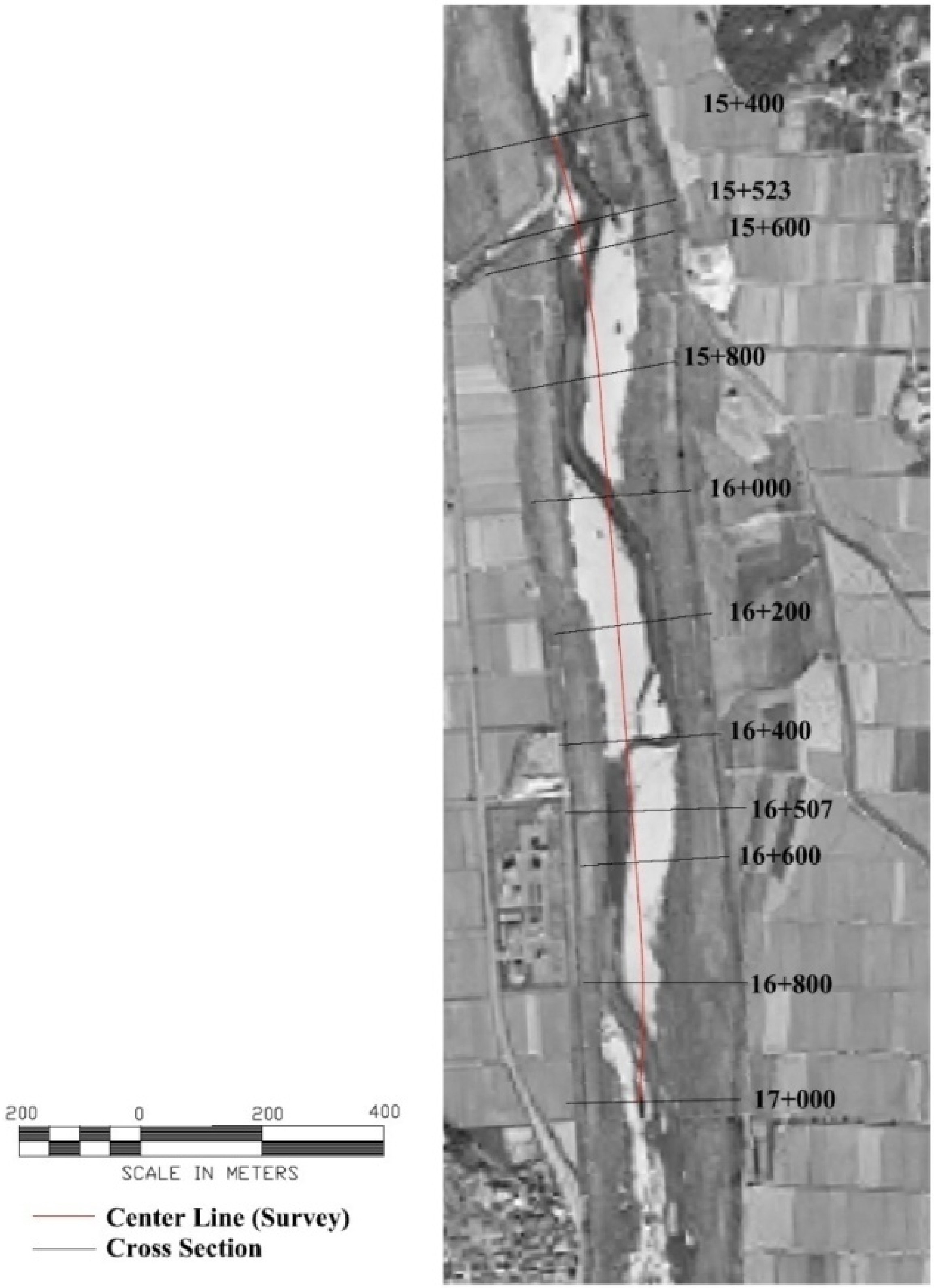

Figure 2-3: Cross Section Map for Study Reach

2.4 AERIAL PHOTOS

Seven aerial photos were provided by KICT. Aerial photos were provided for the following years: 1930, 1969, 1974, 1981, 1992, 2000, and 2006, refer to Appendix A. The scale orientations of the photos were not provided, however some analysis was conducted using the provided images.

Chapter 3 HYDRAULICS

3.1 METHODS

The hydraulic analysis was conducted using HEC-RAS. The Manning's n value of 0.03 is assumed based on initial observations by the surveying team. The hydraulic analysis was conducted on Cheongmi Stream for 12 distinct flow rates.

The bankfull flow rate was not provided; therefore a sensitivity analysis was conducted. The bankfull stage was estimated based on engineering judgment at each cross section within the study reach (17+000 to 15+400). It is difficult to select bankfull discharge because every cross section in study reach has different level of bankfull on either side of banks. In addition, HEC-HMS modeling result value near Sulsung stream tributary with the return interval of 1.58 year and 5 year was 610 cms and 1180 cms respectively. Thus, the discharge between 620 cms and 1200 cms was thought to be bankfull discharge and 980 cms was selected as a reference discharges because later analysis suggested that this value was too high for bankfull.

Flow rates were varied between the 1.58 and 5 year return storms. The input data of reference discharge is shown in Table 3-1.

Table 3-1: Input Data of Reference Discharge

Return Interval (year)	Discharge (cms)		
	CM 6	CM 5	CM 4
1.58	610	620	670
Q_{Ref}	980	980	980
5	1180	1200	1290

The following channel geometry parameters were calculated using HEC-RAS: minimum channel elevation, water surface elevation, energy grade line slope, velocity, cross sectional area, top width, Froude number, hydraulic radius, shear stress, stream power, wetted perimeter, and mean flow depth. Three additional channel geometry properties were determined:

Maximum flow depth = Water Surface Elevation - Minimum Channel Elevation

Width/Depth Ratio, W/D = Top width / Mean Flow Depth

Water surface slope = Water surface elevation / distance between cross sections

These hydraulic parameters were analyzed from each discharge. Two distinct analyses were performed. The first analysis is based on spatial trends for all 12 discharges. The second analysis is based on a reach-averaged value.

3.2 RESULTS

Figure 3-1 shows the spatial trends in the average cross-sectional area, top width, wetted perimeter, mean flow depth, maximum flow depth, channel velocity, Froude number, and width/depth ratio for the study reach at a reference discharge of 980 cms.

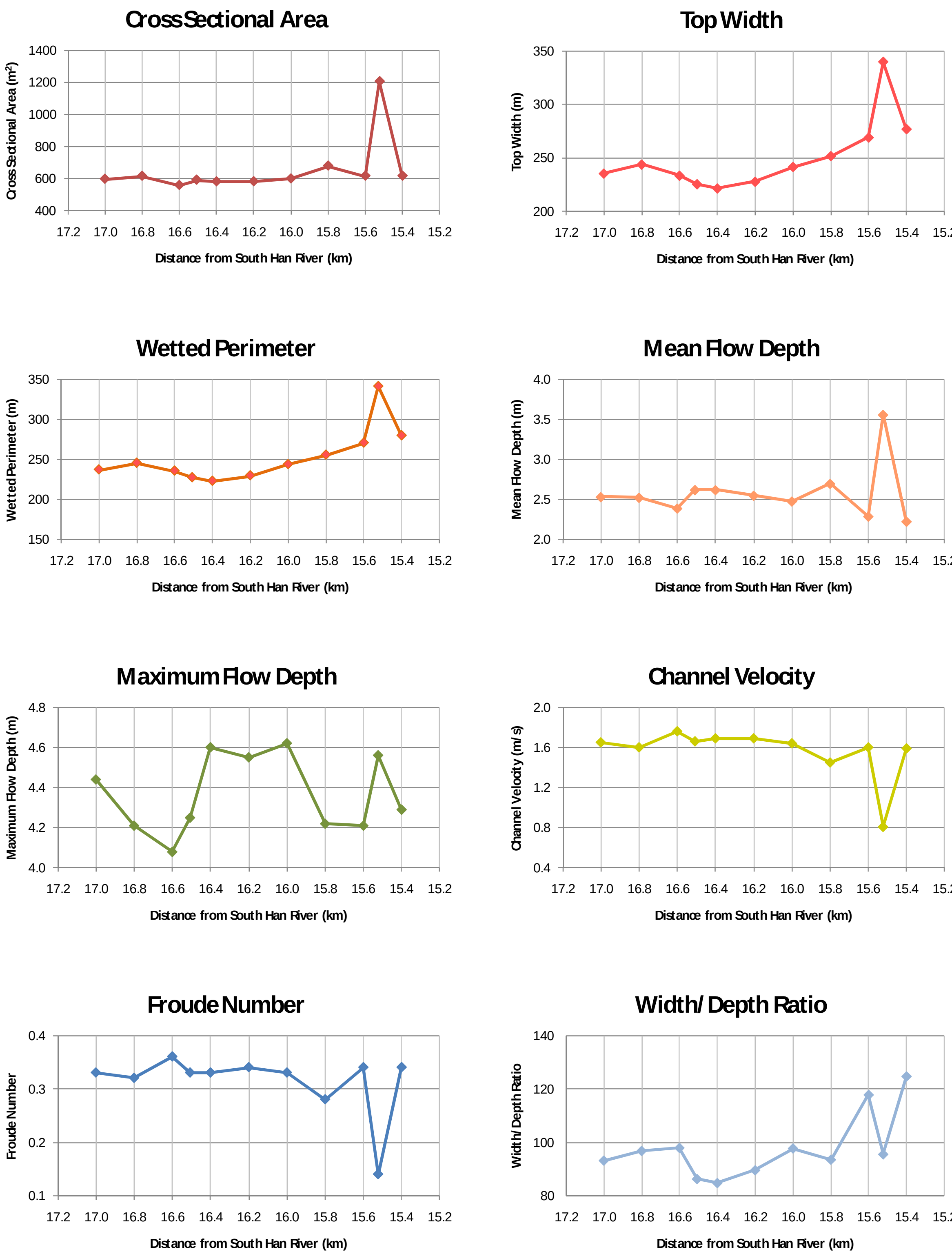

Figure 3-1: Spatial Trends based on Q_{Ref} = 980 cms

The cross sectional area, top width, wetted perimeter, mean flow depth, maximum flow depth, and width/depth ratio increased in the downstream direction, whereas channel velocity and Froude number decreased in the downstream direction. This is due to an increase in flow area. At the cross section 15+523, velocity suddenly decreases because of the confluence between Sulsung Stream and Cheongmi Stream. The results from HEC-RAS are provided in Appendix B and C.

Reach-averaged hydraulic parameters for each return interval were computed and summarized in Figure 3-2. The reach averaged hydraulic parameters increased as discharge increase. The width to depth ratio decreased because the top width did not change significantly. Froude number at the cross section of 15+523 decreased due to increased flow from Sulsung Stream.

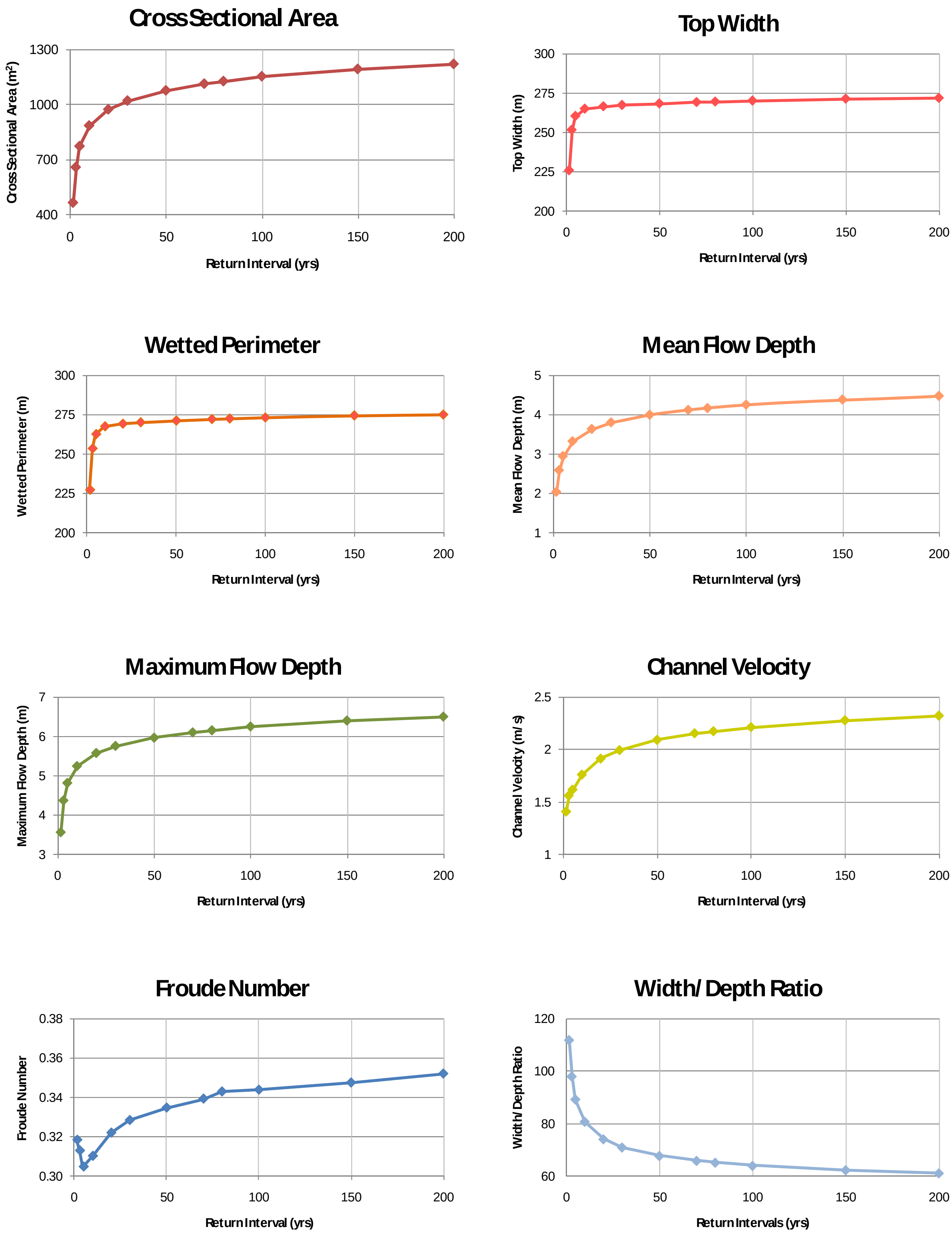

Figure 3-2: Reach Averaged Spatial Trends on Each Return Interval

Chapter 4 SEDIMENT AND BED MATERIAL

4.1 BED MATERIAL

4.1.1 Methods

Bed material measurements within Cheongmi Stream are available for 25.2 km. Samples of the bed material were taken on May 2005 and spaced 1 km apart. The data provided by KICT included the percent finer by weight from five to ninety-five percent for all 26 stations. The particle size distribution was extended to 0 and 100. Table 4-1 is the classification for the bed material (Julien 1998).

Table 4-1: Bed Material Classification (Julien 1998)

Class name	Size range	
	mm	in.
Boulder		
Very large	4,096-2,048	160-80
Large	2,048-1,025	80-40
Medium	1,024-512	40-20
Small	512-256	20-10
Cobble		
Large	256-128	10-5
Small	128-64	5-2.5
Gravel		
Very coarse	64-32	2.5-1.3
Coarse	32-16	1.3-0.6
Medium	16-8	0.6-0.3
Fine	8-4	0.3-0.16
Very fine	4-2	0.16-0.08
Sand		
Very coarse	2.000-1.000	
Coarse	1.000-0.500	
Medium	0.500-0.250	
Fine	0.250-0.125	
Very fine	0.125-0.062	
Silt		
Coarse	0.062-0.031	
Medium	0.031-0.016	
Fine	0.016-0.008	
Very fine	0.008-0.004	
Clay		
Coarse	0.004-0.0020	
Medium	0.0020-0.0010	
Fine	0.0010-0.0005	
Very fine	0.0005-0.00024	

4.1.2 Results

Figure 4-1 shows the bed material particle size distribution for all 26 samples.

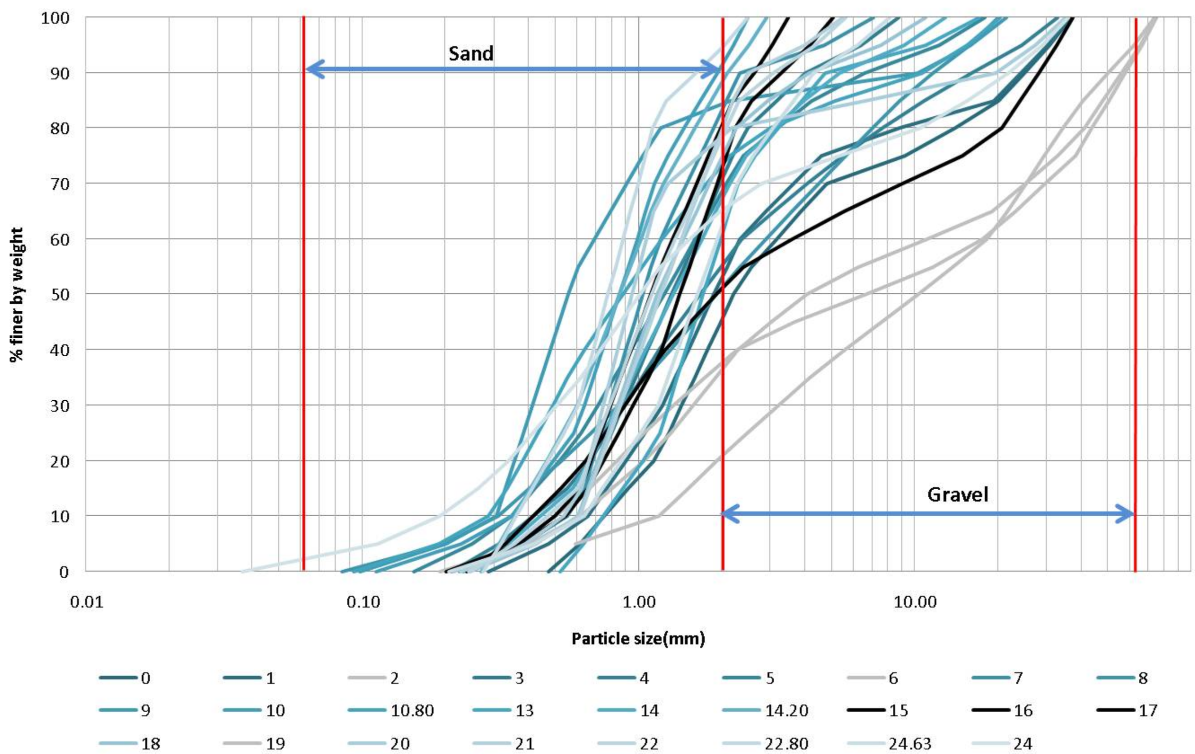

Figure 4-1: Bed Material Distribution for Cheongmi Stream

Most of Cheongmi Stream is composed of sand and fine gravel. The stations of interest are 15+000, 16+000 and 17+000 because they are located closest to or within the study limits. The bed material measured at stations 2+000, 6+000 and 19+000 shows a larger particle size, than the remaining cross section; therefore, they have been excluded from the median grain size calculation. Table 4-2 summarizes the median grain size for Cheongmi Stream and the study reach.

Table 4-2: Median Grain Size

Grain Size	Cheongmi Stream [mm]	No,15+000 to No.17+000 [mm]
d_{10}	0.48	0.49
d_{15}	0.57	0.60
d_{50}	1.29	1.48
d_{85}	6.52	9.60
d_{90}	9.35	11.30

Figure 4-2 shows the particle size distribution for these three locations (15+000, 16+000, and 17+000) within the study reach. In addition, the median grain size for the study reach and Cheongmi Stream are identified.

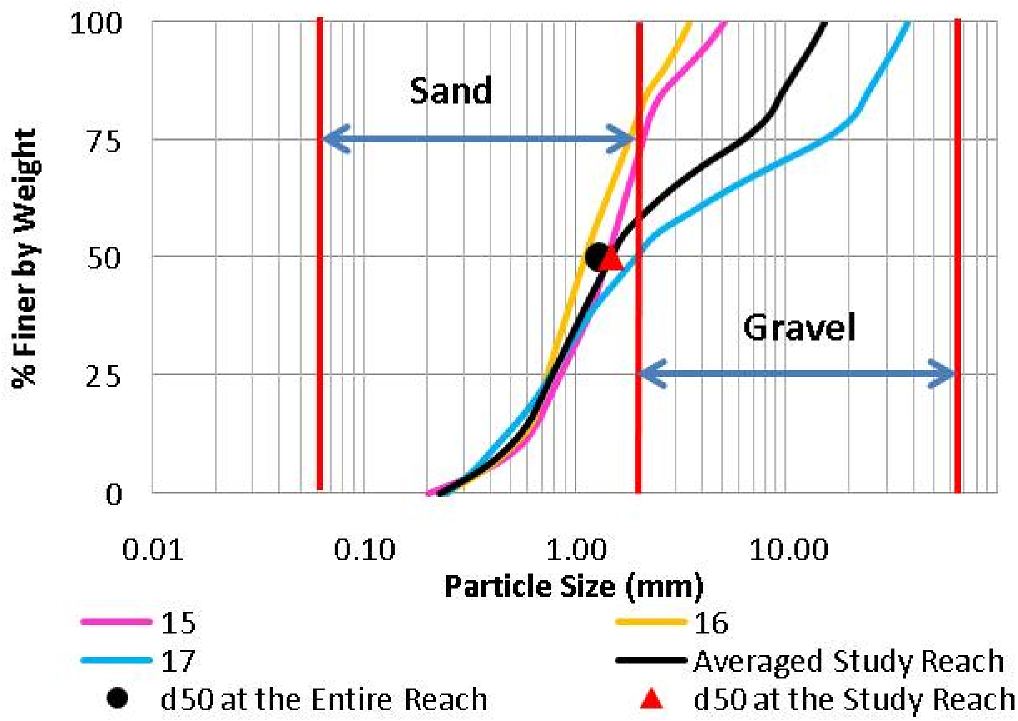

Figure 4-2: Bed Material Distribution for Study Reach

The median grain size within the study reach is higher than that of entire reach. In general, it is expected that the particles have a tendency to get finer in the downstream direction. The entire stream is considered to be a sand bed channel. Figure 4-3 shows the measured d_{50} along the entire 25.2 km.

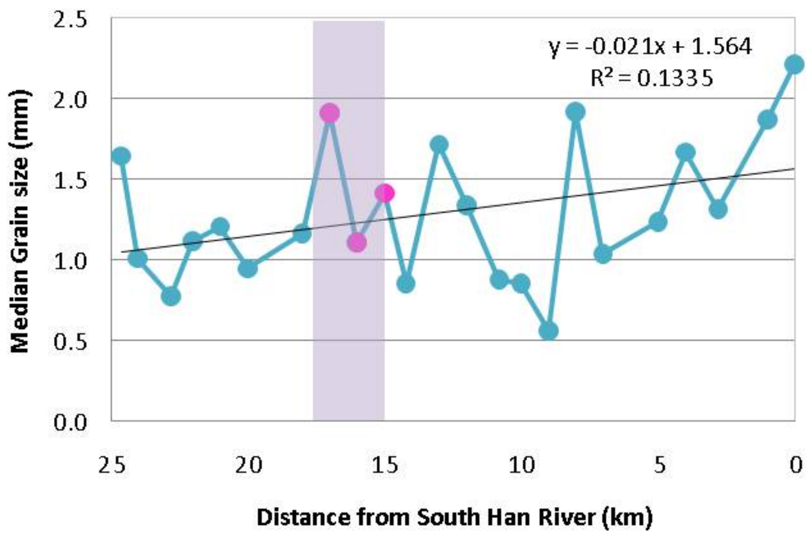

Figure 4-3: d_{50} along Cheongmi Stream

The value of d_{50} ranges from 0.5 mm to 2.0 mm for most of the river. The river contains coarse to very coarse sand. For Cheongmi Stream, the bed material size seems to increase slightly in the downstream direction. This increase may be explained by the Lane's Balance in Figure 4-4.

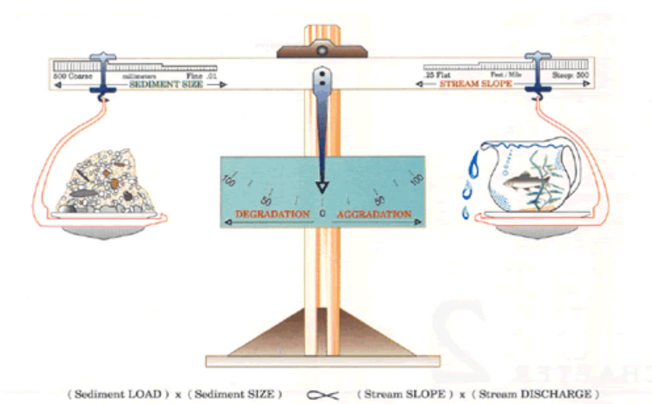

Figure 4-4: Lane's Balance after (Lane 1955)

The Lane relationship is:

$$Q_s \; d_s \; \propto Q \; S$$

where Q_s is the bed material load, d_s is the median size of the bed material, Q is the water discharge, and S is the slope.

This relationship shows that a change in any of the four variables will cause a change in the others, to restore equilibrium. Due to the levee construction, the slope of Cheongmi Stream bas increased, and discharge and sediment rate remained constant. Therefore, the median size of the bed material may increase slightly in the downstream direction.

4.2 MAXIMUM MOVABLE GRAIN SIZE

4.2.1 Methods

From the sediment grain size, the shear stress analysis on particle size was performed to obtain particle size at incipient motion. The dimensionless shear stress is the ratio of hydrodynamic forces to the submerged weight, which is called the Shields parameter (τ_*) and expressed as follows;

$$\tau_* = \frac{\tau_0}{\left(\gamma_s - \gamma_m\right) d_s}$$

Where, τ_* is Shields parameter, τ_0 is boundary shear stress, γ_s is specific weight of a sediment particle, γ_m is specific weight of the fluid mixture, and d_s is particle size.

When the Shields parameter is assumed to be critical (τ_{*c}), the maximum movable particle size can be attained from the following equation.

$$d_s = \frac{R\ S_f}{(G-1)\tau_{*c}}$$

where, R is hydraulic radius and S_f is friction slope.

Based on the critical Shields parameter equation, the maximum movable particle size can be computed iteratively. Table 4-3 contains threshold values for granular material at 20°C (Julien 1998).

Table 4-3: Approximate Threshold Conditions for Granular Material at 20°C

Class name	d_s (mm)	d_*	φ (deg)	τ_{*c}	τ_c (Pa)	u_{*c} (m/s)
Boulder						
Very large	> 2,048	51,800	42	0.054	1,790	1.33
Large	> 1,024	25,900	42	0.054	895	0.94
Medium	> 512	12,950	42	0.054	447	0.67
Small	> 256	6,475	42	0.054	223	0.47
Cobble						
Large	> 128	3,235	42	0.054	111	0.33
Small	> 64	1,620	41	0.052	53	0.23
Gravel						
Very coarse	> 32	810	40	0.05	26	0.16
Coarse	> 16	404	38	0.047	12	0.11
Medium	> 8	202	36	0.044	5.7	0.074
Fine	> 4	101	35	0.042	2.71	0.052
Very fine	> 2	50	33	0.039	1.26	0.036
Sand						
Very coarse	> 1	25	32	0.029	0.47	0.0216
Coarse	> 0.5	12.5	31	0.033	0.27	0.0164
Medium	> 0.25	6.3	30	0.048	0.194	0.0139
Fine	> 0.125	3.2	30	0.072	0.145	0.0120
Very fine	> 0.0625	1.6	30	0.109	0.110	0.0105
Silt						
Coarse	> 0.031	0.8	30	0.165	0.083	0.0091
Medium	> 0.016	0.4	30	0.25	0.065	0.0080

Since the median grain size of the study reach is approximately 1.48 mm, the initial assumed value of d_s is 2 mm, and τ_{*c} is 0.039. The discharge with the return interval of 1.58 year and reference discharge (Q_{Ref}) were selected to get hydraulic radius (R) from HEC-RAS and the slope (S) of 0.00058 m/m from survey data. This critical Shields parameter (τ_{*c}) is identified from Table 4-3 and then an iteration is performed until the particle size is the same as the assumed particle size.

4.2.2 Results

The results of the maximum movable particle size are summarized in Table 4-4.

Table 4-4: Maximum Movable Particle Size

Return Interval (year)	Discharge (cms)	R (m)	S (m/m)	τ_{*c}	d_s (mm)
1.58	610	2.02	0.00058	0.047	15
Q_{Ref}	980	2.56	0.00058	0.047	19

The maximum movable particle size ranges from 15 mm to 19 mm (Coarse gravel). These values are around 10 times bigger than the median grain size of 1.48 mm of the study reach. This result indicates that the sediment currently in Cheongmi Stream will move until the channel armors with a grain size around 19 mm. Based on Figure 4-2 the channel has not armored and it will continue to transport available sediment.

4.3 SEDIMENT TRANSPORT CAPACITY

4.3.1 Methods

The sediment transport capacity was calculated using HEC-RAS. The program has the capability to predict transport capacity for non-cohesive sediment at multiple cross sections based on the hydraulic parameters and known bed material properties for a given river. It does not take into account sediment inflow, erosion, or deposition in its computations. Classically, the sediment transport capacity is comprised of both bed load and suspended load, both of which can be accounted for in the various sediment transport predictors available in HEC-RAS. Results can be used to develop sediment discharge rating curves, which help to understand and predict the fluvial processes found in natural rivers and streams.

HEC-RAS calculates sediment transport capacity using several different methods including those developed by, Ackers & White, Engelund & Hansen, Laursen, Meyer-Peter & Müller, Toffaleti, and Yang (sand). All methods except Meyer-Peter & Müller provide an estimate of the total bed material load. Meyer-Peter & Müller estimates bed load only. For a list of the limitations of each method refer to Appendix E.

4.3.2 Results

The program was used to calculate the sediment transport capacity for all six methods at all twelve discharges. The water temperature was assumed to be 15°C and the bed material particle size for the reach was determined to be 1.48 mm.

The results for cross section 16+600 are shown in Figure 4-5.

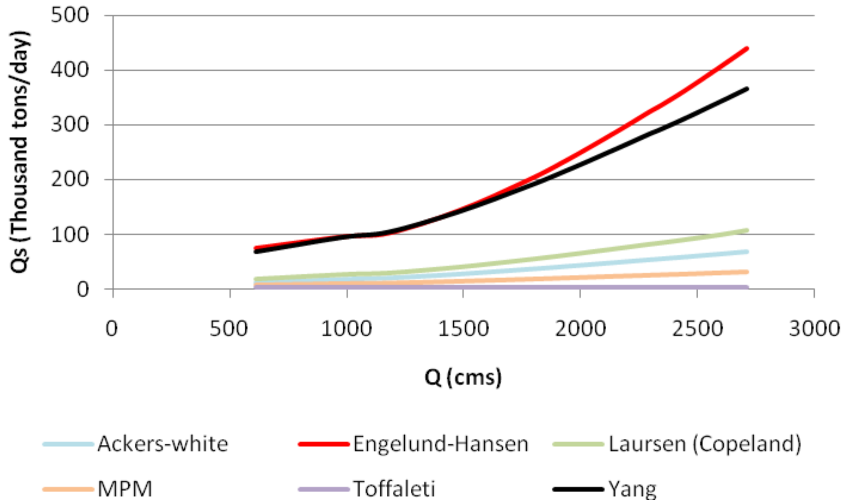

Figure 4-5: Sediment Rating Curve at the Cross Section 16+600

Engelund-Hansen and Yang's equation are the most appropriate for Cheongmi Stream based on the equation applicability and limitation outlined in Appendix E. Engelund-Hansen method is a total bed material load predictor, which gives adequate results for sandy rivers with substantial suspended load. Yang's method is applicable when the particle size ranges from 0.062 and 7.0 mm which is coarse silt to fine gravel. Even though Toffaleti method calculates total bed material load, their results were significantly low because Toffaleti method suggests that mean particle diameters as low as 0.095 mm are acceptable.

Table 4-5 shows the comparison of sediment transport loads between the method of Engelund-Hansen and Yang with different return interval at the cross section of 16+600.

Table 4-5: Sediment Transport Capacity with Engelund-Hansen and Yang Method

Return Interval	Q	Qs (tons/day)	
(yrs)	(cms)	Engelund-Hansen	Yang
1.58	610	74,380	68,750
Q_{Ref}	980	95,050	95,050
50	2150	286,100	256,100
100	2440	360,300	310,700

A comparison of the sediment transport capacity between the measured sediment loads collected at Wonbu Bridge in 2008 and calculated sediment load at cross section 15+400 are shown in Figure 4-6.

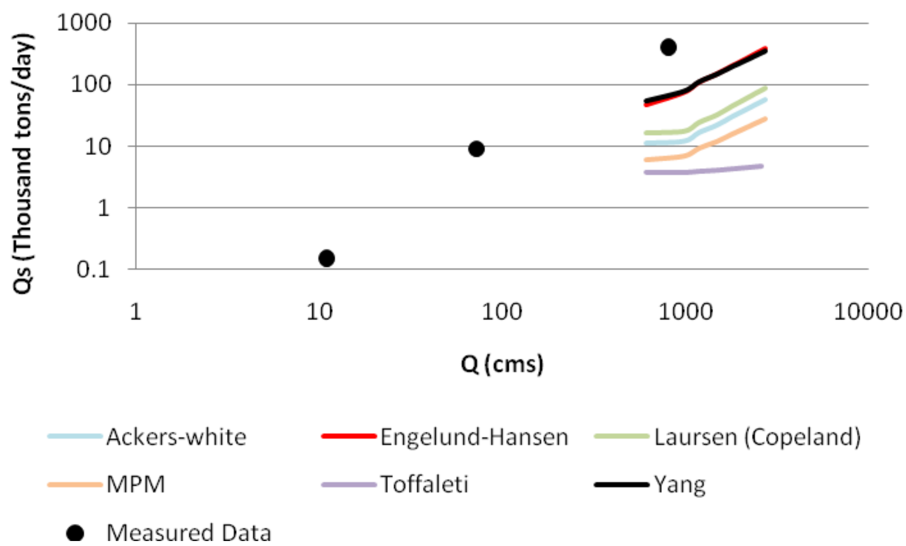

Figure 4-6: Sediment Rating Curve with Measured Data at the Cross Setion 15+400

The black dots are the total load based on BORAMEP at Wonbu Bridge in 2008, which has a higher sediment transport compared to the calculated sediment capacity.

The sediment concentration was calculated by the following equation (Julien 1998).

$$Q_s\,(metric\ tons/\,d) = 0.0864 \times C_{mg/l} \times Q\,(m^3/\,s)$$

$$C_{mg/l} = \frac{Q_s\,(metric\ tons\,/\,d)}{0.0864 \times Q(m^3\,/\,s)}$$

The input data used in the above equation are discharge and sediment load, which are shown in Table 2-3. This data were obtained from BORAMEP result based on the measurement at Wonbu Bridge. Cheongmi Stream was design for a 100 year flood event, of 2,440 cms and the sediment concentration was determined by developing a discharge-sediment curve, refer to Figure 4-7. Table 4-6 summarizes the sediment concentration at various discharges.

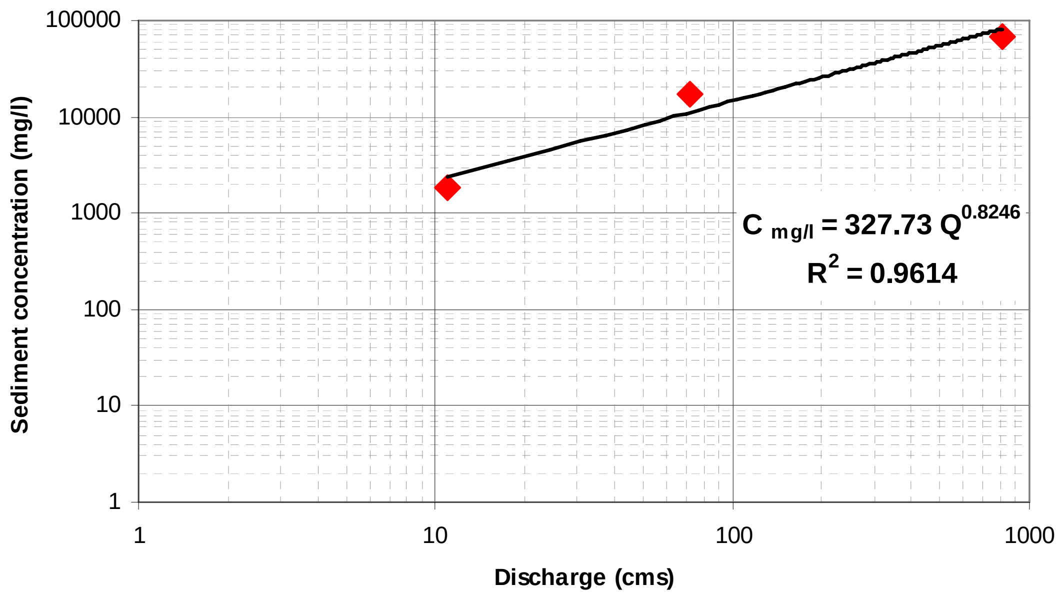

Figure 4-7: Discharge-Sediment Concentration Curve at Wonbu Bridge

Table 4-6: Sediment Concentration

Q (cms)	Qs (tons/d)	**C (mg/l)**
11	153	**1,872**
72	9,118	**16,877**
810	413,840	**68,474**
2440	3,708,316*	**203,591**

* Calculated from Figure 4-7

Sediment concentration will be very high during floods. It is recommended that flow diversion into the abandoned channel only occur during low flow periods to prevent the abandoned channel from plugging with sediment. Addition sediment measurements are recommended at high discharges to improve the sediment transport predictions.

4.4 STABLE CHANNEL DESIGN ANALYSIS

4.4.1 Methods

The stable channel design functions are based on the methods used in the SAM Hydraulic Design Package for channels, developed by the U.S. Army Corps of Engineers Waterways Experiment Station. In this study only the Copeland method was used. It is based on an analytical approach to solve stable channel design based on the depth, width, and slope. This approach is primarily analytical on a foundation of empirically-derived equations and uses the sediment discharge and flow depth prediction methods of Brownlie (1981) to ultimately solve for stable depth and slope for a given channel. The model uses idealized trapezoidal cross sections to determine the stable channel design. This method assumes bed load movement above the bed, and separates hydraulic roughness into bed and bank components.

Sound judgment must be used when selecting the appropriate design discharge for performing a stability analysis. Suggested design discharges that may represent the channel forming discharge are a 2 year to frequency flood, 10 year frequency flood, bankfull discharge, and effective discharge.

4.4.2 Results

For this study the following return flows were selected: 1.58 year, reference discharge of 980 cms, and 5 year discharges. The two main input variables for SAM are side slope and bottom width. To estimate a starting point for the analysis, the reach averaged side slope and bottom width were determined based on the existing cross sections within the reach. Other input data came from the hydraulic analysis using HEC-RAS. Input data of side slope and bottom width are summarized in Table 4-7. The stable channel design results using SAM are shown in Figure 4-8 and Figure 4-9.

Table 4-7: Important Input Data

Return Interval (year)	Discharge (cms)	Reach averaged Side slope		Bottom width (m)
		Left	Right	
1.58	610	2	3	237
Q_{Ref}	980	2	3	237
5	1180	2	3	237

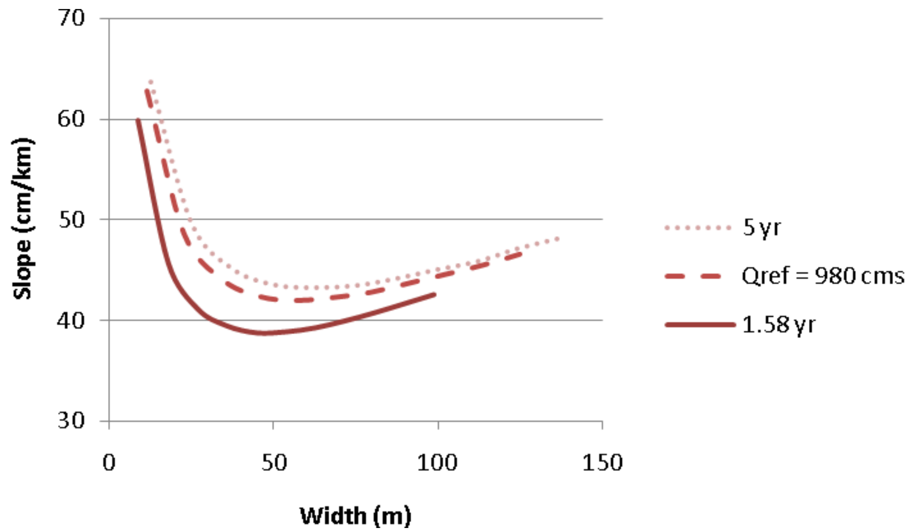

Figure 4-8: Stable Channel Slope and Width from SAM

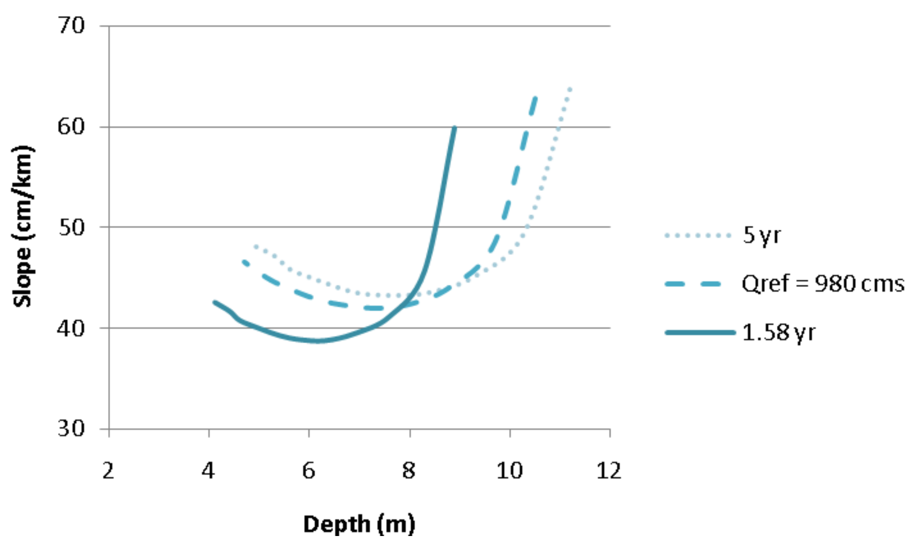

Figure 4-9: Stable Channel Slope and Depth from SAM

The stable width will increase with increasing return interval. There is a small difference between slope and width for the reference discharge and 5 year. This is due to small difference of discharges. The results using SAM were compared with actual slope, width, and depth in Table 4-8.

Table 4-8: Comparison between SAM Results and Actual Values

Return Interval	Discharge	SAM Result			HEC-RAS modeling Results		
		Slope	Width	Depth	Slope	Width	Depth
(year)	(cms)	(m/m)	(m)	(m)	(m/m)	(m)	(m)
1.58	610	0.00039	48	6.1	0.00058	226	2.03
Q_{Ref}	980	0.00042	58	7.2	0.00058	251	2.58
5	1180	0.00043	63	7.7	0.00058	260	2.94

The stable slope was smaller than actual slope. When the width was compared there was a high degree of variability between the actual and stable width. The stable width has a tendency to be less than the actual width, thus explaining why the channel has a tendency to develop alternate bars. The stable depth was deeper than actual depth. A narrow, deeper channel may be more hydraulically efficient.

Chapter 5 EQUILIBRIUM

5.1 METHODS

Several hydraulic geometry equations were used to determine the equilibrium channel width. These methods use channel characteristics such as channel width and slope, sediment concentration, and discharge. All of the equilibrium width equations were developed in simplified conditions such as man-made channels.

Julien and Wargadalam (1995) used the concepts of resistance, sediment transport, continuity, and secondary flow to develop semi-theoretical hydraulic geometry equations.

$$h = 0.2\, Q^{\frac{2}{5+6m}}\, d_s^{\frac{6m}{5+6m}}\, S^{\frac{-1}{5+6m}}$$

$$W = 1.33\, Q^{\frac{2+4m}{5+6m}}\, d_s^{\frac{-4m}{5+6m}}\, S^{\frac{-1-2m}{5+6m}}$$

$$V = 3.76\, Q^{\frac{1+2m}{5+6m}}\, d_s^{\frac{-2m}{5+6m}}\, S^{\frac{2+2m}{5+6m}}$$

$$\tau_* = 0.121\, Q^{\frac{2}{5+6m}}\, d_s^{\frac{-5}{5+6m}}\, S^{\frac{4+6m}{5+6m}}$$

$$\text{given} \quad m = \frac{1}{\ln\left(\frac{12.2\ h}{d_{50}}\right)}$$

where h (m) is the average flow depth, W (m) is the average width, V (m/s) is the average one-dimensional velocity, and τ_* is the Shields parameter, and d_{50} (m) is the median grain size diameter.

Simons and Albertson (1963) used five sets of data from canals in India and America to develop equations to determine equilibrium channel width. Simons and Bender collected data from irrigation canals in Wyoming, Colorado and

Nebraska. These canals had both cohesive and non-cohesive bank material. Data were collected on the Punjab and Sind canals in India. The average bed material diameter found in the Indian canals varied from 0.43 mm in the Punjab canals to between 0.0346 mm and 0.1642 mm in the Sind canals. The USBR data was collected in the San Luis Valley in Colorado and consisted of coarse non-cohesive material. The final data set was collected in the Imperial Valley canal system, which have conditions similar to those seen in the Indian canals and the Simons and Bender canals.

Two figures were developed by Simons and Albertson to obtain the equilibrium width. Figure 5-1 and Figure 5-2 show the relationships between wetted perimeter and discharge and average width and wetted perimeter, respectively.

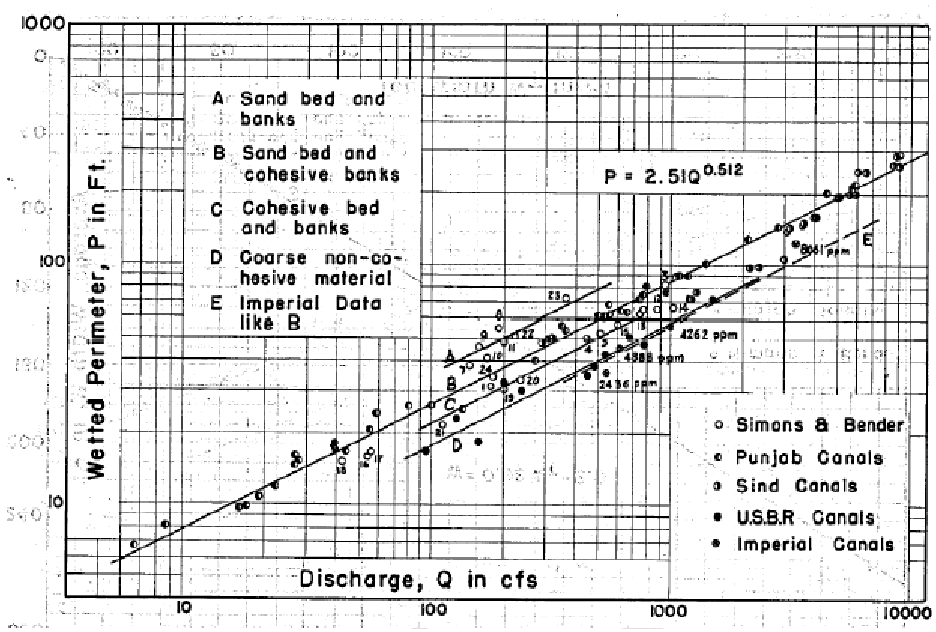

Figure 5-1: Variation of Wetted Perimeter P with Discharge Q and Type of Channel (after Simons and Albertson 1963)

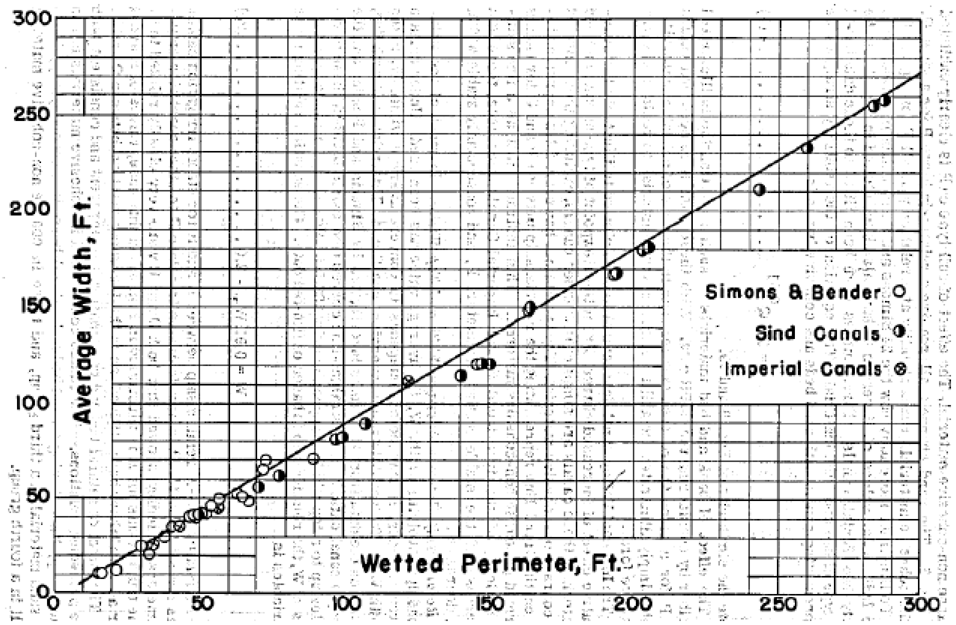

Figure 5-2: Variation of Average Width W with Wetted Perimeter P (Simons and Albertson 1963)

Blench (1957) used flume data to develop regime equations. A bed and a side factor (F_s) were developed to account for differences in bed and bank material.

$$W = \left(\frac{9.6\ (1 + 0.012\ c)}{F_s} \right)^{1/2} d^{1/4}\ Q^{1/2}$$

Where, W (ft) is channel width, c (ppm) is the sediment load concentration, d (mm) is the median grain diameter, and Q (cfs) is the discharge. The side factor, F_s =0.1 for slight bank cohesiveness.

Lacey (from Wargadalam 1993)) developed a power relationship for determining wetted perimeter based on discharge.

$$P = 2.667\, Q^{0.5}$$

Where P (ft) is wetted perimeter and Q (cfs) is discharge. For wide, shallow channels, the wetted perimeter is approximately equal to the width.

Klaassen and Vermeer (1988) used data from the Jamuna River in Bangladesh to develop a width relationship for braided rivers.

$$W = 16.1\, Q^{0.53}$$

Where W (m) is width, and Q (m^3/s) is discharge.

Nouh (1988) developed regime equations based on data collected in extremely arid regions of south and southwest Saudi Arabia.

$$W = 2.83\left(\frac{Q_{50}}{Q}\right)^{0.83} + 0.018\ (1+d)^{0.93}\ c^{1.25}$$

Where W (m) is channel width, Q_{50} (m^3/s) is the peak discharge for a 50 year return period, Q (m^3/s) is annual mean discharge, d (mm) is mean grain diameter, and c (kg/m^3) is mean suspended sediment concentration.

5.2 RESULTS

The input data used to calculate equilibrium widths are summarized in Table 5-1.

Table 5-1: Hydraulic Geometry Calculation Input

Return Interval	Q (cms)	d_{50} (mm)	Channel Slope (m/m)
1.58	610	1.48	0.00058
Q_{Ref}	980	1.48	0.00058
5	1180	1.48	0.00058

Table 5-2 summarizes the equilibrium channel widths predicted by the hydraulic geometry equations.

Table 5-2: Predicted Equilibrium Widths from Hydraulic Geometry Equations

Return Interval	Discharge	Reach Averaged HEC-RAS Main Channel Width	Predicted Width (m)			
(year)	(cms)	(m)	Simons and Albertson	Klaassen and Vermeer	Lacey	Julien and Wargadalam
1.58	610	226	176	482	119	166
Q_{Ref}	980	251	225	620	151	201
5	1180	260	247	684	166	215

Julien and Wargadalam method tends to under predict the channel width compared to main channel width. This suggests that the channel most likely was designed for the higher flow events. The Simons and Albertson method tends to predict the channel widths determined from HEC-RAS at lower flows. However, the Klaassen and Vermeer method tends to completely overestimate channel width whereas Lacey underestimates. The equations of method of Simons and Albertson and Julien-Wargadalam predict similar equilibrium channel widths.

The comparison between predicted and measured width are shown in Figure 5-3.

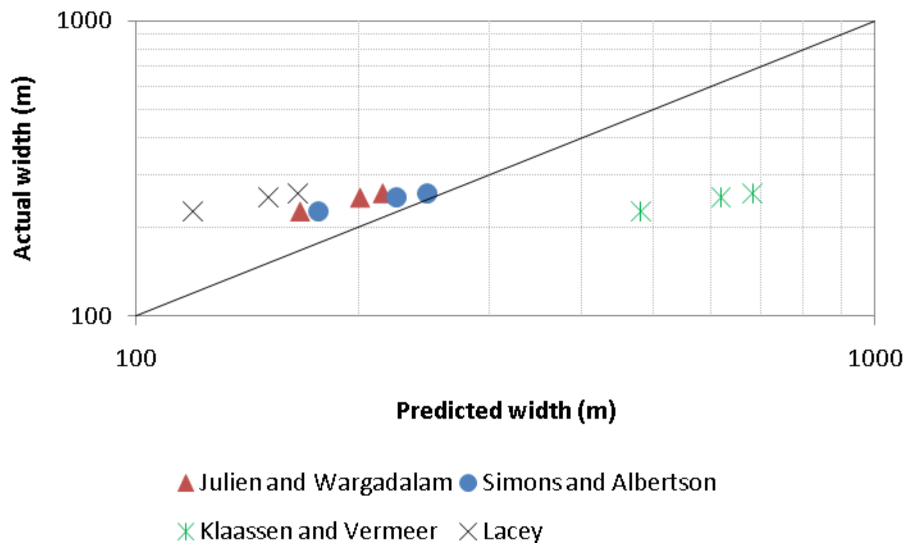

Figure 5-3: Predicted Width and Actual Width

Julien-Wargadalam's method was also used to predict the equilibrium slope. Input data came from reach averaged values and were analyzed with respect to return interval. The Shields parameter (τ_*) is needed for prediction of equilibrium slope. Table 5-3 shows the predicted equilibrium slope.

Table 5-3: Equilibrium Slope Prediction

Return Interval (year)	Discharge (cms)	τ_*	Reach Averaged HEC-RAS Main Channel Slope (m)	Predicted Slope Julien and Wargadalam (m/m)
1.58	610	0.48	0.00058	0.00027
Q_{Ref}	980	0.62	0.00058	0.00029
5	1180	0.70	0.00058	0.00031

The results of the equilibrium slope calculations indicate that the channel had a steeper slope than the predicted slope for each return interval. Thus, due to the levees the channel cannot meander to create a flatter slope.

Using the chapter 4.3 stable channel design results, slope, width, and depth were compared with equlibrium results and HEC-RAS modeling results and are summarized in Table 5-4.

Table 5-4: Comparison SAM, Equilibrium, with HEC-RAS Modeling Results

Recurrence	Discharge	SAM Result			Equilibrium		HEC-RAS Modeling Results		
Interval		Slope	Width	Depth	Slope	Width	Slope	Width	Depth
(year)	(cms)	(m/m)	(m)	(m)	(m/m)	(m)	(m)	(m)	(m)
1.58	610	0.00039	48	6.1	0.00027	166	0.00058	226	2.03
Q_{Ref}	980	0.00042	58	7.2	0.00029	201	0.00058	251	2.58
5	1180	0.00043	63	7.7	0.00031	215	0.00058	260	2.94

The channel width using Julien and Wargadalam method was close to actual width. Overall the channel has developed alternate bars to reduce its slope and to create a more stable channel.

Chapter 6 GEOMORPHOLOGY

6.1 CHANNEL PLANFORM

6.1.1 Methods

A number of channel classification methods were investigated to determine which method was most applicable for Cheongmi Stream. A qualitative classification of the channel was made, based on observations of aerial photographs (1930 and 2006) and AutoCAD survey file from 2004. The channel was classified based on slope-discharge relationships including Leopold and Wolman (1957), Lane (from Richardson et al. 2001), Henderson (1966), and Schumm and Khan (1972). Channel morphology methods by Rosgen (1996) and Parker (1976) were also used, along with stream power relationships developed by Nanson and Croke (1992) and Chang (1979). Two additional methods were also investigated, but found to be inapplicable for Cheongmi Stream. These methods include Ackers and Charlton(1982) and van den Berg (1995). Ackers and Charlton (1982) was developed for gravel-bed rivers and van den Berg (1995) was developed for channels with a sinuosity greater than 1.3 were not used.

6.1.1.1 *Aerial Photo*

The visual planform was analyzed from aerial photo. Due to poor quality of resolution, channel planform was examined from only two year data. Using the 2004 AutoCAD survey data, the aerial images from 1930 and 2006 were scaled.

6.1.1.2 *Slope-Discharge Methods*

Leopold and Wolman (1957) determined a critical slope value, based on discharge, which classifies a stream as either braided or meandering. The following equation shows the slope-discharge relationship:

$$S = 0.6\,Q^{-0.44}$$

Where, S is the critical slope and Q is the channel discharge (cfs). Channels with slopes greater than the critical slope will have a braided planform, while channels with slopes less than the critical slope will have a meandering planform. Straight channels may fall on either side of the critical slope. Leopold and Wolman identified channels with a sinuosity greater than 1.5 as meandering and channels with a sinuosity less than 1.5 as straight. Using the slope-discharge relationship and the critical sinuosity value, channels can be divided into straight, meandering, braided, or straight/braided channels.

Lane (1955) developed a slope-discharge threshold value, k, calculated by this equation:

$$k = S\,Q^{0.25}$$

Where, S is the channel slope and Q is the channel discharge (cfs). The classification of the stream is based on the value of k as shown below:

Meandering: $k \le 0.0017$
Intermediate: $0.010 > k > 0.0017$
Braided: $k \ge 0.010$

These threshold values are based on English units. Values of k are also available for SI units.

Henderson (1966) developed a slope-discharge method that also accounts for the median bed size by plotting the critical slope as defined by Leopold and Wolman against the median bed size. The following equation resulted:

$$S = 0.64 \ d_s^{1.14} \ Q^{-0.44}$$

Where, S is the critical slope, d_s is the median grain size (ft), and Q is the discharge (cfs). For slope values that plot close to this line, the channel planform is expected to be straight or meandering. Braided channels plot well above this line.

Schumm and Khan (1972) developed empirical relationships between valley slope (S_v) and channel planform based on flume experiments. Thresholds were determined for each channel classification as follows:

Straight: S_v < 0.0026

Meandering Thalweg: 0.0026 < S_v < 0.016

Braided: 0.016 < S_v

6.1.1.3 *Channel Morphology Methods*

Rosgen (1996) developed a channel classification method based on entrenchment ratio, width/depth ratio, sinuosity, slope, and bed material. Using these channel characteristics, Rosgen developed eight major classifications and a number of sub-classifications. Figure 6-1 shows Rosgen's method for stream classification.

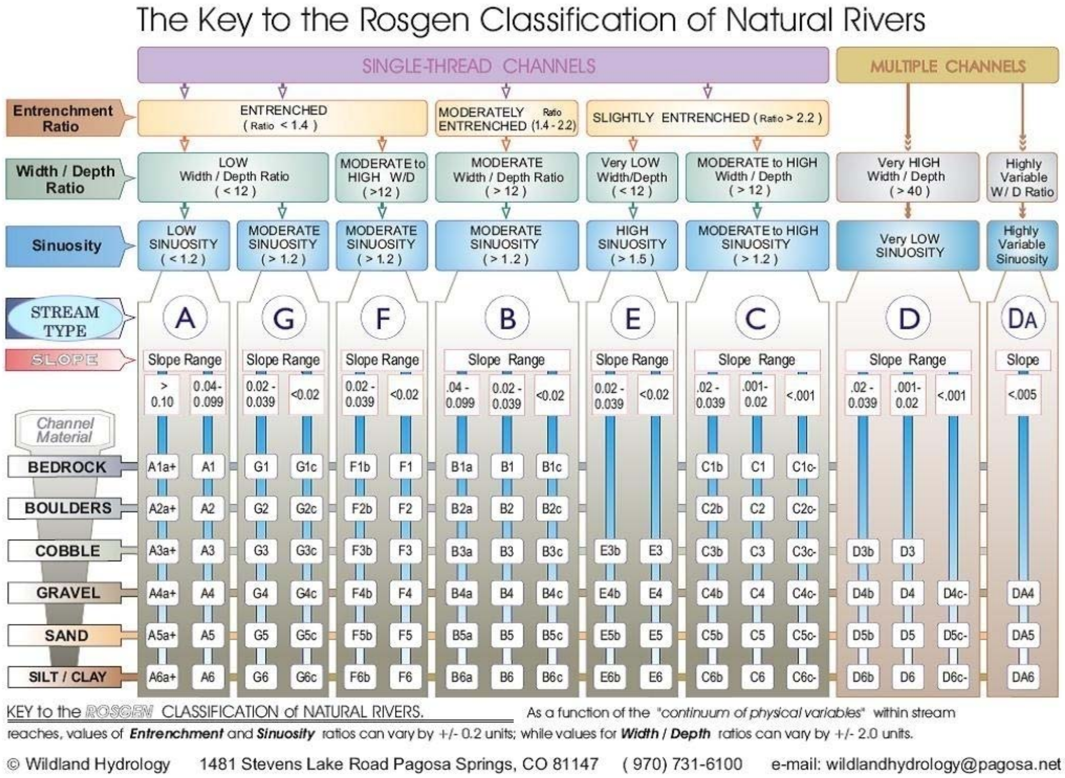

Figure 6-1: Rosgen Channel Classification Key (Rosgen 1996)

<u>Parker (1976)</u> considered the relationship between slope, Froude number, and width to depth ratio. Experiments in laboratory flumes and observations of natural channels lead to the following channel planform classifications:

Meandering: $S/Fr << h/W$

Transitional: $S/Fr \sim h/W$

Braided: $S/Fr >> h/W$

Where S is the channel slope, Fr is the Froude number, and W/h represents the width to depth ratio.

6.1.1.4 *Stream Power Methods*

Nanson and Croke (1992) made use of specific stream power and sediment characteristics to distinguish between types of channel planforms. The equation to determine specific stream power is as follows:

$$\omega = \gamma QS / W$$

Where, ω is specific stream power (W/m^2), γ is the specific weight of water (N/m^3), S is channel slope, and W is channel width (m).

Specific stream power and expected sediment type are shown below:

Braided-river floodplains (braided):
ω = 50-300
gravels, sand, and occasional silt

Meandering river, lateral migration floodplains (meandering):
ω = 10-60
gravels, sands, and silts

Laterally stable, single-channel floodplains (straight):
ω <10
silts and clays

Chang (1979) used data from numerous rivers and canals to build channel classifications based on stream power. The classifications show in terms of valley slope and discharge. Figure 6.2 present the four classification regions defined by Chang for sand streams.

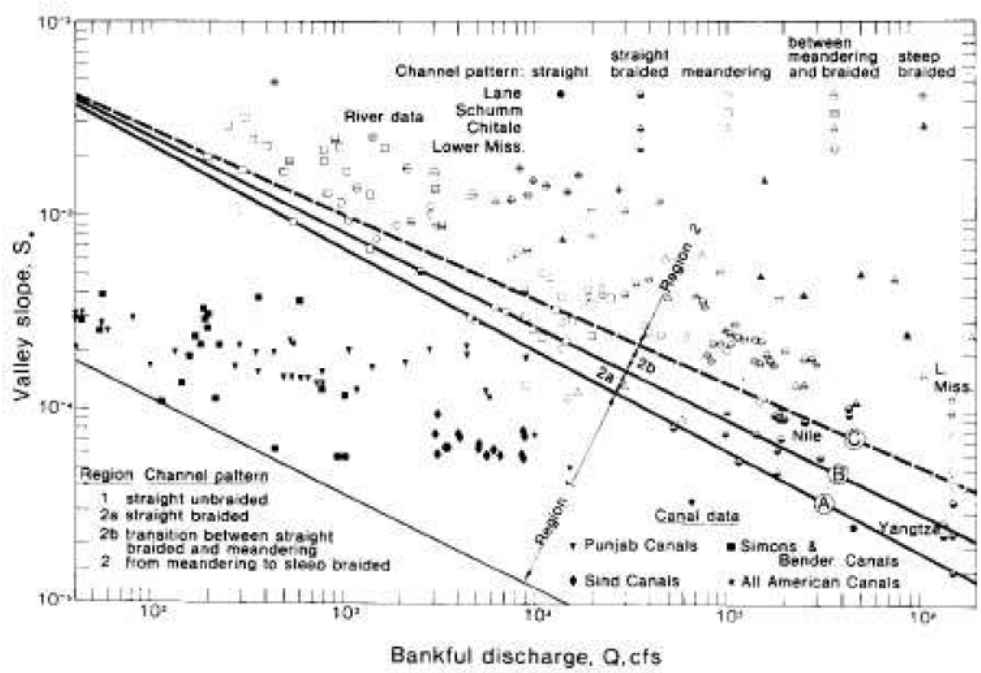

Figure 6-2: Chang's Stream Classification Method Diagram

Chang found that river will have a straight planform at low valley slopes. An increasing valley slope will cause the channel to change to a braided or meandering planform with constant discharge.

6.1.2 Results

Visual characterization of the channel was performed by channel planforms delineated from aerial photographs using AutoCAD in 1930 and 2006. Figure 6-3 shows the historical planforms for Cheongmi Stream.

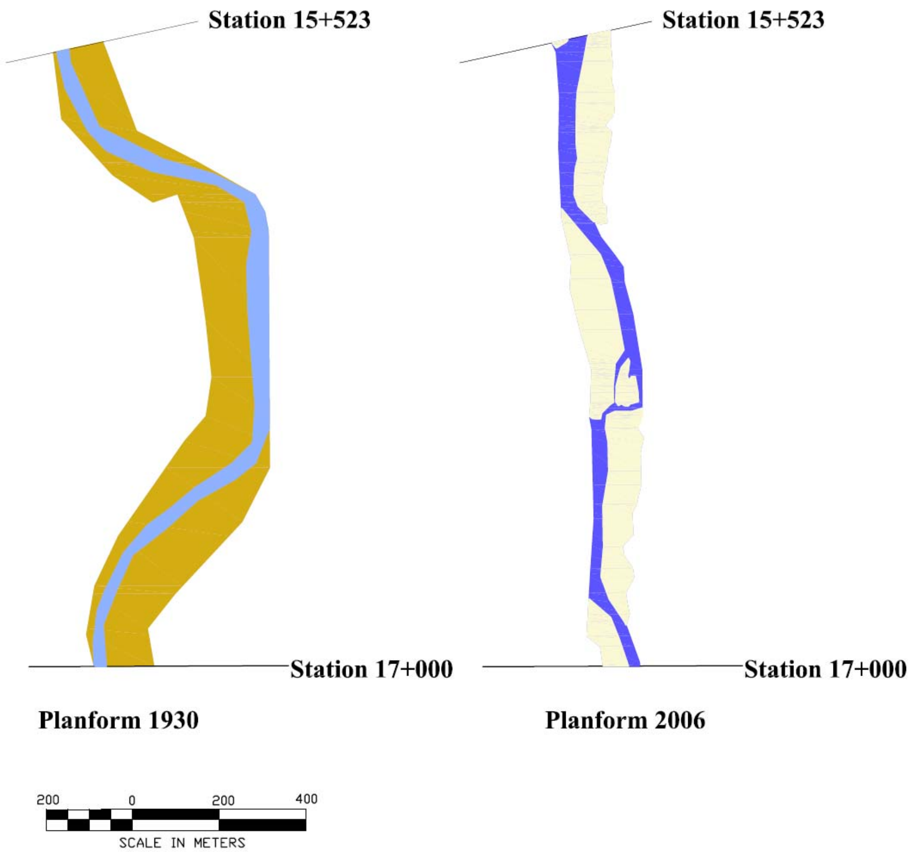

Figure 6-3: Historical Planform

Based on visual observations, the historical channel was somewhat sinuous, but recent planform shows a relatively straight, narrow channel. The planform from 1930 shows the location of the abandoned channel, but the study reach was straightened and levees were constructed for flood protection in 1983. The abandoned channel was created during the channelization of Cheongmi Stream. There are distinct alternate bars in the 2006 planform.

To obtain the values needed in the quantitative channel classification methods, a HEC-RAS model of the reach was run at 12 distinct discharges. Table 6.1 shows the input values obtained from HEC-RAS. Channel characteristics were averaged for each cross section.

Table 6-1: Channel Classification Inputs

Return Interval	Q	Channel Slope	Valley Slope	d_{50}	Bankfull Width	Flood Prone Width	Depth	Fr	EG Slope
(year)	(cms)	(m/m)	(m/m)	(mm)	(m)	(m)	(m)		(m/m)
1.58	610	0.00058	0.00058	1.48	226	279	2.03	0.32	0.00075
Q_{Ref}	980	0.00058	0.00058	1.48	251	279	2.58	0.31	0.00067
5	1180	0.00058	0.00058	1.48	260	279	2.94	0.30	0.00060
10	1480	0.00058	0.00058	1.48	265	279	3.32	0.31	0.00060
20	1770	0.00058	0.00058	1.48	266	279	3.63	0.32	0.00062
30	1940	0.00058	0.00058	1.48	267	279	3.80	0.33	0.00064
50	2150	0.00058	0.00058	1.48	268	279	4.00	0.33	0.00066
70	2290	0.00058	0.00058	1.48	269	279	4.12	0.34	0.00066
80	2340	0.00058	0.00058	1.48	269	279	4.17	0.34	0.00067
100	2440	0.00058	0.00058	1.48	270	279	4.25	0.34	0.00067
150	2600	0.00058	0.00058	1.48	271	279	4.38	0.35	0.00068
200	2710	0.00058	0.00058	1.48	272	279	4.48	0.35	0.00069

The channel classification for each return flow for the study reach is summarized in Table 6-2. The table shows that none of the methods indicates a distinct change in the channel planform over return interval.

Table 6-2: Channel Classification Results

Recurrence Interval (yrs)	D_{50} Type	Slope - Discharge				Channel Morphology		Stream Power	
		Leopold and Wolman	Lane	Henderson	Schumm and Khan	Rosgen Croke	Parker	Nanson and Croke	Chang
1.58	Very Coarse Sand	Straight	Intermediate	Braided	Straight	F5c	Meandering / Transitional	Meandering	Meandering to Steep Braided
Q_{Ref}	Very Coarse Sand	Straight	Intermediate	Braided	Straight	F5c	Meandering / Transitional	Meandering	Meandering to Steep Braided
5	Very Coarse Sand	Braided	Intermediate	Braided	Straight	F5c	Meandering / Transitional	Meandering	Meandering to Steep Braided
10	Very Coarse Sand	Braided/Straight	Intermediate	Braided	Straight	F5c	Meandering / Transitional	Meandering	Meandering to Steep Braided
20	Very Coarse Sand	Braided/Straight	Intermediate	Braided	Straight	F5c	Meandering / Transitional	Meandering	Meandering to Steep Braided
30	Very Coarse Sand	Braided/Straight	Intermediate	Braided	Straight	F5c	Meandering / Transitional	Meandering	Meandering to Steep Braided
50	Very Coarse Sand	Braided/Straight	Intermediate	Braided	Straight	F5c	Meandering / Transitional	Meandering	Meandering to Steep Braided
70	Very Coarse Sand	Braided/Straight	Intermediate	Braided	Straight	F5c	Meandering / Transitional	Meandering	Meandering to Steep Braided

80	Very Coarse Sand	Braided/Straight	Intermediate	Braided	Straight	F5c	Meandering / Transitional	Meandering	Meandering to Steep Braided
100	Very Coarse Sand	Braided/Straight	Intermediate	Braided	Straight	F5c	Meandering / Transitional	Braided/Meandering	Meandering to Steep Braided
150	Very Coarse Sand	Braided/Straight	Braided	Braided	Straight	F5c	Meandering / Transitional	Braided/Meandering	Meandering to Steep Braided
200	Very Coarse Sand	Braided/Straight	Braided	Braided	Straight	F5c	Meandering / Transitional	Braided/Meandering	Meandering to Steep Braided

In slope-discharge analysis, Leopold and Wolman method had gradual change in low flow condition from straight, braided, and braided/straight result. Lane method had different results in high flow conditions from intermediate to braided planform. Henderson, and Schumm and Khan methods had constant results of braided and straight planform respectively.

In channel morphology analysis, Rosgen method indicated that the channel is an F5c planform at all flow conditions, but since the river has been channelized Rosgen's classification may not be appropriate. Parker method had consistent results with meandering/transitional planform.

In stream power analysis, the Nanson and Croke method had different results at high flow conditions from meandering to braided/meandering, whereas Chang method had the same result of meandering to steep braided planform at all flow conditions.

When compared with the observations from the aerial photographs, the methods that indicate a straight or braided channel classification provide the best representation of the current channel characteristics. Since the construction of levee on both sides of river, the straight classification given by Leopold and Wolman's, and Schumm and Khan's methods are the most accurate for all flow conditions. However, Cheongmi Stream has been channelized and is not a natural channel. These results may not be as useful as the actual site observation.

6.2 SINUOSITY

6.2.1 Methods

The sinuosity of the Cheongmi Stream was measured using the AutoCAD survey file from KICT. The valley length was measured for the interested reach as the straight line distance between cross section 17+000 to 15+400. The channel length was measured by estimating the location of the river thalweg profile based on the AutoCAD from survey of the reach. The channel length was divided by the valley length to calculate the sinuosity. Due to lack of survey data and scaled aerial photographs, the sinuosity was obtained from only one year of 2004 survey data.

6.2.2 Results

The sinuosity for the study reach was 1.0. This reach has relatively short distance and levee was constructed on both sides of bank along the stream so the sinuosity is significantly less than 1.5.

6.3 LONGITUDINAL PROFILE

6.3.1 Thalweg Profile

6.3.1.1 *Methods*

The thalweg elevation was calculated as the lowest point in the channel based on 1983 and 1994 (MOCT 2007) and 2004 year survey data from KICT. A thalweg comparison is conducted to determine how the channel bed is changing.

6.3.1.2 *Results*

Figure 6-4 shows the historical thalweg elevation profile of the entire reach.

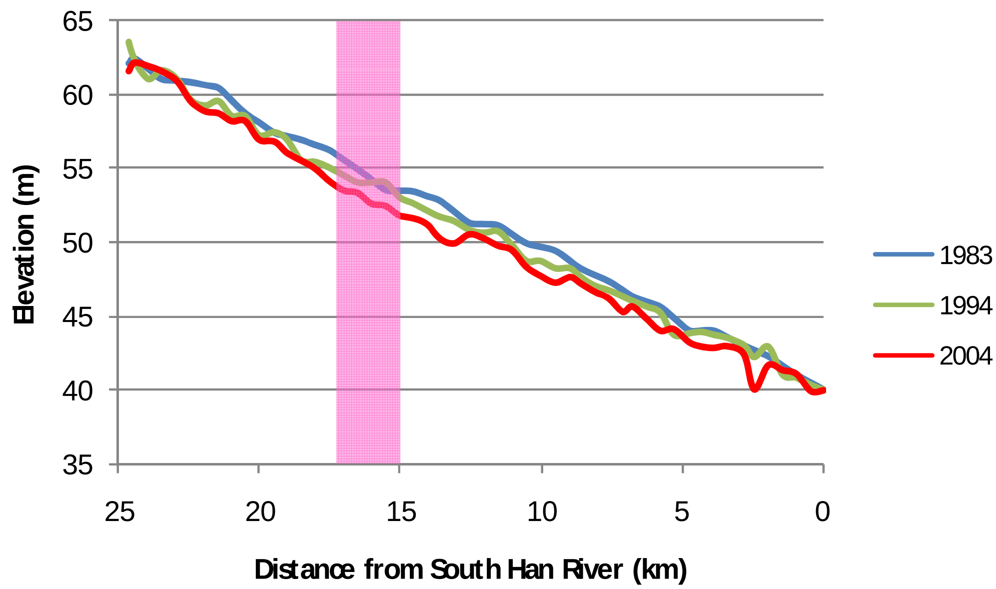

Figure 6-4: Historical Thalweg Profile of Entire Reach

Overall, the results indicate that the reach has degraded since 1983. The area highlighted shows the study reach.

6.3.2 Mean Bed Elevation

6.3.2.1 *Methods*

Trends in mean bed elevation were evaluated using three years in 1983, 1994, and 2004. The three comparisons can be made as 1983-1994 year, 1994-2004 year, and 1983-2004 year. Each evaluation came from the difference between two years. This tendency shows the changes in mean bed elevation through time.

6.3.2.2 *Results*

The change in mean bed elevation for entire reach is shown in Figure 6-5, Figure 6-6, and Figure 6-7.

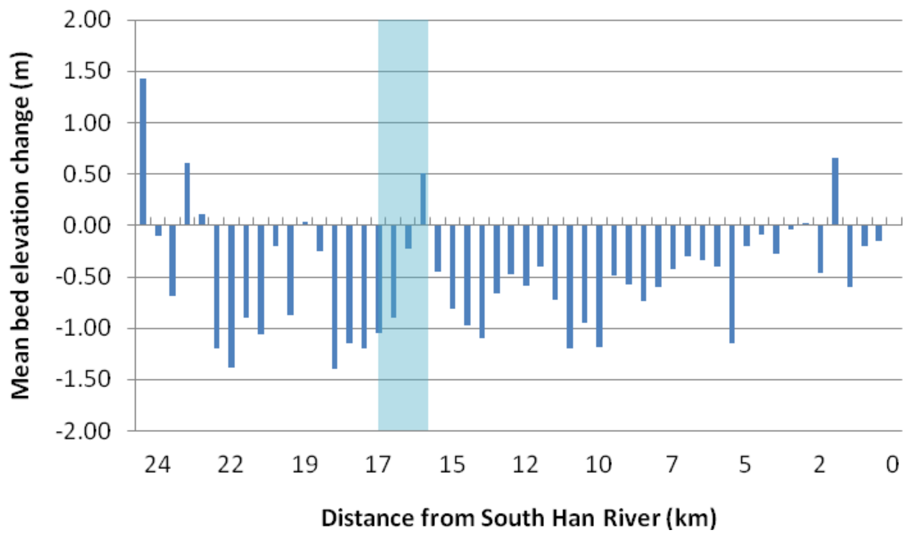

Figure 6-5: Mean Bed Elevation Change between 1983-1994

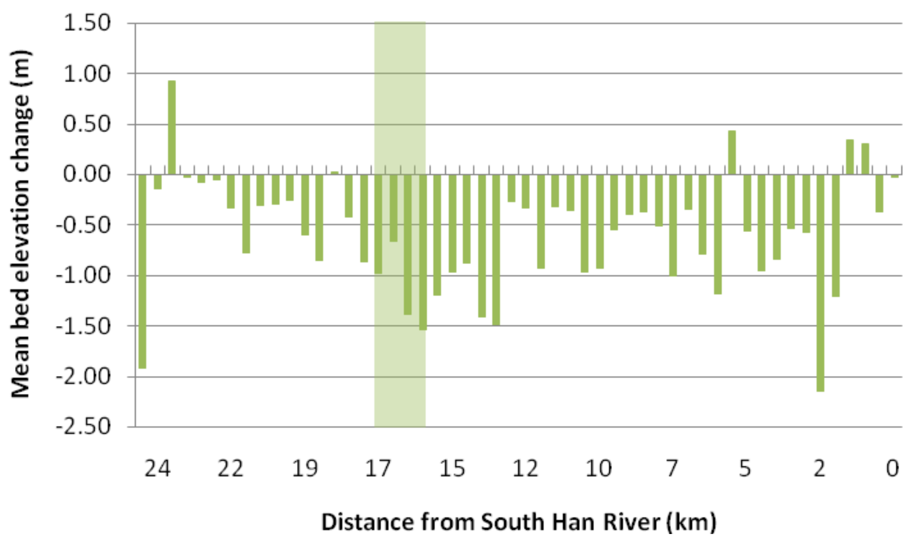

Figure 6-6: Mean Bed Elevation Change between 1994-2004

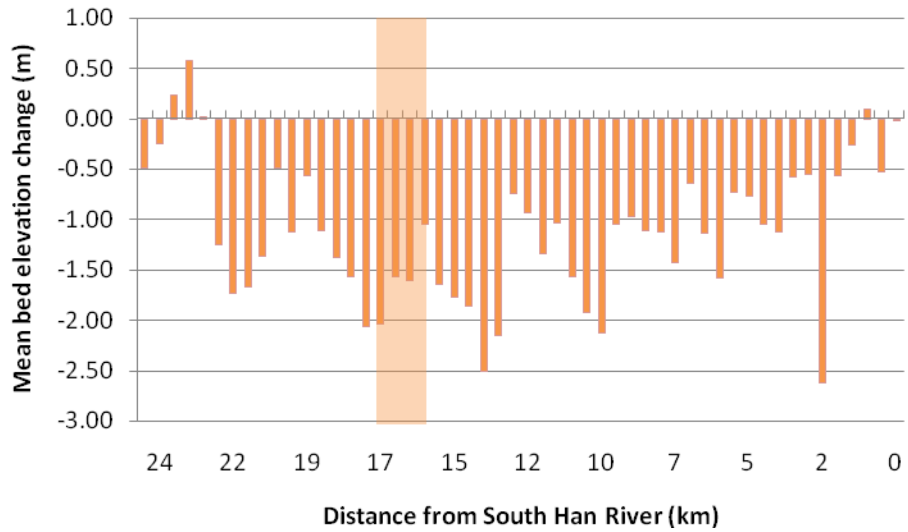

Figure 6-7: Mean Bed Elevation Change between 1983-2004

Overall, the channel has degraded. The river has degraded approximately 2 m along the study reach from 1983 year to 2004 year. This can explain some of the reasons for the alternate bar formation. This may be due to the construction of levee on the both sides of river, which confines the river and prevents the banks from eroding.

Chapter 7 ADDITIONAL CONSIDERATIONS

This Chapter covers responses to questions raised during the review.

7.1 FLOW DURATION ANALYSIS

Daily flow discharge data at Wonbu Bridge became available during the report review. The flow duration curve plots the flow discharge as a function of the percentage of time the discharge is exceeded. Flow duration curves do not represent the actual sequence of flows, but they are useful in predicting the availability and variability of sustained flows. An analysis of the low flow conditions at Cheongmi Stream are performed to determine the appropriate height of the intake structure, so there will be sustainable flows in the reconnected abandoned channel. Figure 7-1 shows the flow duration curve for Cheongmi Stream at Wonbu Bridge. Data was available from 1998 to 2007.

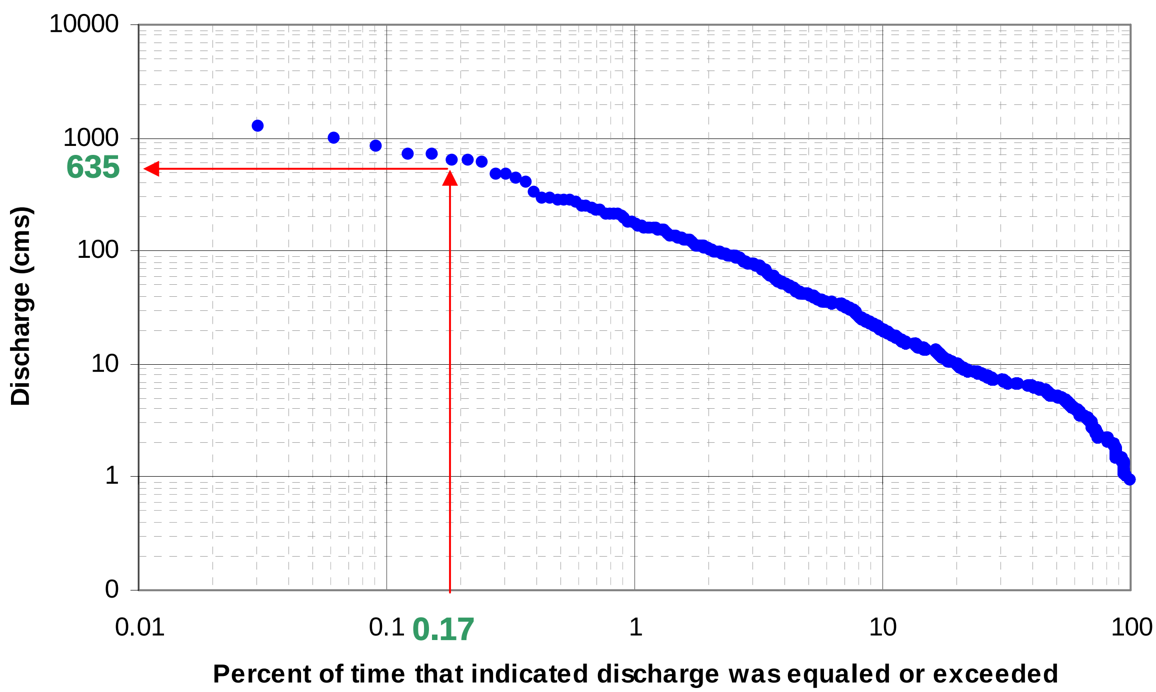

Figure 7-1: Flow Duration Curve for Cheongmi Stream at Wonbu Bridge (1998-2007)

Table 7-1 summarizes the results from the flow duration and HEC-HMS modeling. The flow duration of the study reach is determined based on an area ratio equal to 0.89. Discharges which exceeded one day per 1.58 year, 5 year, and 10 year are computed.

Table 7-1: Comparison of Flow Duration and HEC-HMS modeling

Flow Duration Analysis			HEC-HMS modeling	
Exceeded	Q at Wonbu Bridge (cms)	Q at Study Reach (cms)	Return Interval (yrs)	Location: Just upstream of Sulsung Stream Tributary (CM 5) (cms)
1d / 1.58 yr	635	565	1.58	620
1d / 5 yr	967	860	5	1200
1d / 10 yr	1251	1113	10	1500

The results indicate that the flow rate determined using HEC-HMS is higher than the flow duration analysis. This may be associated with the length of record available to perform flow duration analysis. The 565 cms determined from the flow duration curve is perhaps better suited to design discharge for the study reach. The dominant discharge for Cheongmi Stream is most likely between 565 to 620 cms. This analysis may help determine the flow rate need to provide sustainable flows in Cheongmi Stream.

In the previous section, the reference discharge of 980 cms was used to calculate the hydraulic characteristics within the study reach (15+400 to 17+000).

It is difficult to determine the dominant discharge with great accuracy. The HEC-HMS results are based on a hydrologic analysis and an assumption for Manning's n. On the other hand, the flow duration curve method also includes some uncertainty regarding the drainage area ratio. It is nevertheless considered that a dominant discharge closer to 560-620 cms is probably more appropriate than the reference discharge of 980 cms.

7.2 DEGRADATION

From the thalweg profile analysis in Chapter 6, the average rate of degradation was about 10 cm/year. This result indicates that the bed elevation is degrading. Channel incision will continue until equilibrium is reached. Channel degradation also causes the banks to be unstable. Cheongmi Stream has a levee, which prevents the channel from migrating laterally. In addition, alternate bars located within the active channel width would be eroded. The bed material size should gradually get coarser as degradation progresses.

7.3 ALTERNATE BAR MIGRATION

Alternate bars are regularly spaced depositional features positioned on opposite sides of a straight or slightly sinuous stream. These alternating bars migrate downstream at high flows. This migration may affect the intake structure particularly at low flow. Figure 7-2 shows the potential effect of alternate bar migration in the downstream direction.

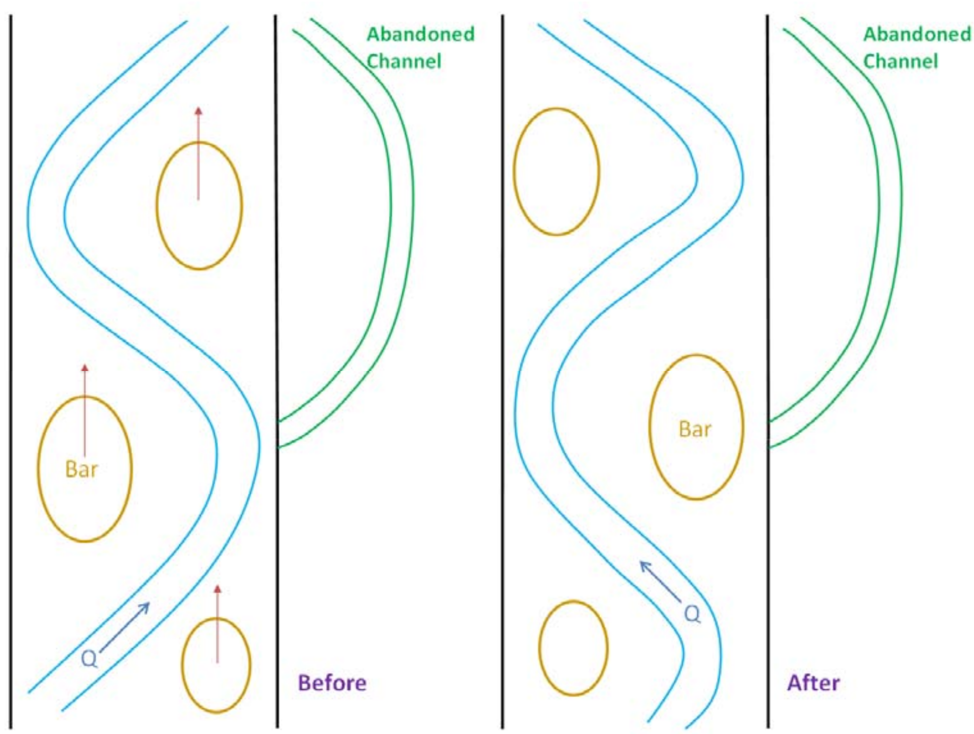

Figure 7-2: Potential Problem with Intake Structure

The migration rate was estimated from available aerial photo. Sparse data was available in 2000 and 2006. Based on two aerial photos, the bar which is easy to be compared was selected and the reference line was drawn. And then the migration length using scale was measured. The bar migration measurement is shown in Figure 7-3

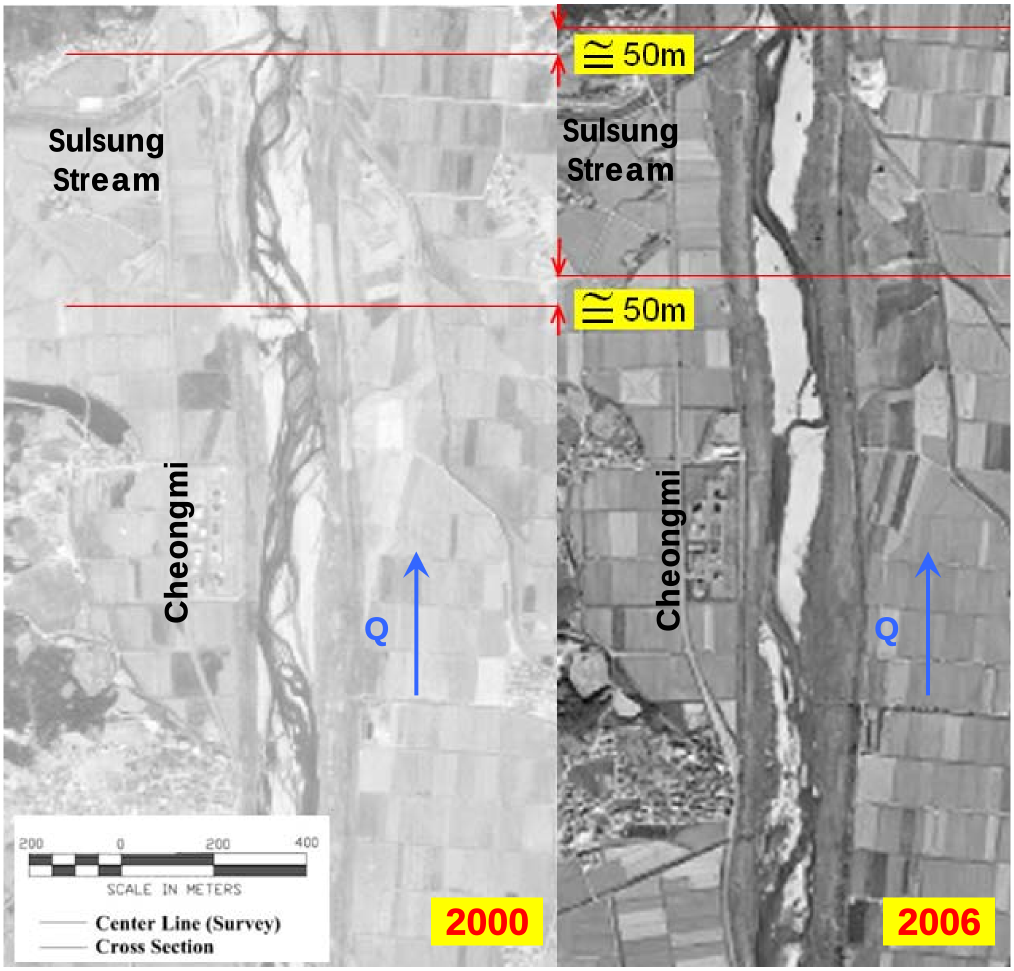

Figure 7-3: Bar Migration Measurement

The bars have a tendency to migrate approximately 8 m per year. This is a very rough estimate and actual rates could greatly increase during flood.

7.4 INTAKE STRUCTURE

For the abandoned channel restoration, the location of the intake structure is very important. To determine the location of the intake structure it is important to analyze flow conditions, degradation and alternate bar migration.

To maintain a sustainable flow within the abandoned channel a sill across Cheongmi Stream is recommended. This sill can be a drop structure or weir, which would maintain a certain minimum water head. The sill should be located downstream of the intake structure, where the effects of degradation and alternate bar migration can be avoided (Julien 2002). A sample sketch of the sill placement is provided Figure 7-4. Figure 7-4 shows that by constructing a sill the problems associated with the alternate bar migration and channel degradation can be alleviated. Flow diversions at low flows are recommended and the insert of the intake structure can be controlled by the sill elevation. During floods, flow diversions are not recommended because high discharges may provide the abandoned channel with the ability to deform and migrate. Also the diversion of sediment laden water at high flows may result in sedimentation in the abandoned channel area.

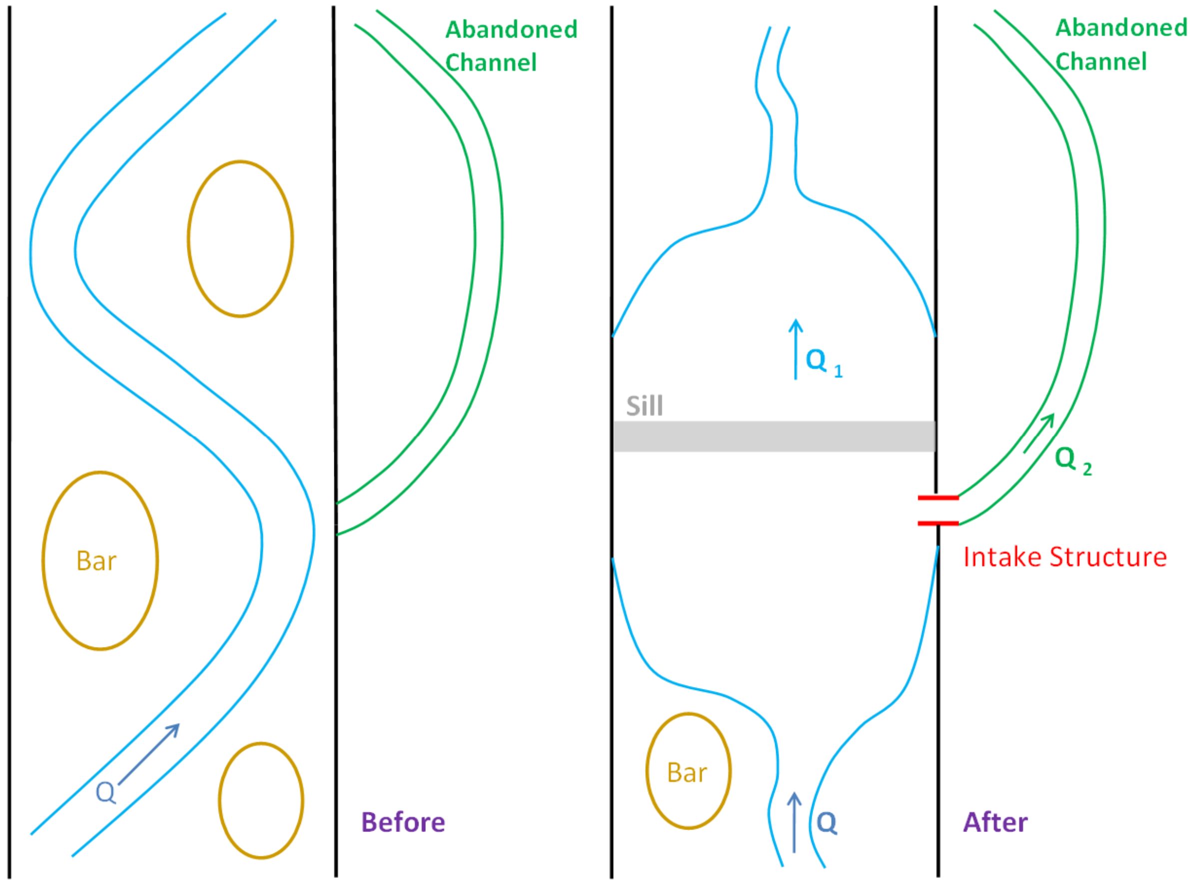

Figure 7-4: Appropriate Design of Intake Structure

Chapter 8 SUMMARY

This study provides a hydraulic modeling analysis of Cheongmi Stream. This stream is 59.5 km long and the reach of interest extends 1.6 km (Station 15+400 to 17+000). The purpose of the analysis is to examine the possibilities of reconnecting an abandoned channel. The primary focus is on the changes in flow discharge, hydraulic parameters, equilibrium hydraulic geometry, sediment transport, bed material characteristics and fluvial geomorphology.

Flow Discharge Analysis

Flow discharges were obtained using three methods in this report and summarized in Table 8-1.

Table 8-1: Flow Summary

Method	Discharge (cms)	Range (cms)
HEC-HMS modeling result (KICT Report)		
1.58 year	620	
5 year	1200	
Cross Section (HEC-RAS)		
Bankfull	502	330 - 800
Reference discharge (Based on the levee discharge)	**980**	820 - 1150
Flow Duration Curve		
1 day / 1.1 year	502	
1 day / 1.58 year	565	
1 day / 2 year	625	
1 day / 3 year	741	
1 day / 5.9 year	980	

HEC-HMS modeling result came from KICT. The station CM 5 is located just upstream of Sulsung stream. Flow discharges with a return interval of 1.58 and 5 years are 620 cms and 1200 cms respectively.

The bankfull discharge varied greatly at different cross sections along this reach. The average bankfull discharge for the reach was approximately 502 cms, from cross section observations, refer to Appendix H. Appropriate discharges to characterize the flow conditions in this reach ranged between 620 cms and 1200 cms and a reference discharge of 980 cms was selected for the hydraulic modeling analysis. Based on the flow duration curve analysis, the bankfull discharge of 502 cms corresponds to a period of return of 1 day per 1.1 year. The reference discharge of 980 cms corresponds to a period of return of 1 day per 5.9 year.

Hydraulic Analysis

The input data for the hydraulic analysis was obtained from the hydrologic analysis performed by KICT. Fifteen hydraulic parameters were analyzed with respect to discharge. At a reference discharge of 980 cms, the average values of the following parameters are obtained. The reach-averaged cross sectional area is 657 m^2, the top width is 251 m, the wetted perimeter is 254 m, the mean flow depth is 2.58 m, the maximum flow depth is 4.4 m, and the width/depth ratio is 98. These values decreased in the downstream direction. The reach-averaged channel velocity is 1.56 m/s and Froude number is 0.3 and these values decreased slightly in the downstream direction due to an increase in cross sectional area at section 15+523.

All hydraulic parameters increased with respect to discharge except the width/depth ratio. This ratio did not follow the same trend due to a minimal change in top width due to the levees. The Froude number also decreased at section 15+523 downstream of the confluence with Sulsung Stream.

Sediment Analysis

The bed material data was available in 2005. The median bed material size d_{50}, for the entire reach was 1.29 mm, while the study reach had a slightly coarser particle size of 1.48 mm. The d_{50} slightly increased in size in the downstream direction. The maximum movable grain size is 19 mm at the reference discharge. The bed sediment of this study reach is mobile.

The sediment transport capacity was calculated using several formulas: Ackers-White, Engelund-Hansen, Laursen, MPM, Toffaleti and Yang. The results of the methods of Engelund-Hansen and Yang at a reference discharge were comparable at approximately 95,000 tons/day. Other methods were significantly lower than the sparse field measurements available for this study. The result from the measured total load at Wonbu Bridge using BORAMEP was 413,840 tons/day at a discharge of 810 cms. At cross section 15+400, near Wonbu Bridge, the results from the sediment transport capacity analysis by the methods of Engelund-Hansen and Yang were also comparable around 77,000 tons/ day. The measured sediment load was higher than the calculated sediment transport capacity from both methods. This may explain why sediment accumulated on alternate bars in the study reach.

The sediment concentration was also computed using BORAMEP based on the measurements at Wonbu Bridge. At a discharge of 810 cms the sediment concentration reached 68,474 mg/l. At such high concentrations, it is not recommended to divert flow into the abandoned channel, due to potential sedimentation.

The stable channel analysis was performed using SAM. When the results from SAM were compared with HEC-RAS at the reference discharge, a stable slope of 0.00042 m/m remained slightly less than the actual slope of 0.00058 m/m. However, the 58 m channel width from SAM was much less than the 251 m measured channel width. The depth from SAM was 7.2 m, which is deeper than the measured depth of 2.58 m at the reference discharge.

Equilibrium Analysis

Four equations were used to determine the equilibrium width of this channel. These results were compared with the actual width from field measurements. The method of Julien-Wargadalam and Simons and Albertson showed reasonable channel width predictions at 201 m and 225 m respectively, compared to the measured width of 251 m.

Geomorphologic Analysis

The channel planform geometry was examined using aerial photographs from 1930 to 2006. In 1930, the planform geometry showed a sinuous stream; however, channelization has resulted in a much straighter channel. The analysis based on slope-discharge, channel morphology, and stream power methods indicated that the methods of Leopold and Wolman, and Schumm and Khan are most appropriate. Both methods predicted straight planform geometry. Today, this channel may have a slight tendency to meander within its levees and to form alternate bars. The formation of alternate bars since levee construction has a tendency to reduce the bed slope. Most important is that based on the surveyed thalweg elevation profiles, the study reach of Cheongmi Stream has degraded about 2 m from 1983 to 2004.

Additional Considerations for Stream Restoration

The flow duration analysis at Wonbu Bridge was performed to determine the sustained flow level within Cheongmi Stream. The flow duration with a period of return of 1.58 years is 565 cms, which is close to 620 cms from the HEC-HMS modeling frequency analysis. The 565 cms is the best estimate of the dominant discharge for the Cheongmi Stream upstream of the confluence with Sulsung Stream (the corresponding discharge is 635 cms). Over the years the channel has been degrading at an average rate of 10 cm/year and there is continued potential for further degradation. From a rough estimate from 2000 to 2006, the alternate bars have a tendency to migrate downstream at approximately of 8m/year. This may potentially adversely affect the operation of the intake structure. A sill, such as a drop structure or a weir, could be built just downstream of the intake structure to maintain a sufficient water level at low flow conditions. Flow diversions to the abandoned channel at low flows are recommended. During floods, sediment concentrations are expected to be high (in excess of 100,000 mg/l). This may result in sedimentation in the abandoned channel area.

The collective observations of the reach indicate that this is a dynamic reach that has not yet reached an equilibrium state and the levees actively prevent the river from lateral migration. More sediment concentration measurements during floods would be desirable to confirm the sediment concentration and transport rate estimates at high flows.

Chapter 9 REFERENCES

Ackers, P. (1982). "Meandering Channels and the Influence of Bed Material." Gravel Bed Rivers: Fluvial Processes, Engineering and Management, R. D. Hey, J. C. Bathurst, and C. R. Thorne, eds., John Wiley & Sons Ltd. , 389-414.

Blench, T. (1957). *Regime Behavior of Canals and Rivers*, Butterworths Scientific Publications, London.

Brownlie, W. R. (1981). "Prediction of Flow Depth and Sediment Discharge in Open Channels." California Institute of Technology, Pasadena, CA.

Chang, H. H. (1979). "Stream Power and River Channel Patterns." *Journal of Hydrology*, 41, 303-327.

Chow, V. T. (1959). *Open Channel Hydraulics*, McGraw-Hill.

Henderson, F. M. (1966). *Open Channel Flow*, Macmillan Publishing Co., Inc., New York, NY.

Ji, U. (2008). "Total Load Analysis Using Boramep on Cheongmi Stream ", Myongji University, Yongin.

Julien, P. Y., and Wargadalam, J. (1995). "Alluvial Channel Geometry: Theory and Applications." *Journal of Hydraulic Engineering*, 121(4), 312-325.

Julien, P. Y. (1998). *Erosion and Sedimentation*, Cambridge University Press, NY.

Julien, P. Y. (2002). *River Mechanics*, Cambridge University, Cambridge, NY.

KICT. (2008). "Http://Www.Kict.Re.Kr." Korea Institute of Construction Technology, Goyang-Si, Gyeonggi-Do, Republic of Korea.

Klaassen, G. J., and Vermeer, K. (1988). "Channel Characteristics of the Braiding Jamuna River, Bangladesh." International Conference on River Regime, 18-20 May 1988, W. R. White, ed., Hydraulics Research Ltd., Wallingford, UK, 173-189.

KRA. (2008). "Www.Riverlove.Or.Kr." Korea River Association, Republic of Korea.

Lane, E. W. (1955). "The Importance of Fluvial Morphology in Hydraulic Engineering." *Proc. ASCE*, 81(745), 1-17.

Leopold, L. B., and Wolman, M. G. (1957). "River Channel Patterns: Braided, Meandering, and Straight." *USGS Professional Paper* 282-B, 85.

MOCT. (2007). "Cheongmi Stream Restoration Master Plan." Ministry of Construction and Transport, Republic of Korea.

Nanson, G. C., and Croke, J. C. (1992). "A Genetic Classification of Floodplains." *Geomorphology*, 4, 459-486.

Nouh, M. (1988). "Regime Channels of an Extremely Arid Zone." International Conference of River Regime, 18-20 May 1988, W. R. White, ed., Hydraulics Research Ltd., Wallingford, UK, 55-66.

Parker, G. (1976). "On the Cause and Characteristic Scales of Meandering and Braiding in Rivers." *Journal of Fluid Mechanics*, 76(Part 3), 457-480.

Richardson, E. V., Simons, D. B., and Lagasse, P. F. (2001). *River Engineering for Highway Encroachments, Highways in the River Environment*, United States Department of the Transportation, Federal Highway Administration.

Rosgen, D. (1996). *Applied River Morphology*, Wildland Hydrology, Pagosa Springs, CO.

Schumm, S. A., and Khan, H. R. (1972). "Experimental Study of Channel Patterns." *Geological Society of America Bulletin*, 83, 1755-1770.

Simons, D. B., and Albertson, M. L. (1963). "Uniform Water Conveyance Channels in Alluvial Material." *Transactions of the American Society of Civil Engineers*, 128, 65-107.

USBR. (2006). *User's Manual for Boramep Ver 1.0* U.S. Department of the Interior Bureau of Reclamation Technical Service Center Denver, Colorado.

van den Berg, J. H. (1995). "Prediction of Alluvial Channel Pattern of Perennial Rivers." *Geomorphology*, 12, 259-279.

Wargadalam, J. (1993). "Hydraulic Geometry of Alluvial Channels," Ph.D. Dissertation, Colorado State University, Fort Collins, CO.

Watson, C. C., Biedenharn, D. S., and Thorne, C. R. (2007). *Stream Rehabilitation*, Colorado State University, Fort Collins, CO.

APPENDIX A - Aerial Photo Images

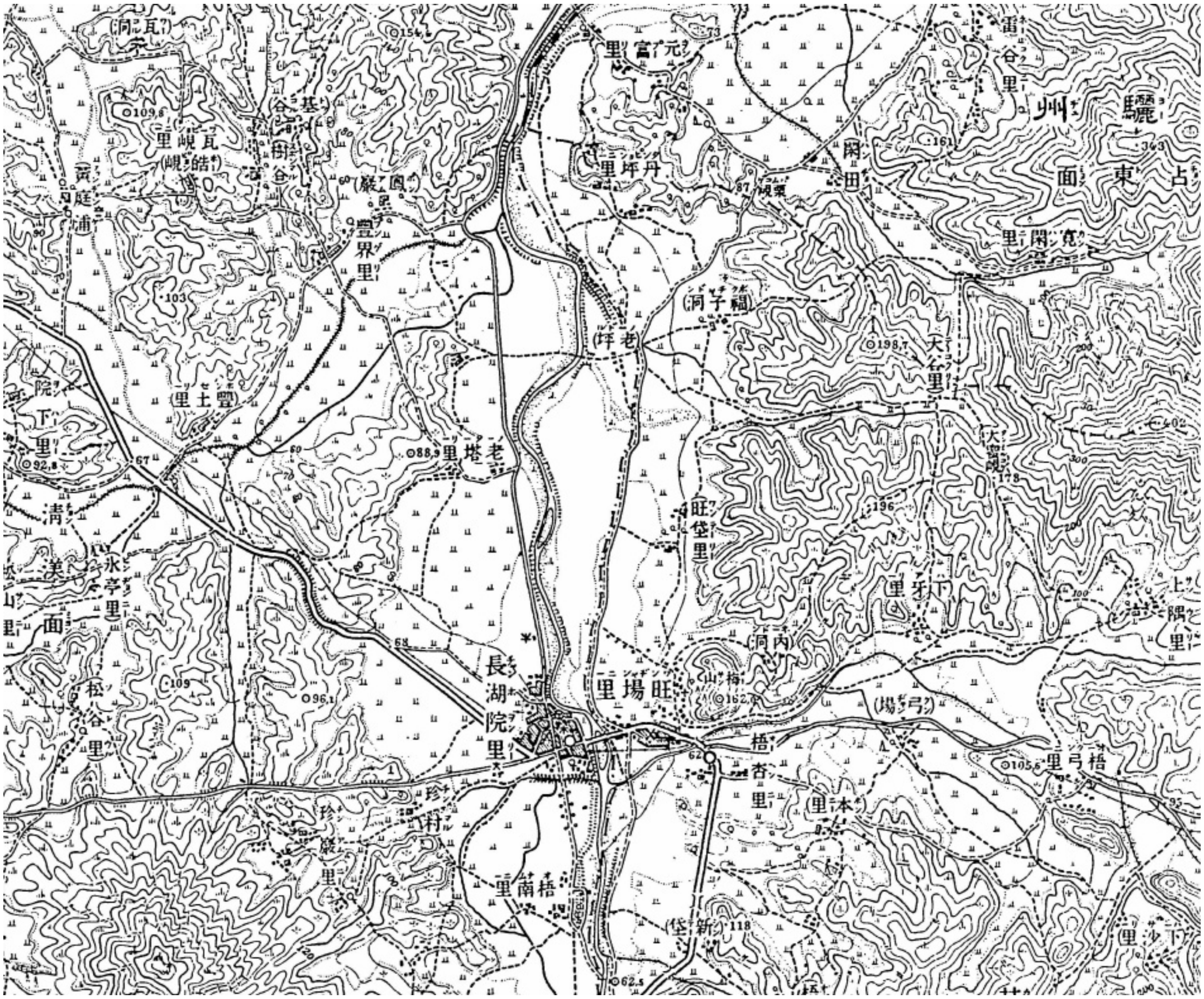

Figure A-1: Aerial Photo Image in 1930

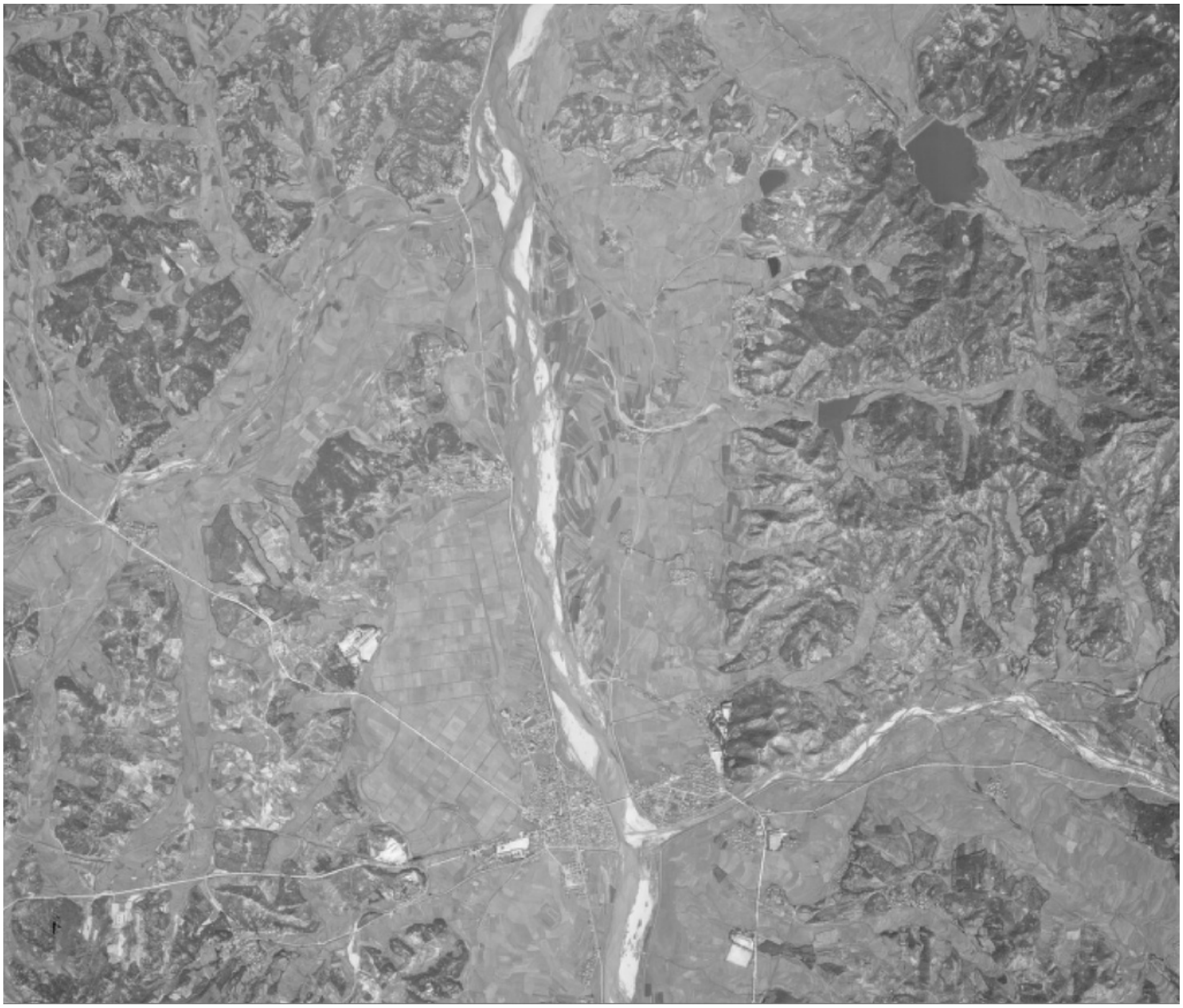

Figure A-2: Aerial Photo Image in 1969

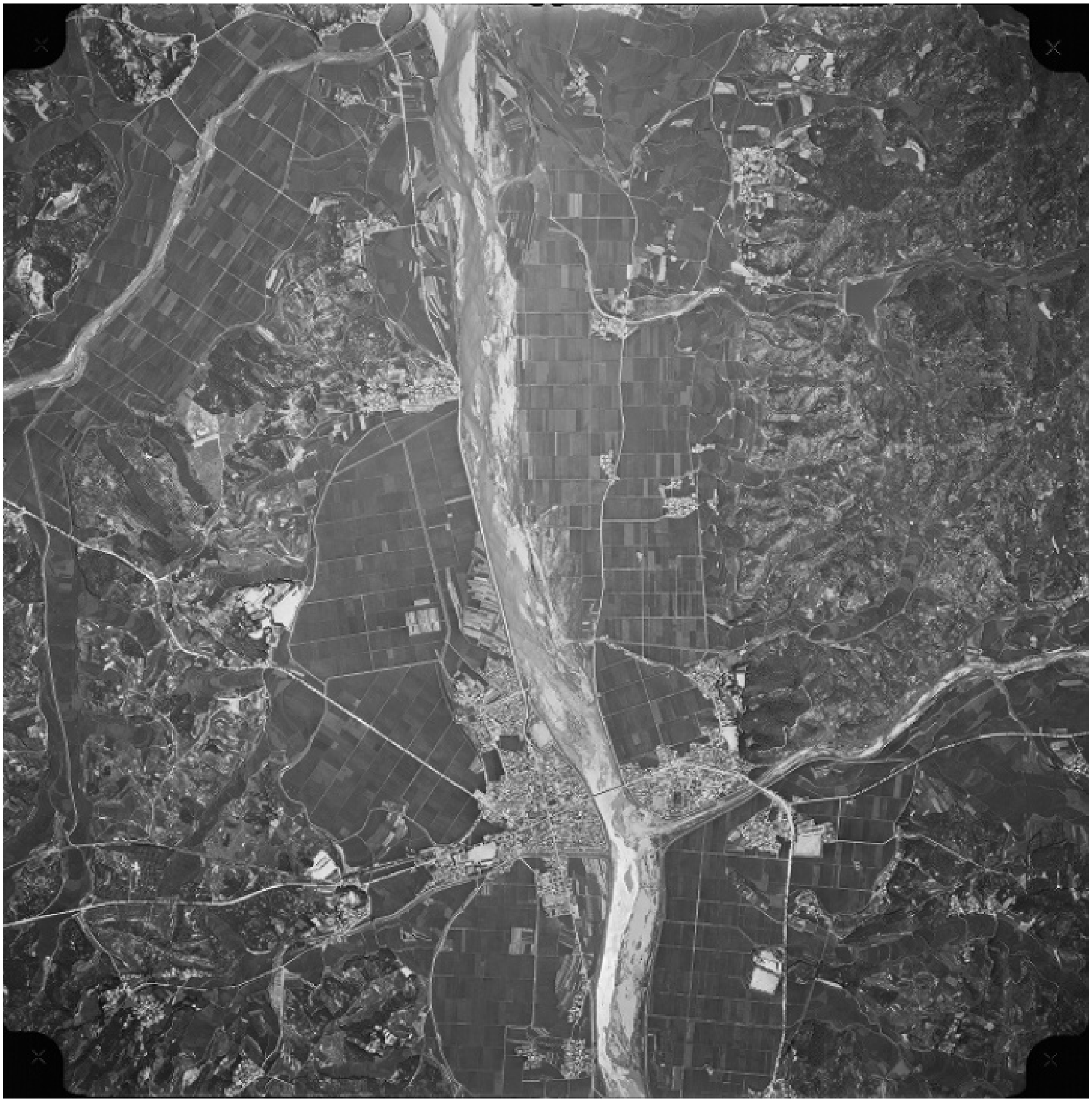

Figure A-3: Aerial Photo Image in 1974

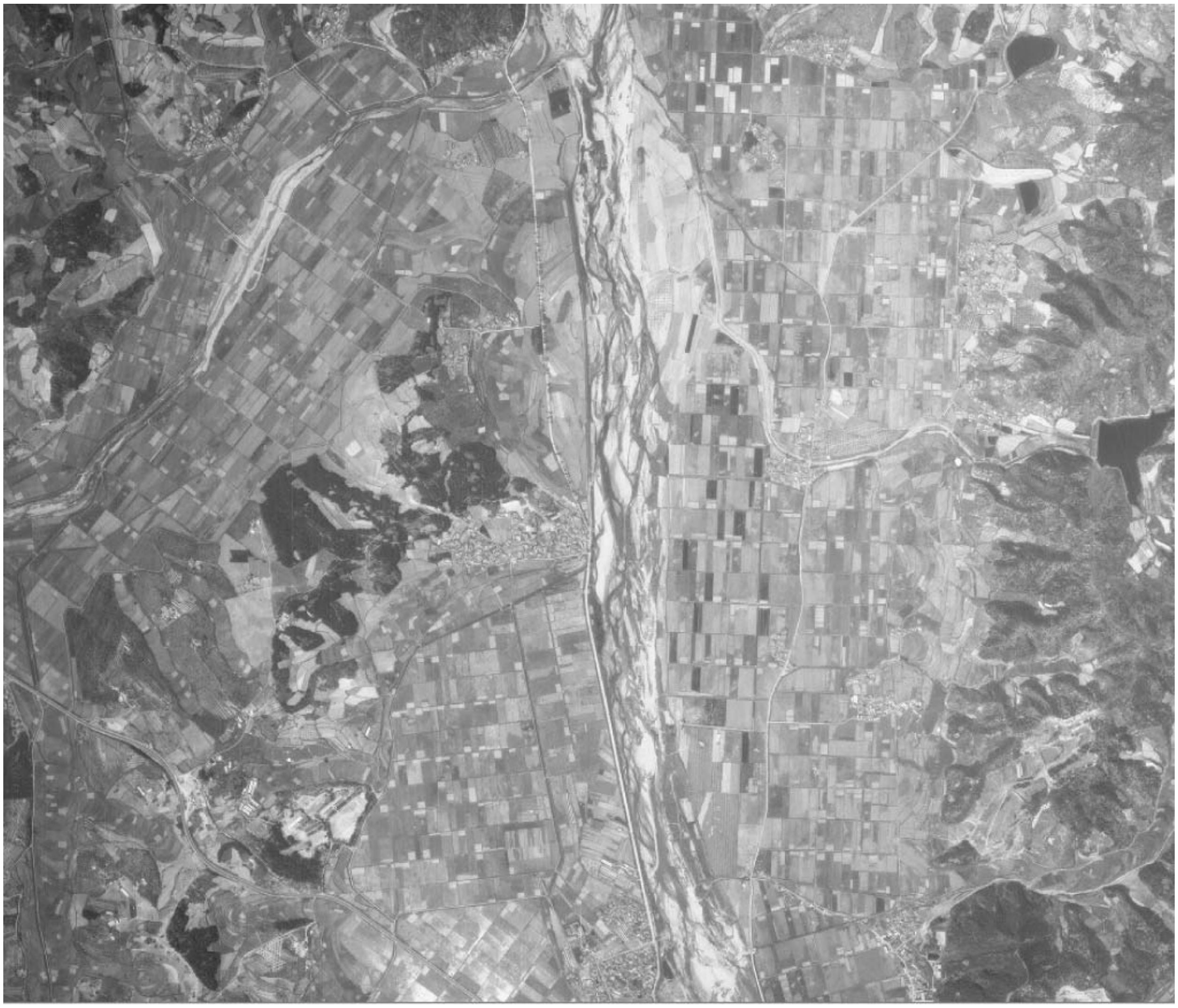

Figure A-4: Aerial Photo Image in 1981

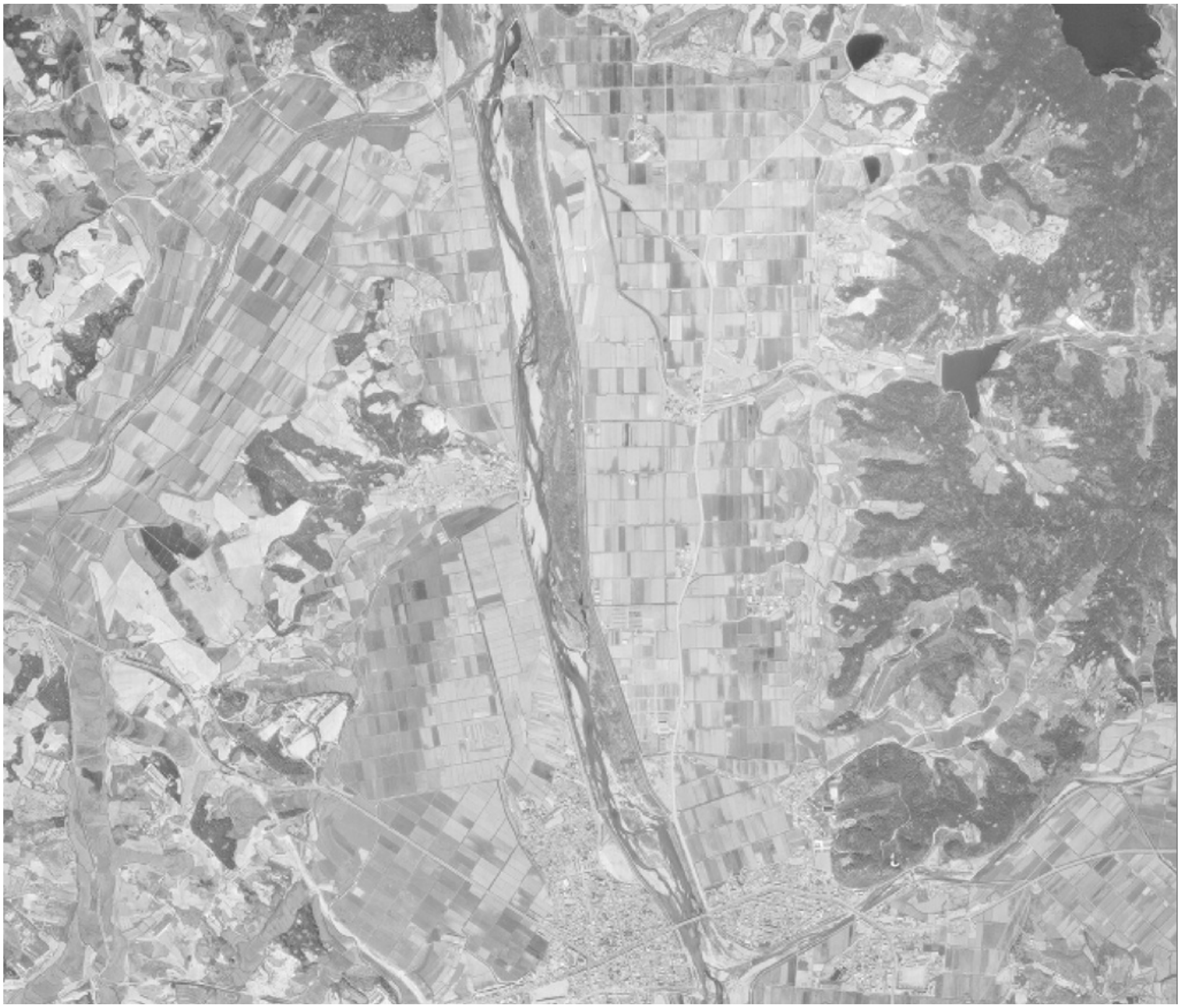

Figure A-5: Aerial Photo Image in 1992

Figure A-6: Aerial Photo Image in 2000

Figure A-7: Aerial Photo Image in 2006

APPENDIX B - Raw Data for HEC-RAS Modeling

Table B-1: Raw Data for HEC-RAS Modeling

River Sta	Profile	Q Total (m^3/s)	Min Ch El (m)	W.S Elev (m)	E.G. Slope (m/m)	Vel Chnl (m/s)	Flow Area (m^2)	Top Width (m)	Froude # Chl	Hydr Radius (m)	Shear Chan (N/m^2)	Power Chan (N/m s)	W.P. Channel (m)	Hydraulic Depth (m)
17	1.58 yr	610	53.53	57.27	0.000784	1.42	430.86	229.29	0.33	1.87	14.36	20.34	230.64	1.88
17	Q_{Ref}	980	53.53	57.97	0.000715	1.65	595.08	235.41	0.33	2.51	17.61	29	237.01	2.53
17	5 yr	1180	53.53	58.35	0.000665	1.73	683.74	238.73	0.33	2.84	18.55	32.02	240.46	2.86
17	10 yr	1480	53.53	58.78	0.000667	1.88	787.12	242.08	0.33	3.23	21.12	39.7	243.96	3.25
17	20 yr	1770	53.53	59.13	0.000683	2.03	873.07	243.81	0.34	3.55	23.78	48.2	245.84	3.58
17	30 yr	1940	53.53	59.32	0.000693	2.11	920	244.76	0.35	3.73	25.31	53.38	246.86	3.76
17	50 yr	2150	53.53	59.55	0.000705	2.2	975.12	245.86	0.35	3.93	27.19	59.94	248.06	3.97
17	70 yr	2290	53.53	59.69	0.000712	2.27	1011.04	246.57	0.36	4.06	28.38	64.27	248.84	4.10
17	80 yr	2340	53.53	59.75	0.000713	2.28	1024.25	246.83	0.36	4.11	28.75	65.69	249.12	4.15
17	100 yr	2440	53.53	59.85	0.000717	2.32	1049.58	247.34	0.36	4.2	29.55	68.71	249.67	4.24
17	150 yr	2600	53.53	60.01	0.000724	2.39	1088.56	247.99	0.36	4.35	30.85	73.68	250.4	4.39
17	200 yr	2710	53.53	60.11	0.000727	2.43	1114.95	248.36	0.37	4.45	31.71	77.08	250.82	4.49
16.8	1.58 yr	610	53.63	57.11	0.000787	1.39	438.03	239.77	0.33	1.82	14.03	19.53	241.05	1.83
16.8	Q_{Ref}	980	53.63	57.84	0.000675	1.6	614.11	243.75	0.32	2.5	16.55	26.42	245.38	2.52
16.8	5 yr	1180	53.63	58.23	0.000618	1.66	708.94	247.38	0.31	2.85	17.25	28.72	249.13	2.87
16.8	10 yr	1480	53.63	58.66	0.000621	1.81	816.35	251.34	0.32	3.22	19.64	35.6	253.22	3.25
16.8	20 yr	1770	53.63	59.01	0.000635	1.96	905.12	252.77	0.33	3.55	22.12	43.26	254.81	3.58
16.8	30 yr	1940	53.63	59.2	0.000644	2.03	953.45	253.54	0.33	3.73	23.56	47.94	255.68	3.76
16.8	50 yr	2150	53.63	59.42	0.000656	2.13	1010.13	254.45	0.34	3.94	25.33	53.9	256.69	3.97
16.8	70 yr	2290	53.63	59.57	0.000663	2.19	1047.1	255.01	0.34	4.07	26.44	57.83	257.32	4.11
16.8	80 yr	2340	53.63	59.62	0.000663	2.21	1060.76	255.21	0.35	4.12	26.79	59.11	257.55	4.16
16.8	100 yr	2440	53.63	59.72	0.000667	2.24	1086.87	255.59	0.35	4.21	27.54	61.83	257.98	4.25
16.8	150 yr	2600	53.63	59.88	0.000673	2.31	1126.97	256.18	0.35	4.36	28.76	66.35	258.65	4.40
16.8	200 yr	2710	53.63	59.99	0.000677	2.35	1154.14	256.58	0.35	4.45	29.57	69.44	259.1	4.50
16.6	1.58 yr	610	53.58	56.88	0.001174	1.61	379.57	225.52	0.4	1.67	19.22	30.88	227.46	1.68
16.6	Q_{Ref}	980	53.58	57.66	0.000887	1.76	556.5	233.39	0.36	2.36	20.55	36.19	235.53	2.38
16.6	5 yr	1180	53.58	58.06	0.000778	1.81	651.75	237.52	0.35	2.72	20.73	37.53	239.77	2.74
16.6	10 yr	1480	53.58	58.49	0.000765	1.96	754.26	240.62	0.35	3.1	23.3	45.71	243.01	3.13
16.6	20 yr	1770	53.58	58.83	0.00078	2.11	837.54	242.29	0.36	3.42	26.16	55.29	244.82	3.46
16.6	30 yr	1940	53.58	59.02	0.00079	2.2	882.76	243.2	0.37	3.59	27.83	61.17	245.8	3.63
16.6	50 yr	2150	53.58	59.24	0.000804	2.3	935.69	244.25	0.37	3.79	29.89	68.68	246.94	3.83
16.6	70 yr	2290	53.58	59.38	0.000812	2.36	970.36	244.94	0.38	3.92	31.18	73.59	247.69	3.96
16.6	80 yr	2340	53.58	59.43	0.000812	2.38	983.31	245.2	0.38	3.97	31.58	75.14	247.97	4.01
16.6	100 yr	2440	53.58	59.53	0.000815	2.42	1007.91	245.69	0.38	4.06	32.43	78.52	248.49	4.10
16.6	150 yr	2600	53.58	59.68	0.000823	2.49	1045.57	246.43	0.39	4.19	33.84	84.15	249.3	4.24
16.6	200 yr	2710	53.58	59.79	0.000827	2.53	1071.15	246.93	0.39	4.29	34.78	87.98	249.84	4.34
16.507	1.58 yr	610	53.34	56.82	0.000733	1.45	420.49	204.8	0.32	2.04	14.65	21.26	206.41	2.05
16.507	Q_{Ref}	980	53.34	57.59	0.000697	1.66	589.69	225.47	0.33	2.6	17.74	29.48	227.23	2.62
16.507	5 yr	1180	53.34	58.01	0.000641	1.73	683.84	232.1	0.32	2.92	18.38	31.72	233.98	2.95
16.507	10 yr	1480	53.34	58.43	0.000648	1.89	783.52	233.93	0.33	3.32	21.11	39.87	236	3.35
16.507	20 yr	1770	53.34	58.78	0.000676	2.05	863.86	235.4	0.34	3.64	24.1	49.37	237.62	3.67
16.507	30 yr	1940	53.34	58.96	0.000693	2.14	907.41	236.19	0.35	3.8	25.84	55.25	238.5	3.84
16.507	50 yr	2150	53.34	59.18	0.000713	2.24	958.32	237.11	0.36	4	27.98	62.78	239.51	4.04
16.507	70 yr	2290	53.34	59.32	0.000725	2.31	991.68	237.71	0.36	4.13	29.34	67.74	240.18	4.17
16.507	80 yr	2340	53.34	59.37	0.000727	2.33	1004.2	237.94	0.36	4.18	29.76	69.34	240.43	4.22
16.507	100 yr	2440	53.34	59.47	0.000733	2.37	1027.9	238.36	0.36	4.27	30.66	72.78	240.9	4.31
16.507	150 yr	2600	53.34	59.62	0.000744	2.44	1064.06	239.01	0.37	4.4	32.15	78.55	241.62	4.45
16.507	200 yr	2710	53.34	59.72	0.000751	2.49	1088.66	239.45	0.37	4.5	33.13	82.48	242.1	4.55
16.4	1.58 yr	610	52.91	56.72	0.000903	1.51	404.78	218.48	0.35	1.84	16.34	24.63	219.4	1.85
16.4	Q_{Ref}	980	52.91	57.51	0.000721	1.69	579.29	221.52	0.33	2.6	18.37	31.08	222.84	2.62
16.4	5 yr	1180	52.91	57.93	0.000656	1.75	673.2	227.28	0.33	2.94	18.92	33.17	228.79	2.96
16.4	10 yr	1480	52.91	58.36	0.000666	1.92	770.23	229.15	0.33	3.34	21.81	41.9	230.84	3.36
16.4	20 yr	1770	52.91	58.69	0.000699	2.09	847.72	230.63	0.35	3.65	25	52.19	232.47	3.68
16.4	30 yr	1940	52.91	58.87	0.000719	2.18	889.64	231.43	0.36	3.81	26.87	58.58	233.34	3.84
16.4	50 yr	2150	52.91	59.09	0.000743	2.29	938.59	232.35	0.36	4	29.16	66.8	234.36	4.04
16.4	70 yr	2290	52.91	59.22	0.000756	2.36	970.73	232.96	0.37	4.13	30.61	72.22	235.03	4.17
16.4	80 yr	2340	52.91	59.28	0.000758	2.38	982.87	233.19	0.37	4.18	31.06	73.95	235.28	4.21
16.4	100 yr	2440	52.91	59.37	0.000766	2.43	1005.76	233.62	0.37	4.27	32.03	77.7	235.76	4.31
16.4	150 yr	2600	52.91	59.52	0.000779	2.5	1040.6	234.27	0.38	4.4	33.62	84.01	236.48	4.44
16.4	200 yr	2710	52.91	59.62	0.000787	2.55	1064.34	234.72	0.38	4.49	34.68	88.3	236.97	4.53

16.2	1.58 yr	610	52.82	56.55	0.000812	1.51	402.97	198.71	0.34	2.01	16.02	24.25	200.33	2.03
16.2	Q_{Ref}	980	52.82	57.37	0.000748	1.69	579.65	227.77	0.34	2.52	18.53	31.33	229.63	2.54
16.2	5 yr	1180	52.82	57.8	0.00066	1.74	679.09	232.82	0.32	2.89	18.71	32.51	234.98	2.92
16.2	10 yr	1480	52.82	58.22	0.000666	1.9	778.23	234.47	0.33	3.29	21.47	40.83	236.83	3.32
16.2	20 yr	1770	52.82	58.56	0.000699	2.07	856.01	235.75	0.35	3.59	24.64	50.95	238.27	3.63
16.2	30 yr	1940	52.82	58.73	0.000719	2.16	897.95	236.44	0.35	3.76	26.5	57.26	239.05	3.80
16.2	50 yr	2150	52.82	58.94	0.000744	2.27	946.81	237.23	0.36	3.95	28.8	65.4	239.95	3.99
16.2	70 yr	2290	52.82	59.08	0.000758	2.34	979.01	237.76	0.37	4.07	30.24	70.75	240.54	4.12
16.2	80 yr	2340	52.82	59.13	0.00076	2.36	991.31	237.96	0.37	4.12	30.68	72.43	240.76	4.17
16.2	100 yr	2440	52.82	59.22	0.000767	2.41	1014.35	238.33	0.37	4.21	31.64	76.11	241.19	4.26
16.2	150 yr	2600	52.82	59.37	0.000781	2.48	1049.27	238.9	0.38	4.34	33.23	82.33	241.82	4.39
16.2	200 yr	2710	52.82	59.47	0.000789	2.53	1073.1	239.29	0.38	4.43	34.27	86.56	242.26	4.48
16	1.58 yr	610	52.6	56.4	0.000738	1.47	415.11	199.03	0.32	2.07	14.96	21.99	200.86	2.09
16	Q_{Ref}	980	52.6	57.22	0.000733	1.64	597.28	241.54	0.33	2.45	17.62	28.91	243.64	2.47
16	5 yr	1180	52.6	57.68	0.000609	1.67	708.48	243.5	0.31	2.88	17.2	28.65	245.81	2.91
16	10 yr	1480	52.6	58.11	0.000613	1.82	812.38	245.32	0.32	3.28	19.72	35.92	247.82	3.31
16	20 yr	1770	52.6	58.43	0.000646	1.98	892.54	246.72	0.33	3.58	22.69	45	249.36	3.62
16	30 yr	1940	52.6	58.61	0.000666	2.07	935.67	247.46	0.34	3.74	24.44	50.68	250.18	3.78
16	50 yr	2150	52.6	58.81	0.000691	2.18	985.86	248.33	0.35	3.93	26.61	58.03	251.14	3.97
16	70 yr	2290	52.6	58.94	0.000704	2.25	1019.09	248.9	0.35	4.05	27.96	62.84	251.77	4.09
16	80 yr	2340	52.6	59	0.000706	2.27	1031.94	249.12	0.36	4.09	28.37	64.32	252.01	4.14
16	100 yr	2440	52.6	59.09	0.000713	2.31	1055.85	249.53	0.36	4.18	29.26	67.61	252.47	4.23
16	150 yr	2600	52.6	59.24	0.000727	2.38	1091.95	250.15	0.36	4.31	30.74	73.19	253.15	4.37
16	200 yr	2710	52.6	59.34	0.000735	2.43	1116.66	250.57	0.37	4.4	31.72	76.97	253.62	4.46
15.8	1.58 yr	610	52.9	56.28	0.000616	1.29	471.49	237.59	0.29	1.96	11.81	15.28	240.97	1.98
15.8	Q_{Ref}	980	52.9	57.12	0.000512	1.45	677.94	251.69	0.28	2.65	13.32	19.26	255.5	2.69
15.8	5 yr	1180	52.9	57.6	0.000435	1.48	798.55	253.52	0.27	3.1	13.22	19.53	257.57	3.15
15.8	10 yr	1480	52.9	58.03	0.000453	1.63	906.58	255.31	0.28	3.49	15.5	25.31	259.55	3.55
15.8	20 yr	1770	52.9	58.35	0.000489	1.79	988.9	256.86	0.29	3.79	18.14	32.47	261.23	3.85
15.8	30 yr	1940	52.9	58.52	0.00051	1.88	1033.13	257.68	0.3	3.94	19.7	37	262.12	4.01
15.8	50 yr	2150	52.9	58.72	0.000535	1.98	1084.57	258.5	0.31	4.12	21.63	42.88	263.04	4.20
15.8	70 yr	2290	52.9	58.85	0.000549	2.05	1118.75	259.02	0.31	4.24	22.84	46.75	263.62	4.32
15.8	80 yr	2340	52.9	58.9	0.000551	2.07	1132.09	259.22	0.32	4.29	23.21	47.96	263.84	4.37
15.8	100 yr	2440	52.9	59	0.000559	2.11	1156.78	259.59	0.32	4.38	24	50.63	264.26	4.46
15.8	150 yr	2600	52.9	59.14	0.000573	2.18	1193.94	260.15	0.32	4.51	25.34	55.18	264.89	4.59
15.8	200 yr	2710	52.9	59.24	0.000582	2.22	1219.42	260.54	0.33	4.6	26.22	58.27	265.32	4.68
15.6	1.58 yr	610	52.76	56.11	0.000806	1.48	413.04	210.49	0.34	1.95	15.41	22.75	211.78	1.96
15.6	Q_{Ref}	980	52.76	56.97	0.000767	1.6	614.37	268.96	0.34	2.27	17.08	27.25	270.52	2.28
15.6	5 yr	1180	52.76	57.49	0.0006	1.56	756.3	284.6	0.31	2.64	15.54	24.25	286.31	2.66
15.6	10 yr	1480	52.76	57.91	0.000582	1.68	879.46	288.75	0.31	3.03	17.28	29.08	290.64	3.05
15.6	20 yr	1770	52.76	58.23	0.000601	1.82	971.6	289.89	0.32	3.33	19.62	35.74	291.94	3.35
15.6	30 yr	1940	52.76	58.4	0.000614	1.9	1020.96	290.54	0.32	3.49	21.01	39.93	292.68	3.51
15.6	50 yr	2150	52.76	58.6	0.000631	1.99	1078.31	291.3	0.33	3.67	22.74	45.34	293.54	3.70
15.6	70 yr	2290	52.76	58.73	0.000639	2.05	1116.66	291.81	0.33	3.8	23.79	48.79	294.11	3.83
15.6	80 yr	2340	52.76	58.78	0.000639	2.07	1131.83	292.01	0.34	3.85	24.08	49.78	294.33	3.88
15.6	100 yr	2440	52.76	58.88	0.000642	2.1	1159.57	292.37	0.34	3.93	24.75	52.09	294.75	3.97
15.6	150 yr	2600	52.76	59.02	0.000659	2.16	1201.16	296.05	0.34	4.02	26	56.28	298.51	4.06
15.6	200 yr	2710	52.76	59.12	0.000662	2.2	1230.08	296.36	0.35	4.12	26.73	58.89	298.88	4.15
15.523	1.58 yr	670	52.46	56.15	0.000127	0.73	913.26	333.97	0.14	2.72	3.4	2.5	335.37	2.73
15.523	Q_{Ref}	980	52.46	57.02	0.00011	0.81	1207.27	339.5	0.14	3.54	3.82	3.1	341.16	3.56
15.523	5 yr	1290	52.46	57.52	0.000129	0.93	1380.85	353.43	0.15	3.89	4.9	4.58	355.28	3.91
15.523	10 yr	1610	52.46	57.96	0.000142	1.05	1534.49	355.37	0.16	4.29	5.98	6.27	357.43	4.32
15.523	20 yr	1930	52.46	58.28	0.000162	1.17	1650.1	357.56	0.17	4.59	7.27	8.5	359.72	4.61
15.523	30 yr	2110	52.46	58.46	0.000171	1.23	1712.45	358.8	0.18	4.74	7.97	9.83	361.01	4.77
15.523	50 yr	2330	52.46	58.66	0.000183	1.31	1785.16	360.75	0.19	4.92	8.84	11.54	363.03	4.95
15.523	70 yr	2480	52.46	58.79	0.000193	1.35	1833.9	364.64	0.19	5	9.44	12.77	366.96	5.03
15.523	80 yr	2540	52.46	58.84	0.000196	1.37	1853.03	366.16	0.19	5.03	9.68	13.27	368.49	5.06
15.523	100 yr	2650	52.46	58.94	0.000203	1.4	1888.54	368.96	0.2	5.09	10.1	14.18	371.32	5.12
15.523	150 yr	2820	52.46	59.09	0.000212	1.45	1942.11	373.06	0.2	5.17	10.76	15.62	375.46	5.21
15.523	200 yr	2940	52.46	59.19	0.000218	1.49	1979.37	374.62	0.21	5.25	11.2	16.64	377.04	5.28
15.4	1.58 yr	670	52.6	56	0.000801	1.61	415.33	184.39	0.34	2.24	17.57	28.34	185.78	2.25
15.4	Q_{Ref}	980	52.6	56.89	0.000801	1.59	614.63	276.82	0.34	2.2	17.26	27.52	279.62	2.22
15.4	5 yr	1290	52.6	57.38	0.000801	1.7	760.9	311.96	0.35	2.41	18.92	32.08	315.72	2.44
15.4	10 yr	1610	52.6	57.8	0.0008	1.79	897.63	338.03	0.35	2.62	20.59	36.93	342.17	2.66
15.4	20 yr	1930	52.6	58.11	0.000801	1.93	1002.11	339.34	0.36	2.92	22.91	44.13	343.63	2.95
15.4	30 yr	2110	52.6	58.28	0.0008	1.99	1058.55	339.99	0.36	3.07	24.12	48.07	344.37	3.11
15.4	50 yr	2330	52.6	58.47	0.000801	2.07	1124.15	340.71	0.36	3.26	25.58	53.02	345.18	3.30
15.4	70 yr	2480	52.6	58.6	0.000801	2.12	1167.79	341.18	0.37	3.38	26.53	56.34	345.72	3.42
15.4	80 yr	2540	52.6	58.65	0.000801	2.14	1184.79	341.37	0.37	3.42	26.91	57.69	345.93	3.47
15.4	100 yr	2650	52.6	58.74	0.0008	2.18	1216.31	341.71	0.37	3.51	27.56	60.05	346.32	3.56
15.4	150 yr	2820	52.6	58.88	0.0008	2.23	1263.38	342.22	0.37	3.64	28.58	63.8	346.9	3.69
15.4	200 yr	2940	52.6	58.97	0.0008	2.27	1295.96	342.57	0.37	3.73	29.28	66.43	347.3	3.78

APPENDIX C - Hydraulic Geometry Analysis Plots Combined & Averaged

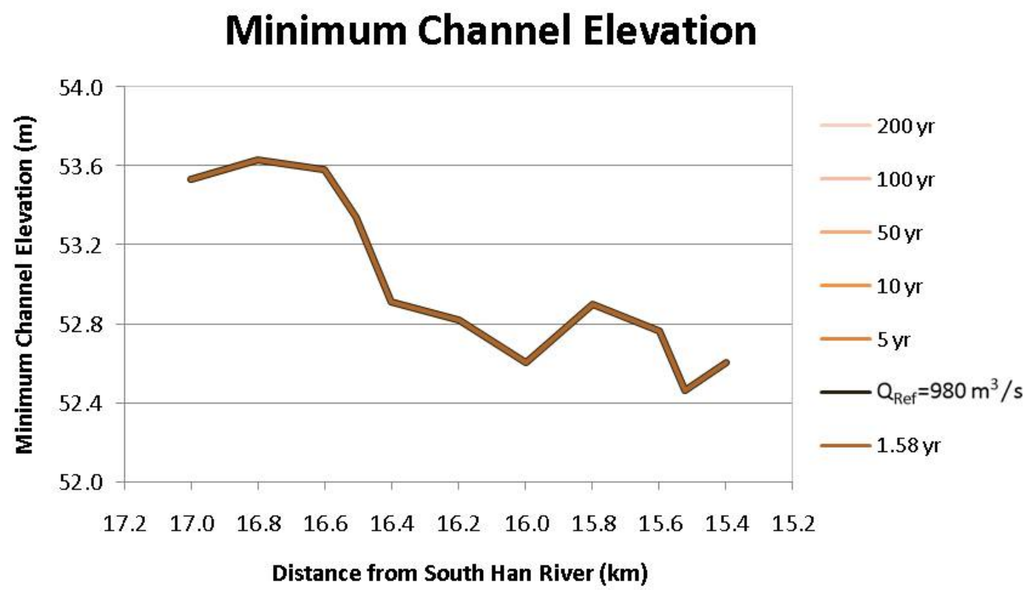

Figure C-1: Combined Minimum Channel Elevation due to Discharge

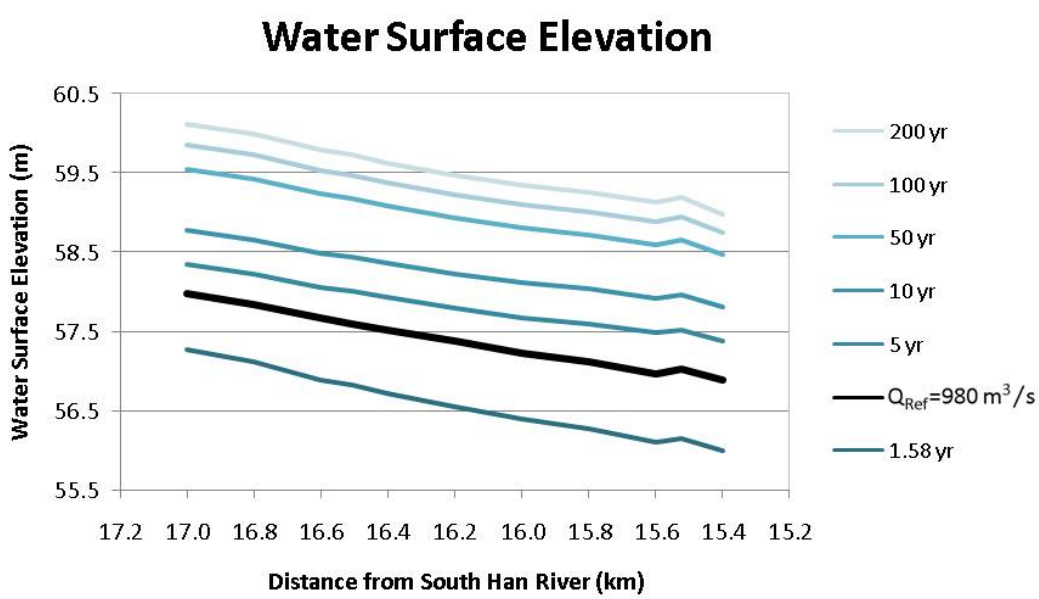

Figure C-2: Combined Water Surface Elevation due to Discharge

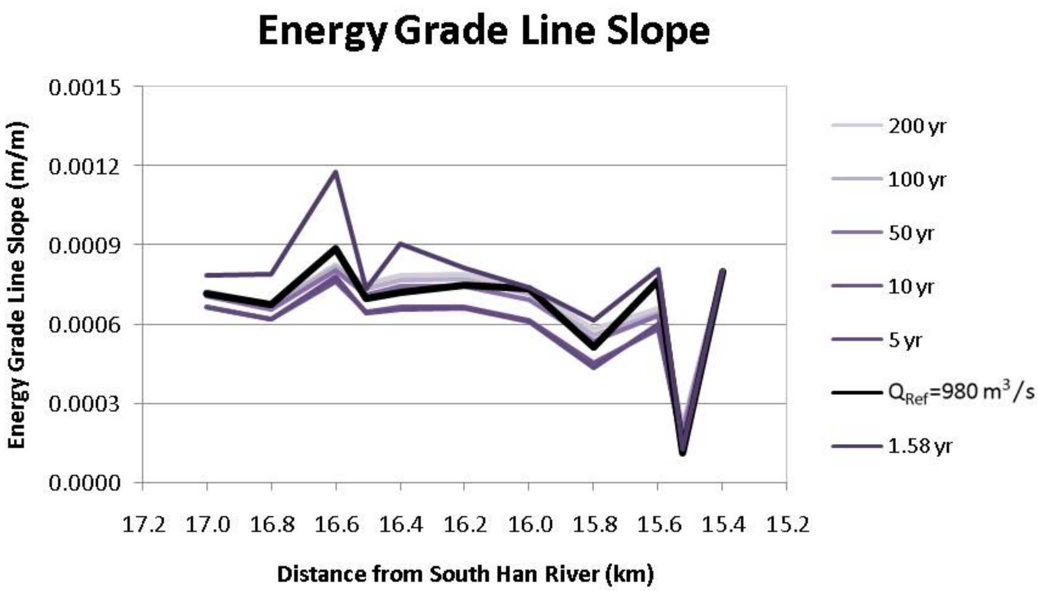

Figure C-3: Combined Energy Grade Line Slope due to Discharge

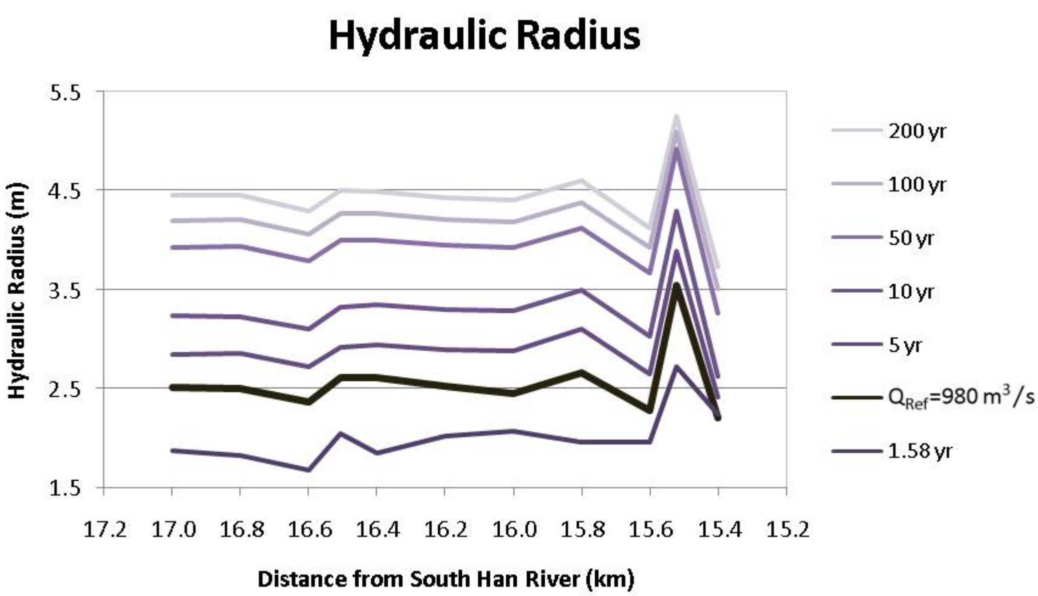

Figure C-4: Combined Hydraulic Radius due to Discharge

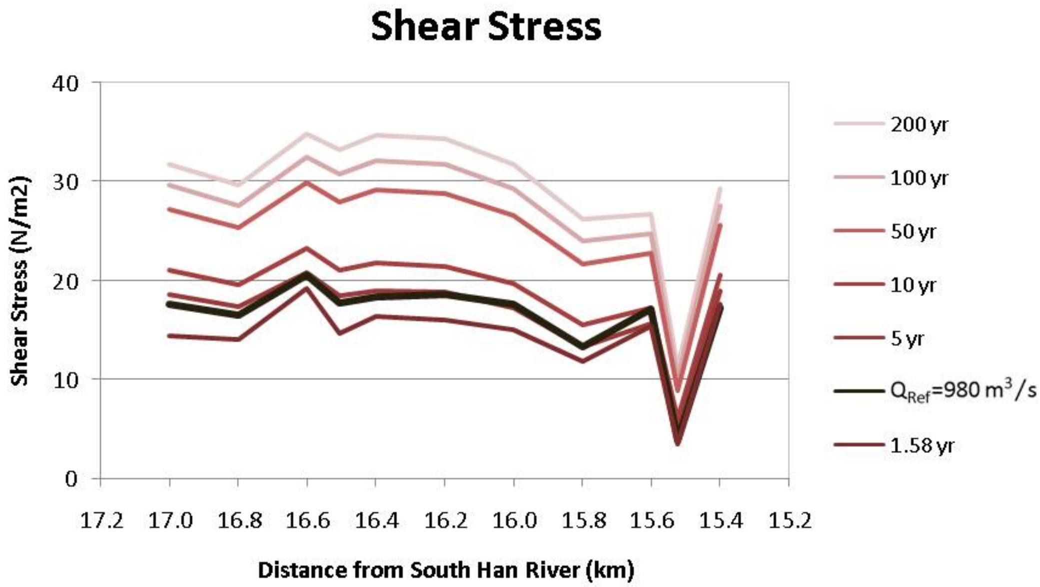

Figure C-5: Combined Shear Stress due to Discharge

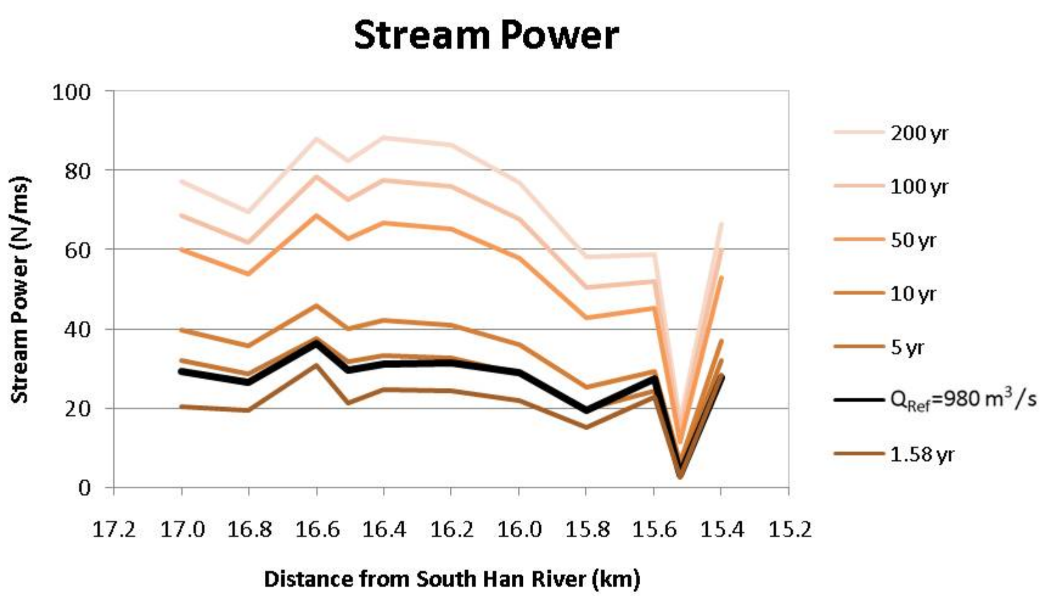

Figure C-6: Combined Stream Power due to Discharge

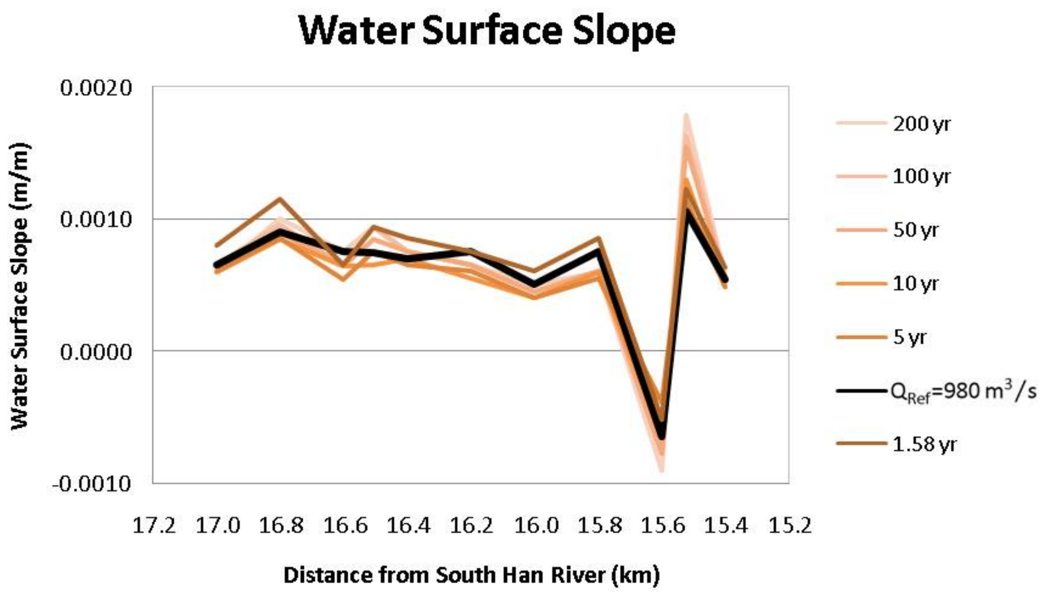

Figure C-7: Combined Water Surface Slope due to Discharge

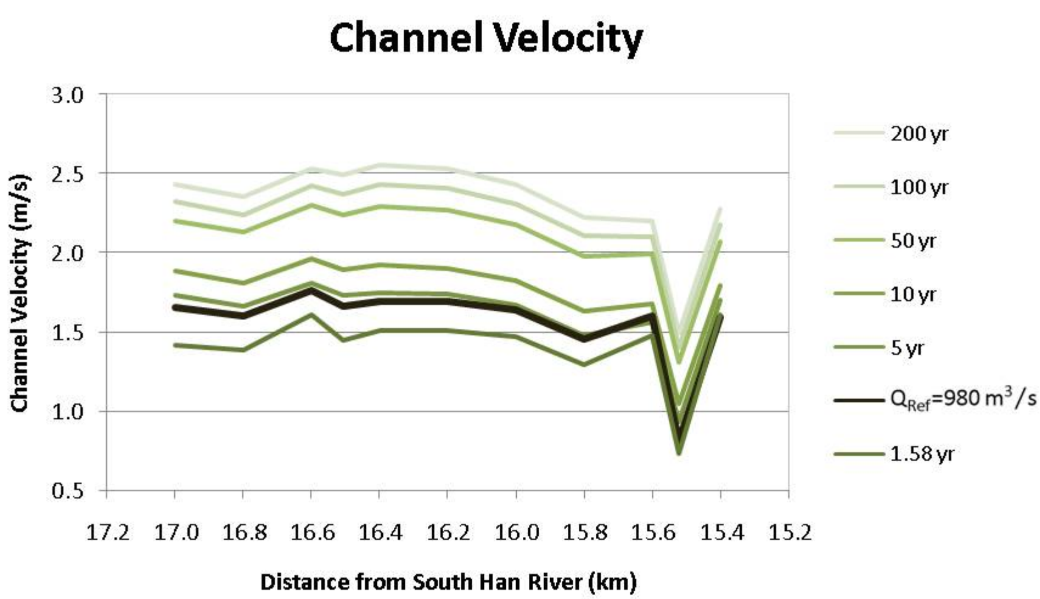

Figure C-8: Combined Channel Velocity due to Discharge

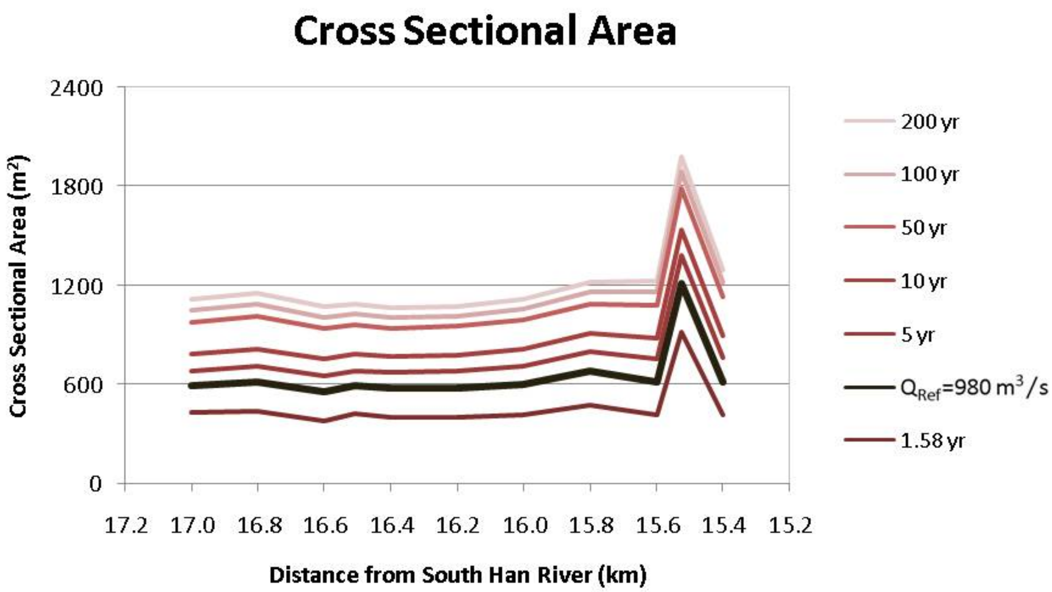

Figure C-9: Combined Cross Sectional Area due to Discharge

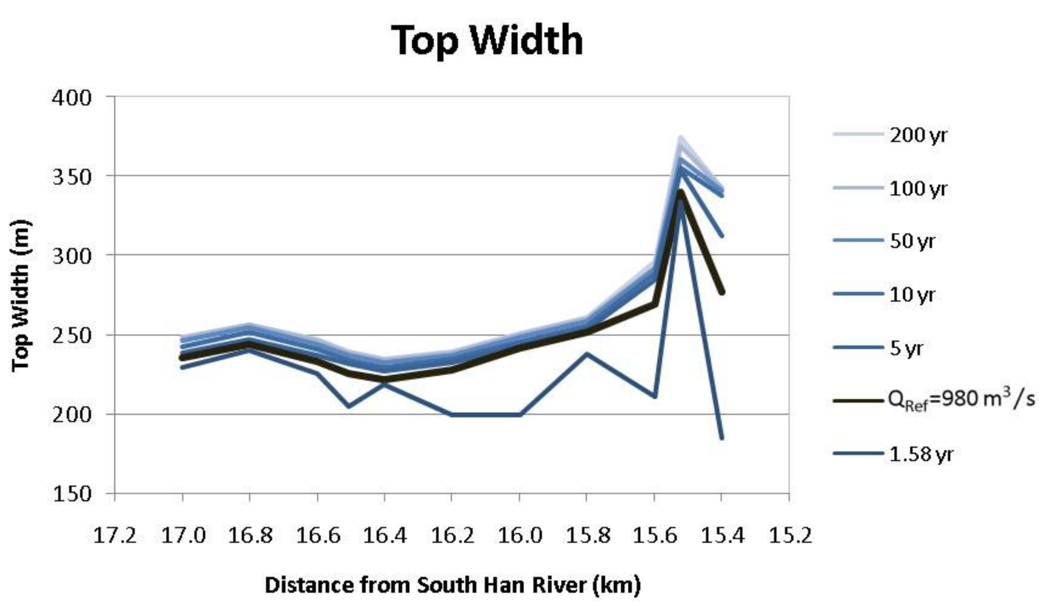

Figure C-10: Combined Top Width due to Discharge

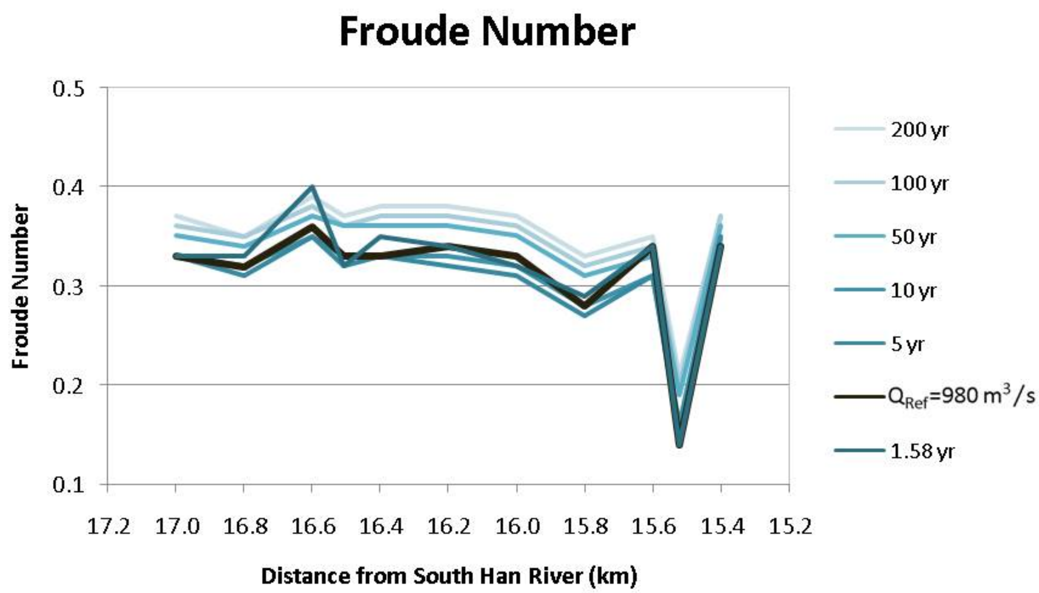

Figure C-11: Combined Froude Number due to Discharge

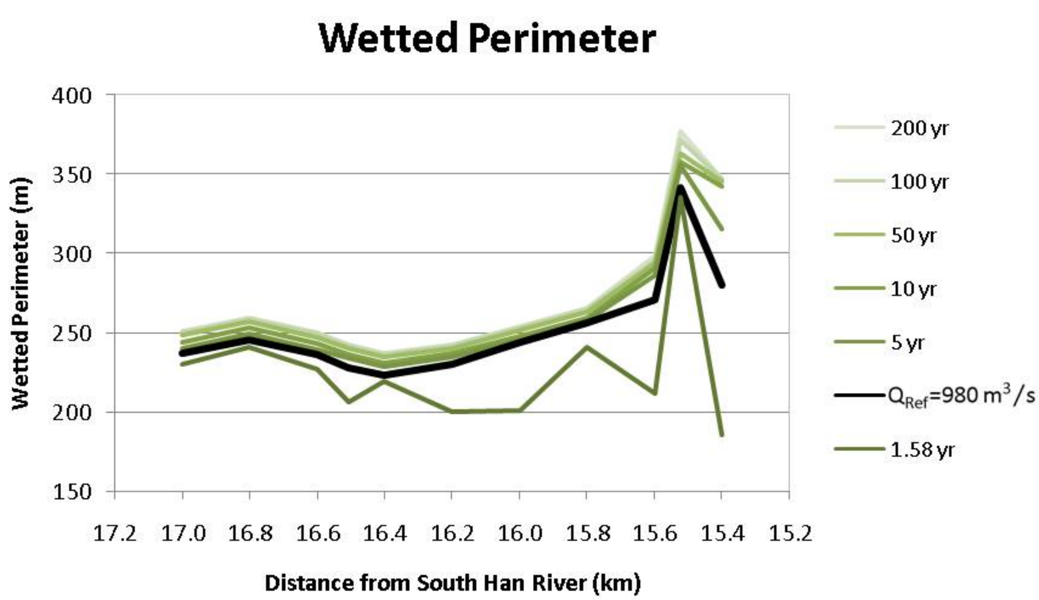

Figure C-12: Combined Wetted Perimeter due to Discharge

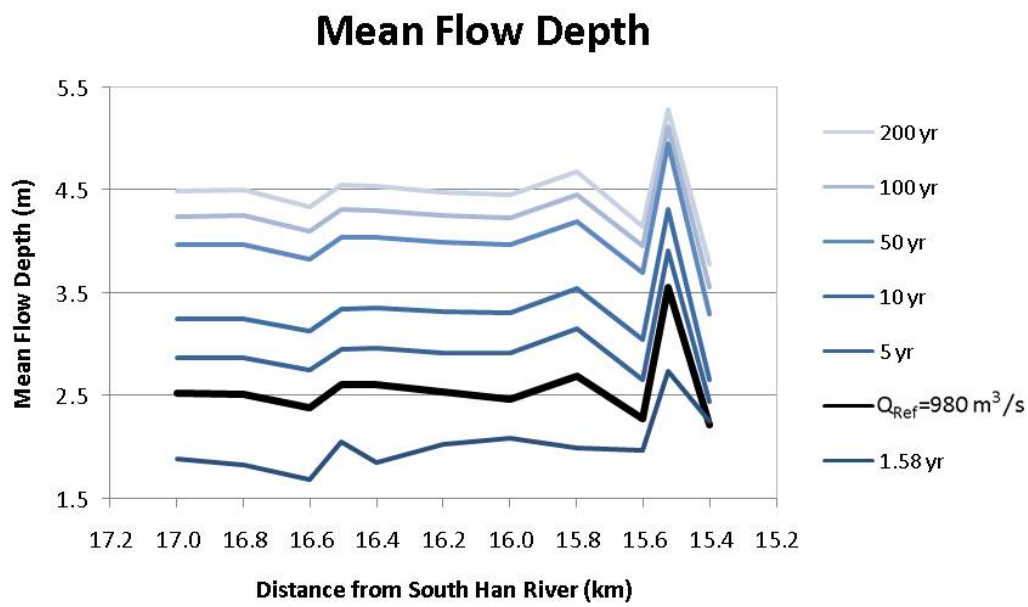

Figure C-13: Combined Mean Flow Depth due to Discharge

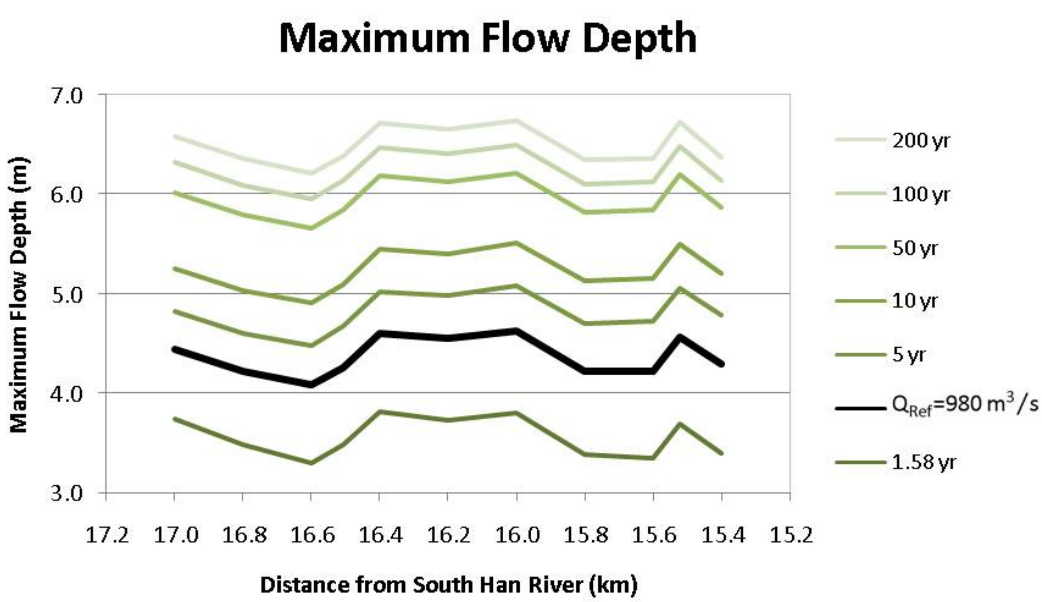

Figure C-14: Combined Maximum Flow Depth due to Discharge

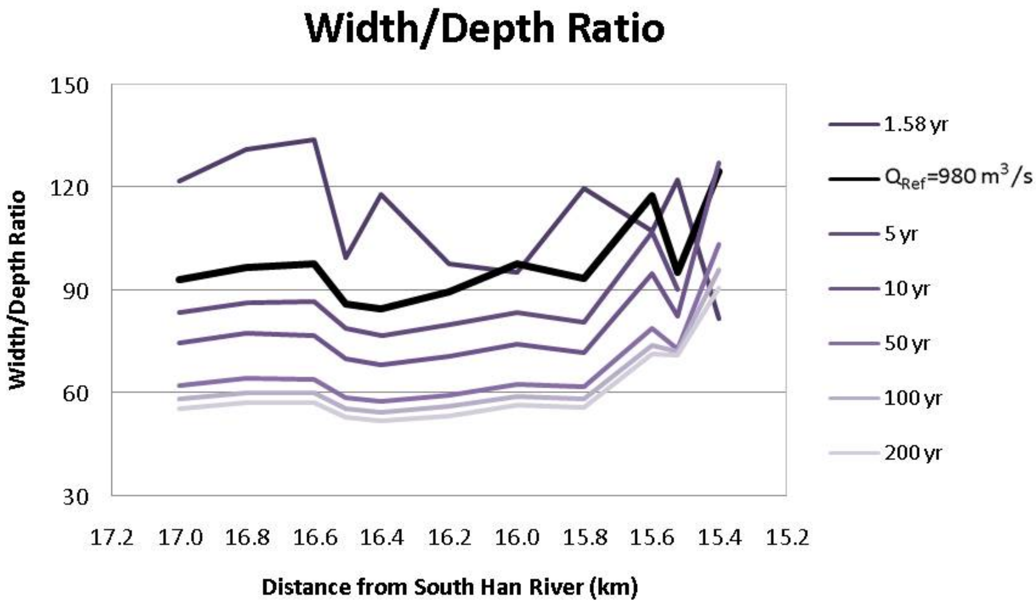

Figure C-15: Combined Width/Depth Ratio due to Discharge

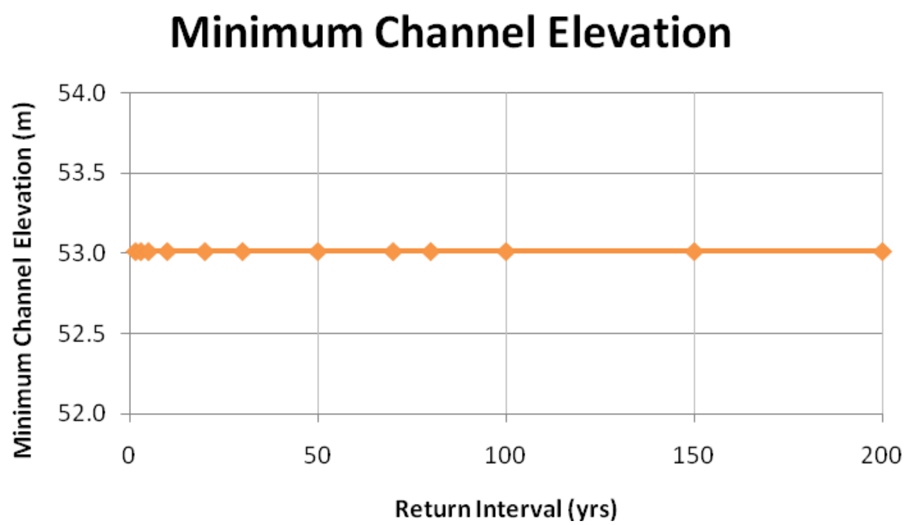

Figure C-16: Averaged Channel Elevation due to Return Interval

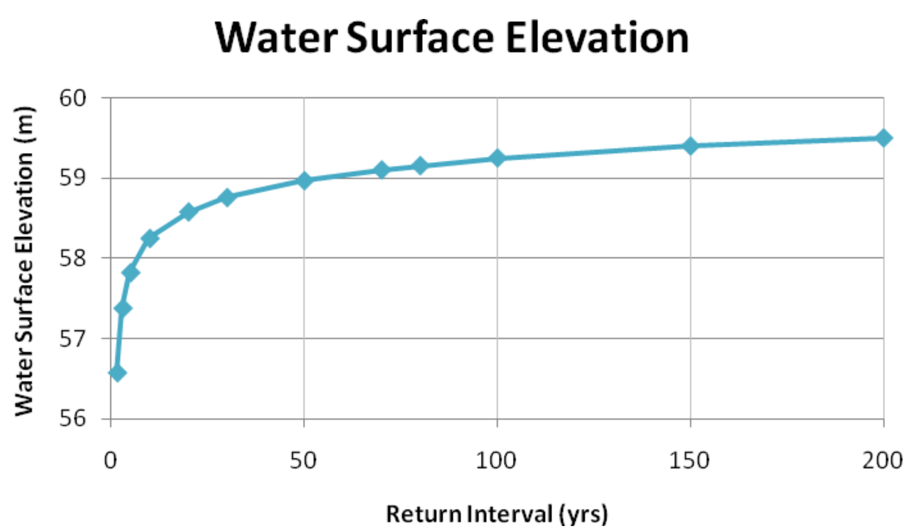

Figure C-17: Averaged Water Surface Elevation due to Return Interval

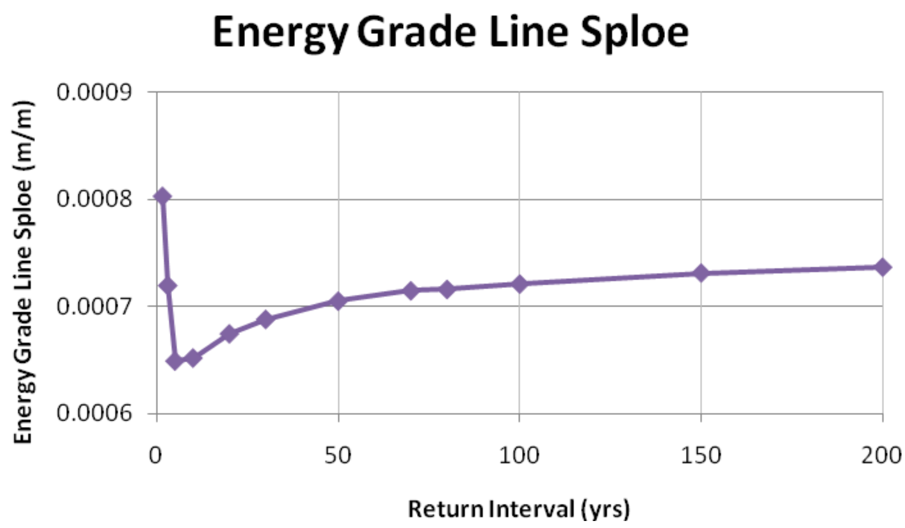

Figure C-18: Averaged Energy Grade Line Slope due to Return Interval

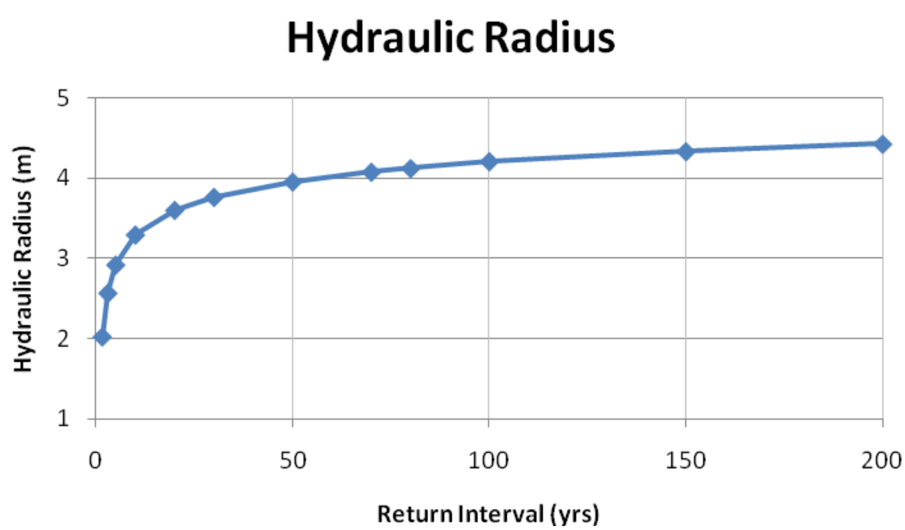

Figure C-19: Averaged Hydraulic Radius due to Return Interval

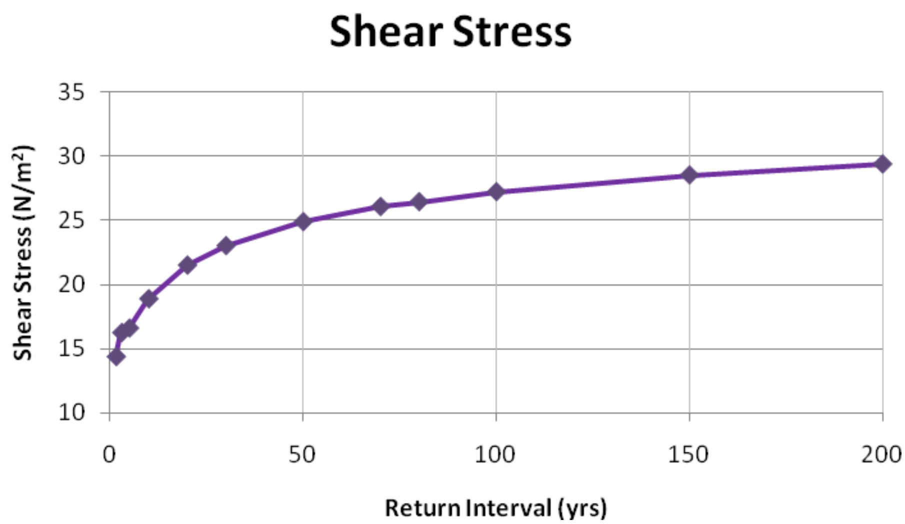

Figure C-20: Averaged Shear Stress due to Return Interval

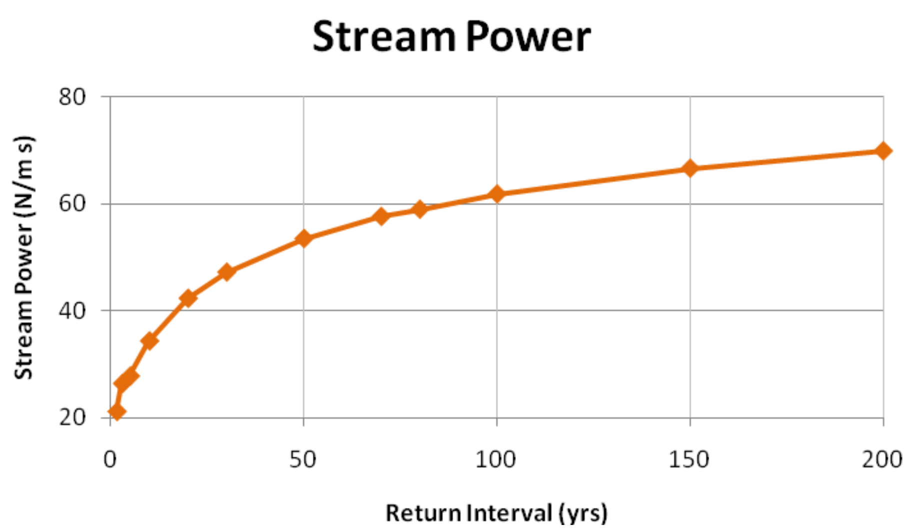

Figure C-21: Averaged Stream Power due to Return Interval

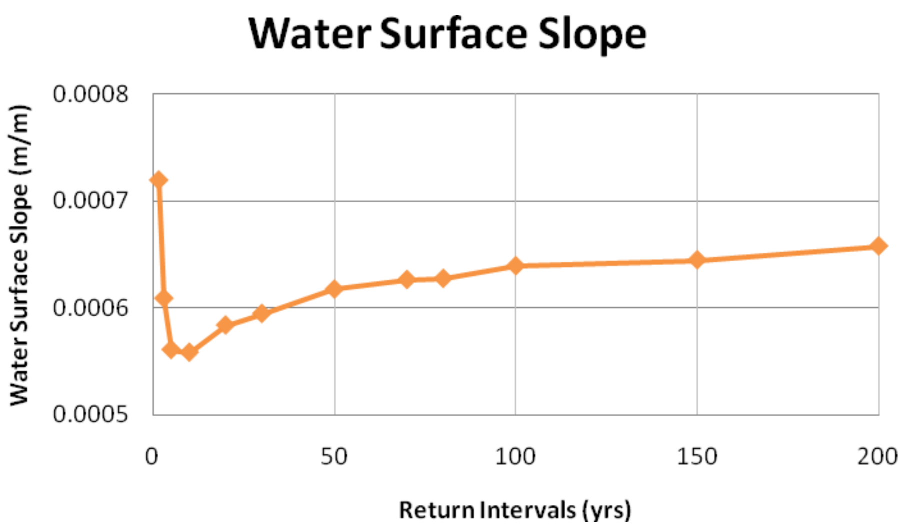

Figure C-22: Averaged Water Surface Slope due to Return Interval

APPENDIX D - Channel Classification Output

Table D-1: Channel Classification Raw Data

Return Interval (yrs)	Q (cms)	Channel Slope (m/m)	Valley Slope (m/m)	d_{50} (mm)	Bankfull Width (m)	Flood Prone Width (m)	Depth (m)	Fr	EG Slope (m/m)	Entrenchment Ratio	Width / Depth Ratio	Sinuosity	D_{50} Type
1.58	610	0.00058	0.00058	1.48	226	279	2.03	0.32	0.00075	1.23	111	1.0	Very Coarse Sand
Q_{ref}	980	0.00058	0.00058	1.48	251	279	2.58	0.31	0.00067	1.11	97	1.0	Very Coarse Sand
5	1180	0.00058	0.00058	1.48	260	279	2.94	0.30	0.00060	1.07	88	1.0	Very Coarse Sand
10	1480	0.00058	0.00058	1.48	265	279	3.32	0.31	0.00060	1.05	80	1.0	Very Coarse Sand
20	1770	0.00058	0.00058	1.48	266	279	3.63	0.32	0.00062	1.05	73	1.0	Very Coarse Sand
30	1940	0.00058	0.00058	1.48	267	279	3.80	0.33	0.00064	1.04	70	1.0	Very Coarse Sand
50	2150	0.00058	0.00058	1.48	268	279	4.00	0.33	0.00066	1.04	67	1.0	Very Coarse Sand
70	2290	0.00058	0.00058	1.48	269	279	4.12	0.34	0.00066	1.04	65	1.0	Very Coarse Sand
80	2340	0.00058	0.00058	1.48	269	279	4.17	0.34	0.00067	1.03	65	1.0	Very Coarse Sand
100	2440	0.00058	0.00058	1.48	270	279	4.25	0.34	0.00067	1.03	63	1.0	Very Coarse Sand
150	2600	0.00058	0.00058	1.48	271	279	4.38	0.35	0.00068	1.03	62	1.0	Very Coarse Sand
200	2710	0.00058	0.00058	1.48	272	279	4.48	0.35	0.00069	1.02	61	1.0	Very Coarse Sand

APPENDIX E - HEC-RAS Sediment Transport Application Limits

Sediment transport capacity is analyzed by HEC-RAS 3.1.3. Transported sediment consists of bed load, suspended load and wash load according to Van Rijn(1993). Suspended load is maintained part in suspension in the flowing water. It moves with same velocity as that of the flowing water. Bed load is the sediment in almost continuous contact with the bed, carried forward by rolling, sliding, or hopping. And wash load is a portion of suspended load. However it is comprised of smaller particles than the bed material and it is not contained in transport capacity of the flow.

In HEC-RAS, the sedimentation transport capacity function has the capability of predicting transport capacity for non-cohesive sediment at one or more cross sections based on existing hydraulic parameters and know bed sediment properties [Hydraulic Reference, HEC-RAS 3.1.3]. Following sediment transport functions are available in HEC-RAS:

- Ackers-White
- Engelund-Hansen
- Laursen
- Meyer-Peter Müller
- Toffaleti
- Yang

To estimate sediment transport capacity by these functions, input data is required to HEC-RAS. Table E-1 shows ranges of input parameters required in HEC-RAS to develop each function. Their ranges are taken from SAM package user's manual and based on range stated by developer in their original paper. In the case of Engelund-Hansen function, the ranges are taken from the database (Guy et al, 1966) primarily used in that function's development.

Table E-1: Range of input values for sediment transport functions

Function	d	d_m	s	V	D	S	W	T
Ackers-White *(flume)*	0.04 - 7.0	NA	1.0 - 2.7	0.07 - 7.0	0.01 - 1.4	0.00006 - 0.037	0.23 - 0.4	46 - 89
Englund-Hansen *(flume)*	NA	0.19 - 0.93	NA	0.65 - 6.34	0.19 - 1.33	0.000055 - 0.019	NA	45 - 93
Laursen *(field)*	NA	0.08 - 0.7	NA	0.068 - 7.8	0.67 - 54	0.0000021 - 0.0018	63 - 3640	32 - 93
Laursen *(flume)*	NA	0.011 - 29	NA	0.7 - 9.4	0.03 - 3.6	000025 - 0.025	0.25 - 6.6	46 - 83
Meyer-Peter Müller *(flume)*	0.4 - 29	NA	1.25 – 4	1.2 - 9.4	0.03 - 3.9	0.0004 - 0.02	0.5 - 6.6	NA
Toffaleti *(field)*	0.062 - 4	0.095 - 0.76	NA	0.7 - 7.8	0.07 - 56.7 (R)	0.000002 - 0.0011	63 - 3640	36 - 93
Toffaleti *(flume)*	0.062 - 4	0.45 - 0.91	NA	0.7 - 6.3	0.07 - 1.1 (R)	0.00014 - 0.019	0.8 - 8	40 - 93
Yang *(field-sand)*	0.15 -1.7	NA	NA	0.8 - 6.4	0.04 - 50	0.000043 - 0.028	0.44 - 1750	32 - 94
Yang *(field-gravel)*	2.5 - 7	NA	NA	1.4 - 5.1	0.08 - 0.72	0.0014 - 0.029	0.44 - 1750	32 - 94

Where, d = Overall particle diameter [mm]

d_m = Median particle diameter [mm]

s = Sediment specific gravity

V = Average channel velocity [ft/sec]

D = Channel depth [ft]

S = Energy gradient

W = Channel width [ft]

T = Water temperature [°F]

(R) = Hydraulic Radius [ft]

NA = Data not available

Ackers-White

The Ackers-White transport function is a total load function based on two assumptions. One of these assumptions is that the fine sediment has best relation with turbulent fluctuations in the water column. Another is that the coarse sediment has best relation with mean velocity used as the representative variable. Based on these, the Ackers-White transport function was developed in terms of grain size, mobility and transport.

In Table E-1, the ranges of input values for Ackers-White transport function are shown. It was developed based on over 1000 flume experiments. An equation for Ackers-White function for a single grain is represented by

$$X = \frac{G_{gr}\, s\, d_s}{D\left(\frac{u_*}{V}\right)^n} \quad \text{and} \quad G_{gr} = C\left(\frac{F_{gr}}{A} - 1\right)$$

Where: X = Sediment concentration, in parts per part

G_{gr} = Sediment transport parameter

s = Specific gravity of sediments

d_s = Mean particle diameter

D = Effective depth

u_* = Shear velocity

V = Average channel velocity

n = Transition exponent, depending on sediment size

C = Coefficient

F_{gr} = Sediment mobility parameter

A = Critical sediment mobility parameter

Engelund-Hansen

The Engelund-Hansen function is used as a total load predictor which gives adequate results for sand rivers with substantial suspended load. This was developed based on flume data with given sediment size in Table E-1, 0.19 to 0.93mm. General equation for Engelund-Hansen function is represented by

$$g_s = 0.05\gamma_s V^2 \sqrt{\frac{d_{50}}{g\left(\frac{\gamma_s}{\gamma}-1\right)}}\left[\frac{\tau_0}{(\gamma_s-\gamma)d_{50}}\right]^{3/2}$$

Where: g_s = Unit sediment transport

$\gamma = \gamma$ = Unit weight of water

γ_s = Unit weight of solid particles

V = Average channel velocity

$\tau_0 = \tau_0$ = Bed level shear stress

d_{50} = Particle size of which 50% is smaller

Laursen

The Laursen function is a total sediment load predictor. It is derived from a combination of qualitative analysis, original experiments, and supplementary data. Transport of sediments is primarily defined based on the hydraulic characteristics of mean channel velocity, depth of flow, energy gradient, and on the sediment characteristics of gradation and fall velocity. Contributions by Copeland (Copeland, 1989) extend the range of applicability to gravel-sized sediments. The range of applicability is 0.011 to 29mm, median particle size as shown Table E-1.

The general transport equation for the Laursen function extended by Copeland for a single grain size is represented by

$$C_m = 0.01\gamma\left(\frac{d_s}{D}\right)^{7/6}\left(\frac{\tau_0}{\tau_c}-1\right)f\left(\frac{u_*}{\omega}\right)$$

Where: C_m = Sediment discharge concentration, in weight/volume

G = Unit weight of water

d_s = Mean particle diameter

D = Effective depth of flow

τ_0 = Bed shear stress due to grain resistance

τ_c = Critical bed shear stress

$f\left(\frac{u_*}{\omega}\right)$ = Function of the ratio of shear velocity to fall velocity as defined in Laursen's

Figure 14 (Laursen, 1958)

Meyer-Peter Müller

The Meyer-Peter Müller (MPM) is bed load transport function based primarily on experimental data. MPM has been extensively tested and used for rivers with relatively coarse sediment. The transport rate is proportional to the difference between the mean shear stress acting on the grain and the critical shear stress. Applicable particle size is between 0.4 and 2.9mm as mention above Table E-1. The Darcy-Weisbach friction factor is used to define bed resistance.

The general transport equation for the Meyer-Peter Müller (MPM) function is represented by

$$\left(\frac{k_r}{k_r^{'}}\right)^{3/2} \gamma R S = 0.047\left(\gamma_s - \gamma\right) d_m + 0.25\left(\frac{\gamma}{g}\right)^{1/3}\left(\frac{\gamma_s - \gamma}{\gamma_s}\right)^{2/3} g_s^{2/3}$$

Where: g_s = Unit sediment transport rate in weight/time/unit width

k_r = A roughness coefficient

$k_r^{'}$ = A roughness coefficient based on grains

γ = Unit weight of water

γ_s = Unit weight of the sediment

g = Acceleration of gravity

d_m = Median particle diameter

R = Hydraulic radius

S = Energy gradient

Toffaleti

The Toffaleti function is a modified-Einstein total load method. This method divided the suspended load distribution into vertical zones, replicating two-dimensional sediment movement. In the sediment distribution, there are four zones, the upper zone, the middle zone, the lower zone and the bed zone. First, the sediment transport is calculated independently and then they are summed as total sediment transport.

This method was developed using an exhaustive collection of both flume and field data. The flume experiments used sediment particles with mean diameter raging from 0.3 to 0.93 mm. However successful application of the Toffaleti method suggests that mean particle diameter as low as 0.095mm is acceptable.

The general transport equations for the Toffaleti function for a single grain size is represented by

$$g_{ssL} = M \frac{\left(\frac{R}{11.24}\right)^{1+n_v-0.756z} - \left(2d_m\right)^{1+n_v-0.756z}}{1+n_v-0.756z} \quad \text{(lower zone)}$$

$$g_{ssM} = M \frac{\left(\frac{R}{11.24}\right)^{0.244z}\left[\left(\frac{R}{2.5}\right)^{1+n_v-z} - \left(\frac{R}{11.24}\right)^{1+n_v-z}\right]}{1+n_v-z} \quad \text{(middle zone)}$$

$$g_{ssU} = M \frac{\left(\frac{R}{11.24}\right)^{0.244z}\left(\frac{R}{2.5}\right)^{0.5z}\left[R^{1+n_v-1.5z} - \left(\frac{R}{2.5}\right)^{1+n_v-1.5z}\right]}{1+n_v-1.5z} \quad \text{(upper zone)}$$

$$g_{sb} = M\left(2\,d_m\right)^{1+n_v-0.756\,z} \quad \text{(Bed zone)}$$

$$M = 43.2\,C_L\left(1+n_v\right)V\,R^{0.756-n_v}$$

$$g_s = g_{ssL} + g_{ssM} + g_{ssU} + g_{sb}$$

Where: g_{ssL} = Suspended sediment transport in the lower zone, in tons/day/ft

g_{ssM} = Suspended sediment transport in the middle zone, in tons/day/ft

g_{ssU} = Suspended sediment transport in the upper zone, in tons/day/ft

g_{sb} = g_{sb} = Bed load sediment transport in tons/day/ft

g_s = Total sediment transport in tons/day/ft

M = Sediment concentration parameter

C_L = Sediment concentration in the lower zone

R = Hydraulic radius

d_m = Median particle diameter

z = Exponent describing the relationship between the sediment and hydraulic characteristics

n_v = Temperature exponent

Yang

Yang's method (1973) is developed under an assumption that unit stream power is the dominant factor in the determination of total sediment concentration. The research is based on data obtained in flume experiments and field data under a wide range conditions found in alluvial channels. Conditions for development and experiments are mentioned in Table E-1.

In 1984, Yang expended the applicability to include gravel sized sediments. The general transport equations for sand and gravel using Yang function for a single grain size is represented by

$$\log C_t = 5.435 - 0.286 \log \frac{\omega d_m}{\nu} - 0.457 \log \frac{u_*}{\omega} + \left(1.799 - 0.409 \log \frac{\omega d_m}{\nu} - 0.314 \log \frac{u_*}{\omega}\right) \log\left(\frac{VS}{\omega} - \frac{V_{cr}S}{\omega}\right)$$

for sand $d_m < 2mm$

$$\log C_t = 6.681 - 0.633 \log \frac{\omega d_m}{\nu} - 4.816 \log \frac{u_*}{\omega} + \left(2.784 - 0.305 \log \frac{\omega d_m}{\nu} - 0.282 \log \frac{u_*}{\omega}\right) \log\left(\frac{VS}{\omega} - \frac{V_{cr}S}{\omega}\right)$$

for sand $d_m \geq 2mm$

Where: C_t = Total sediment concentration

ω = Particle fall velocity

d_m = Median particle diameter

ν = Kinematic viscosity

u_* = Shear velocity

V = Average channel velocity

S = Energy gradient

APPENDIX F - Sediment Transport Capacity Plots

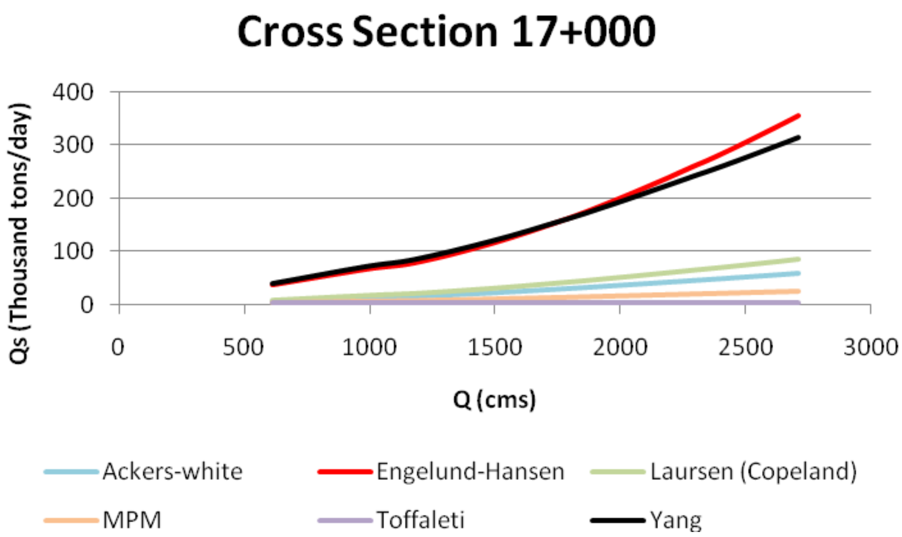

Figure F-1: Sediment Transport Capacity at Cross section 17+000

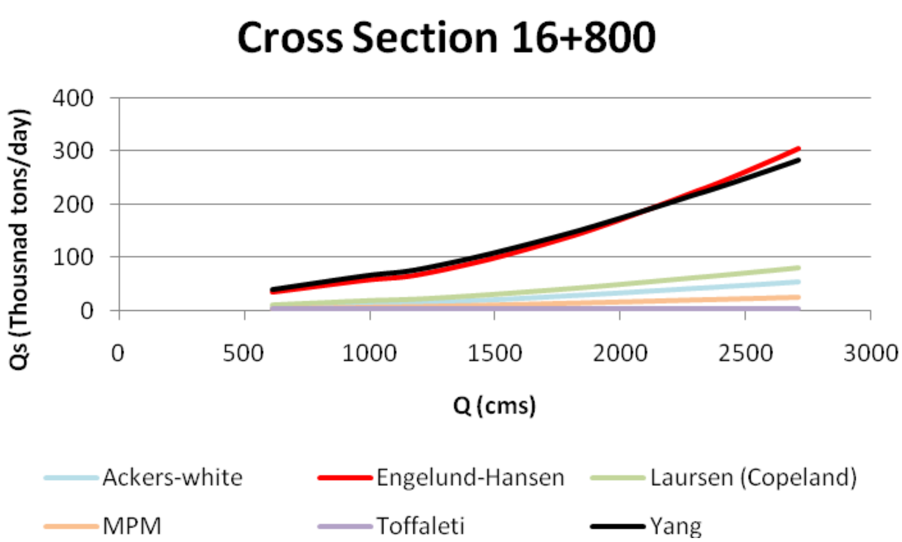

Figure F-2: Sediment Transport Capacity at Cross section 16+800

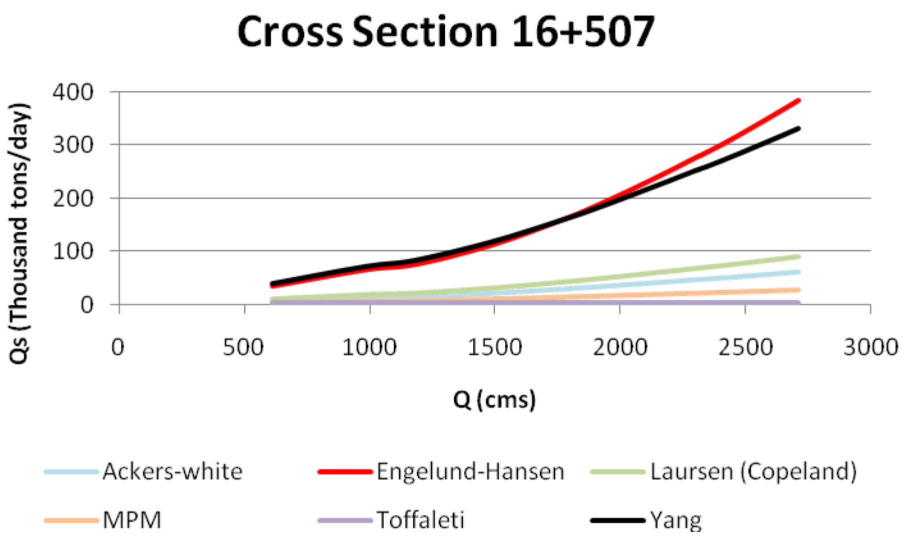

Figure F-3: Sediment Transport Capacity at Cross section 16+507

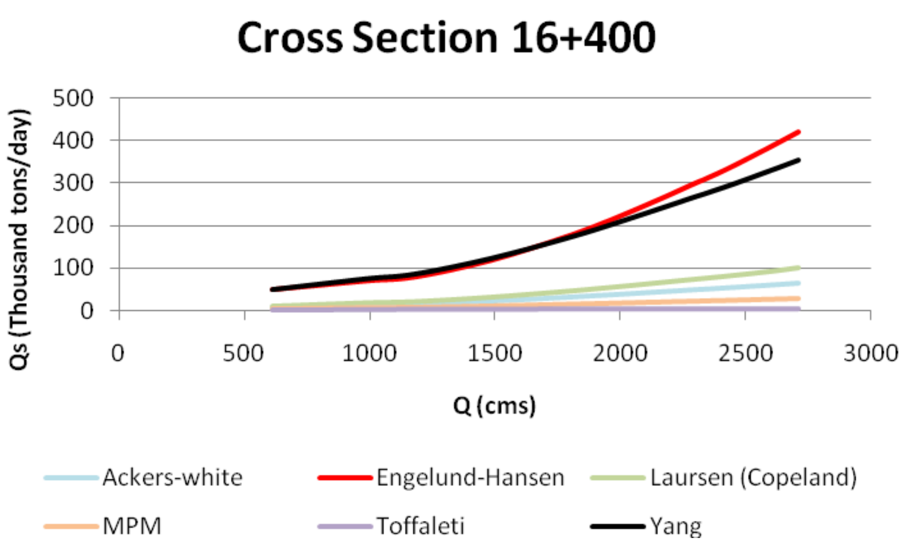

Figure F-4: Sediment Transport Capacity at Cross section 16+400

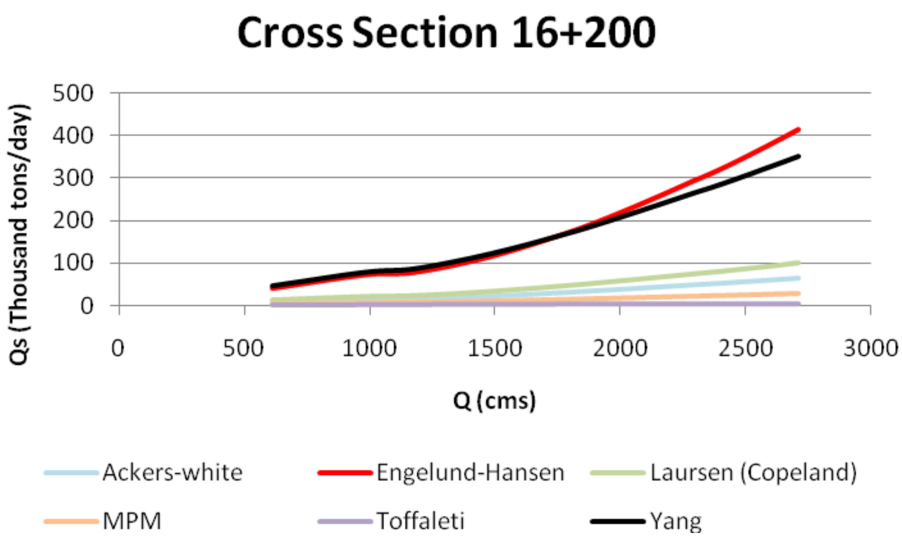

Figure F-5: Sediment Transport Capacity at Cross section 16+200

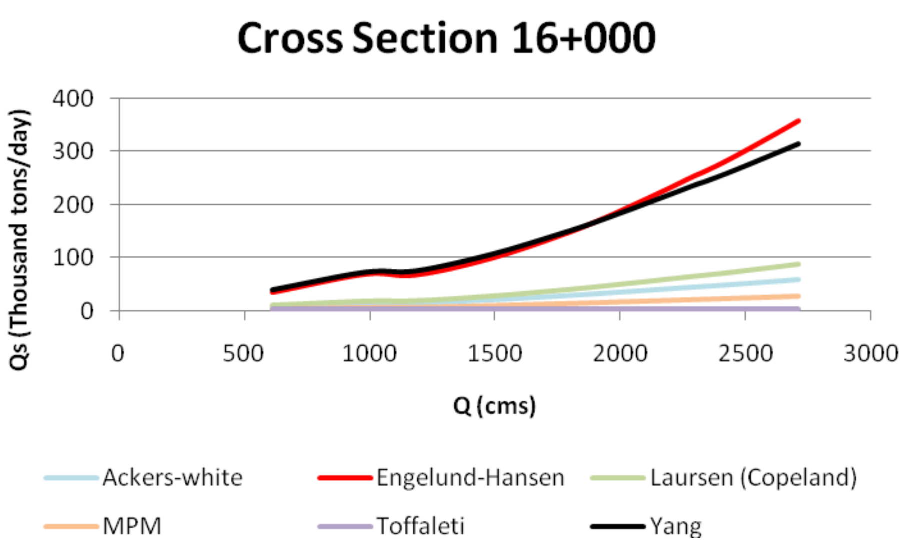

Figure F-6: Sediment Transport Capacity at Cross section 16+000

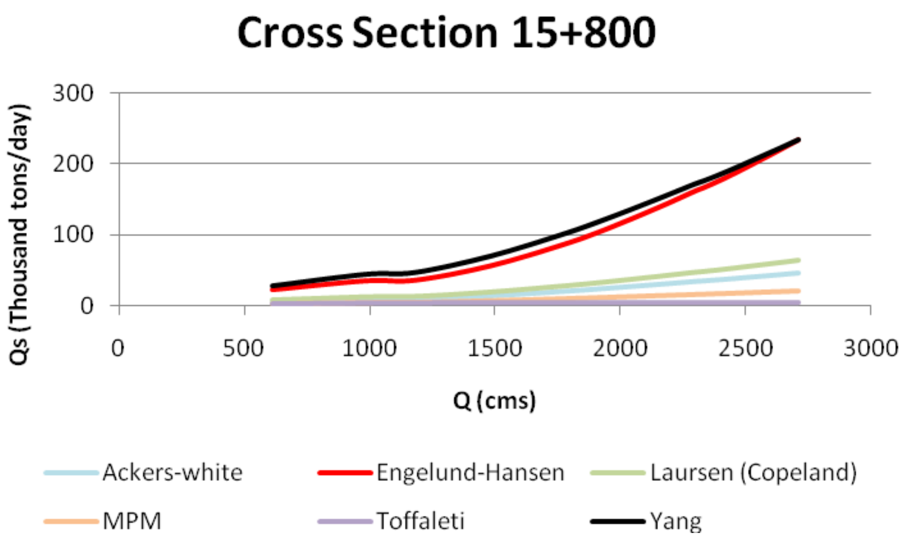

Figure F-7: Sediment Transport Capacity at Cross section 15+800

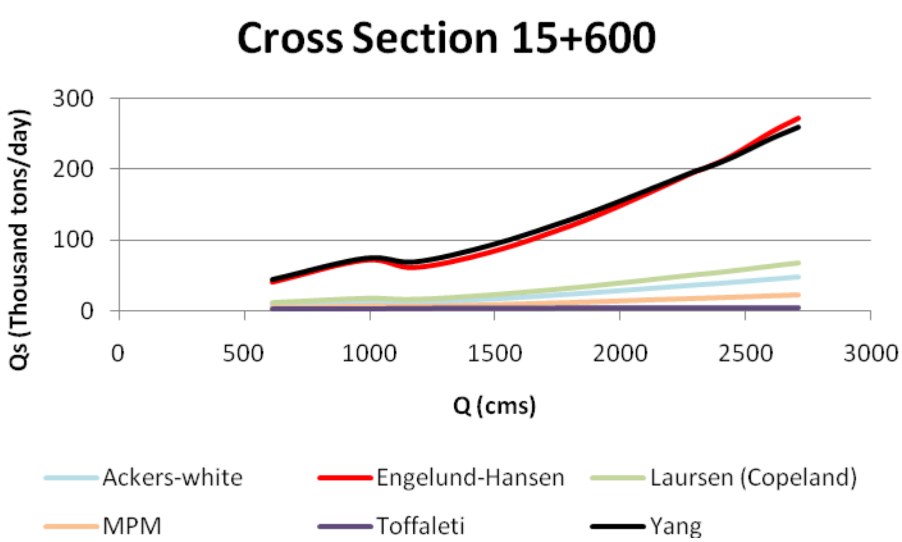

Figure F-8: Sediment Transport Capacity at Cross section 15+600

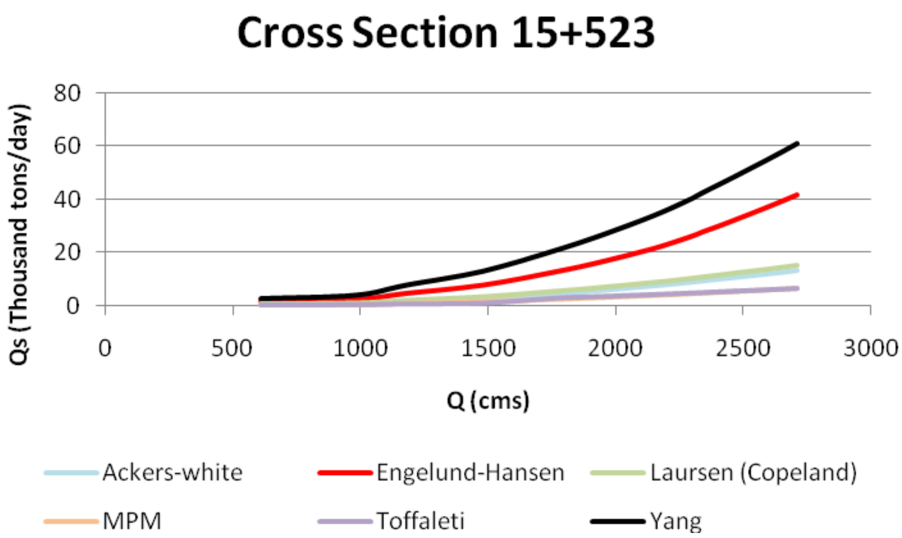

Figure F-9: Sediment Transport Capacity at Cross section 15+523

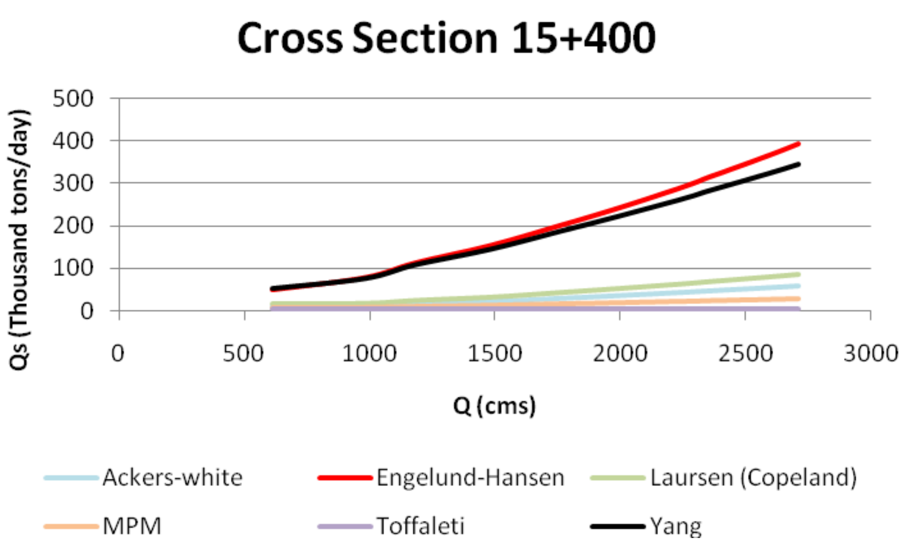

Figure F-10: Sediment Transport Capacity at Cross section 15+400

APPENDIX G - Stable Channel Design Plots

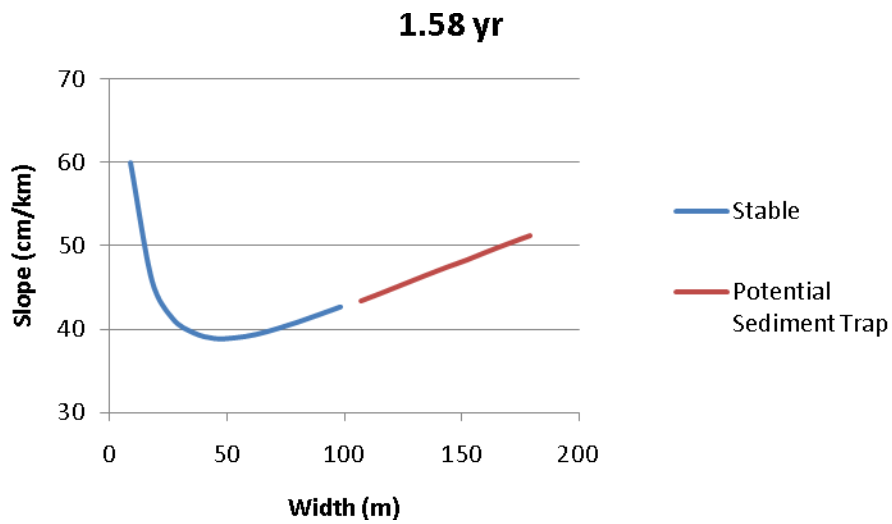

Figure G-1: Stable Channel Slope and Width (1.58yr)

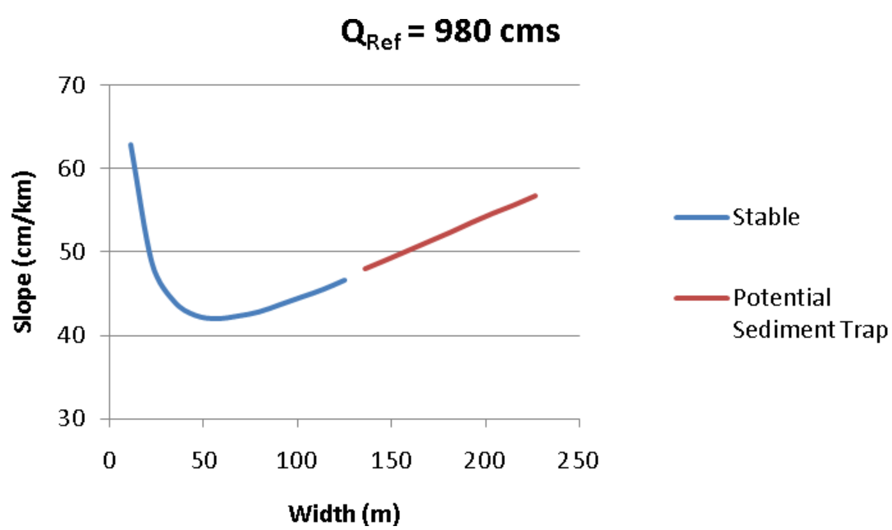

Figure G-2: 2 Stable Channel Slope and Width (Q_{Ref} = 980 cms)

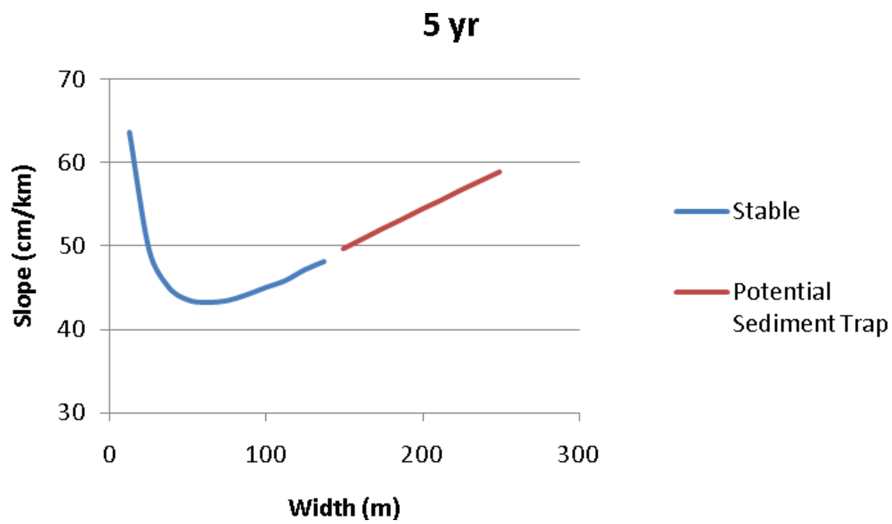

Figure G-3: Stable Channel Slope and Width (5yr)

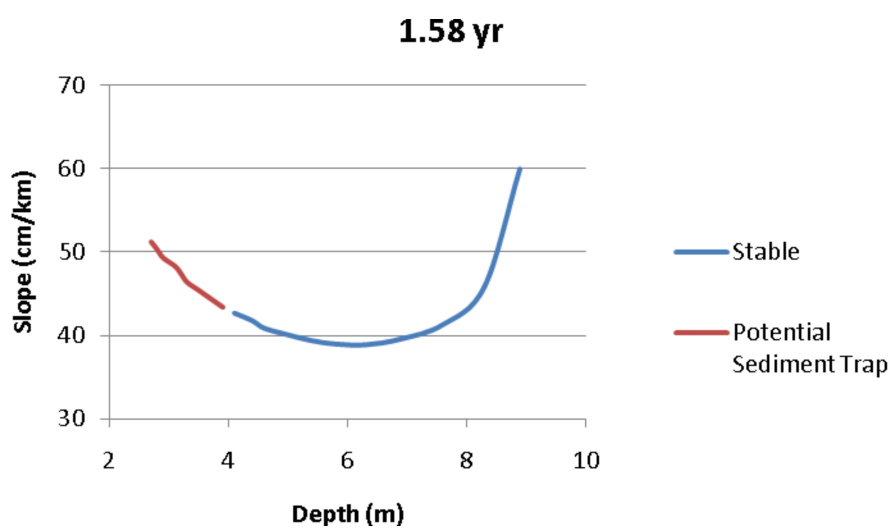

Figure G-4: Stable Channel Slope and Depth (1.58yr)

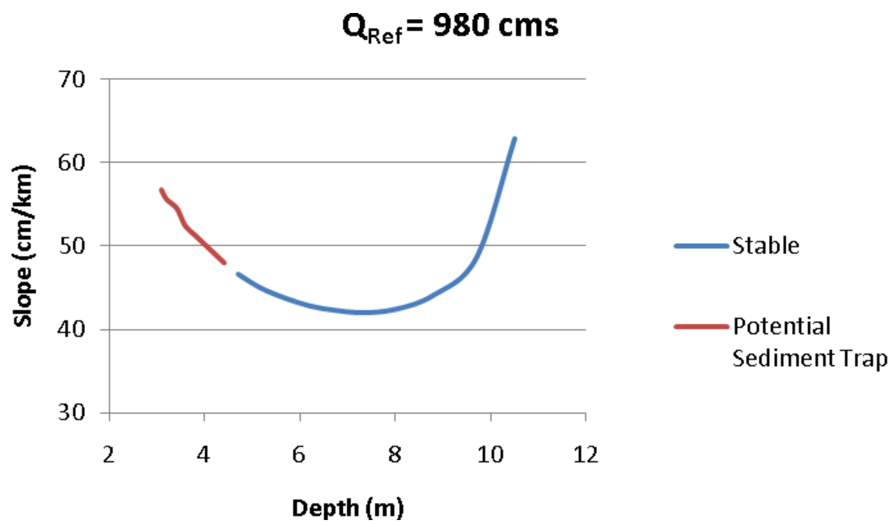

Figure G-5: Stable Channel Slope and Depth (Q_{Ref} = 980 cms)

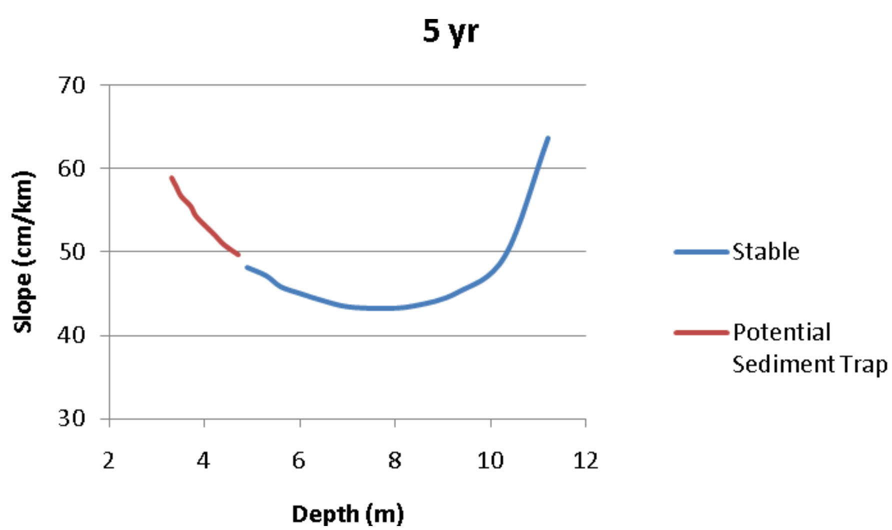

Figure G-6: Stable Channel Slope and Depth (5yr)

APPENDIX H - Cross Sections

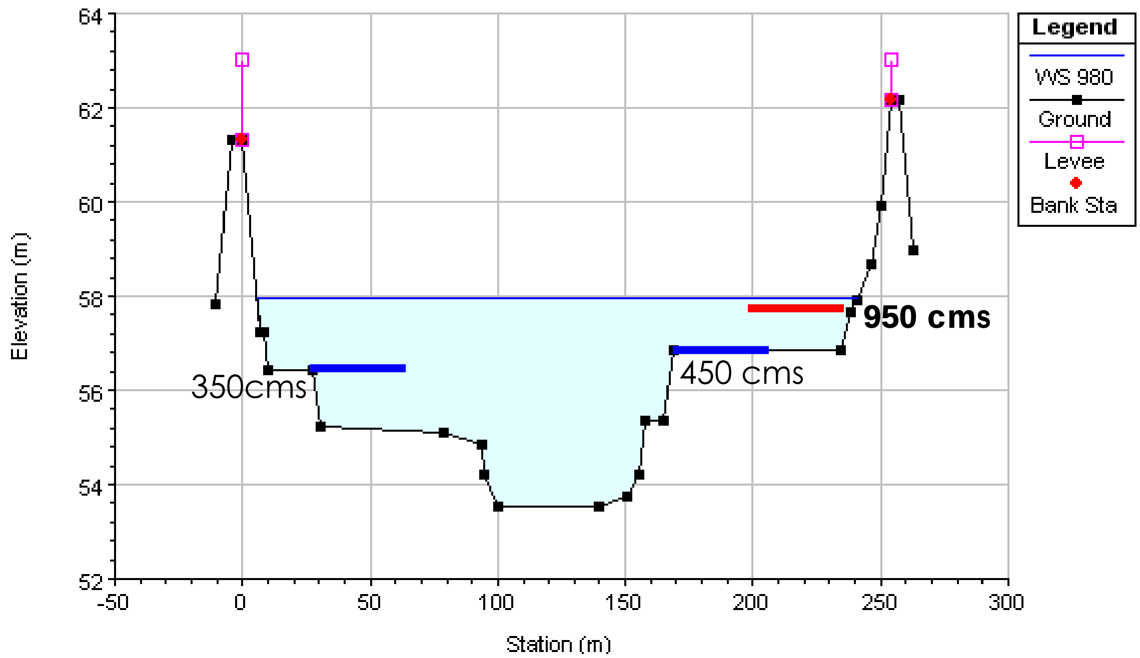

Figure H-1: Cross Section No. 17+000

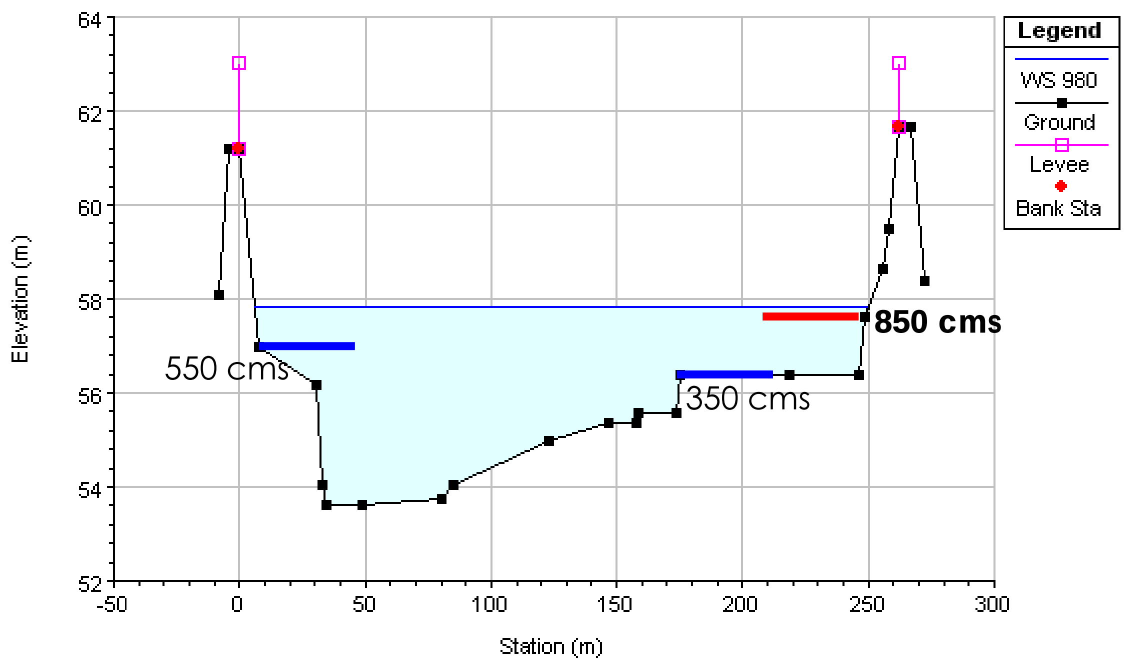

Figure H-2: Cross Section No. 16+800

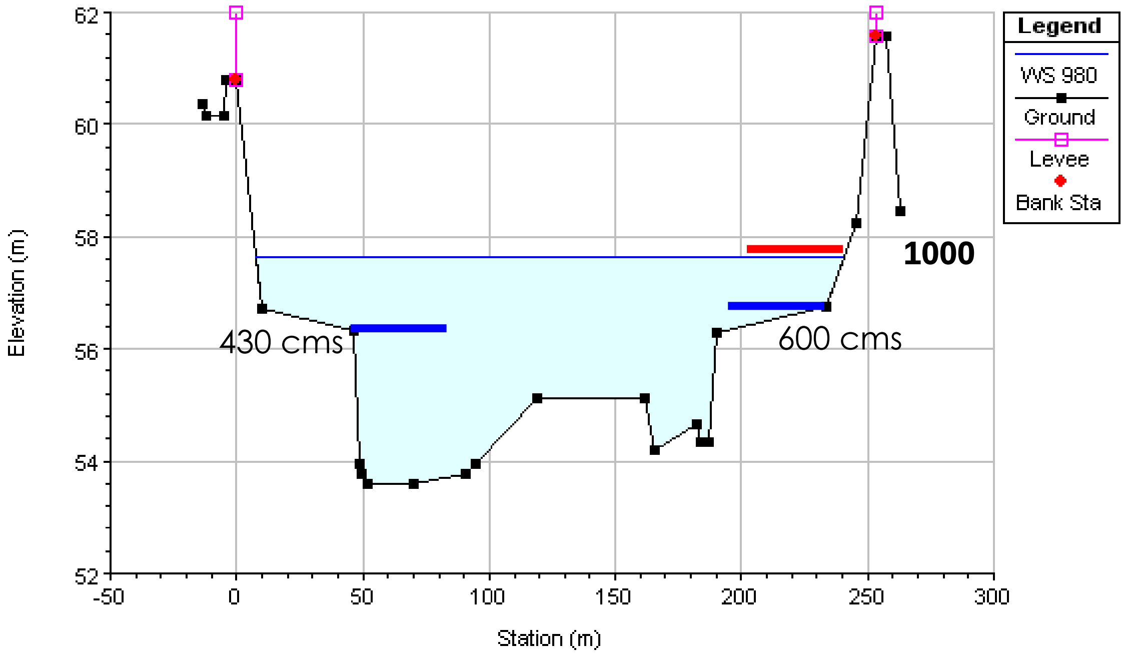

Figure H-3: Cross Section No. 16+600

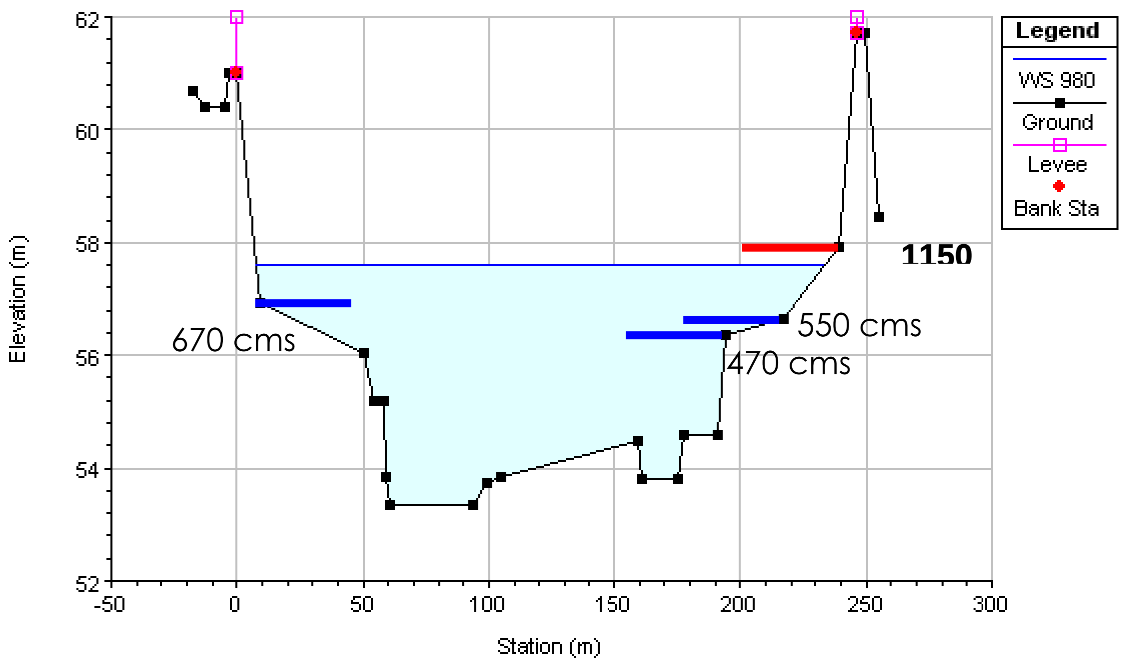

Figure H-4: Cross Section No. 16+507

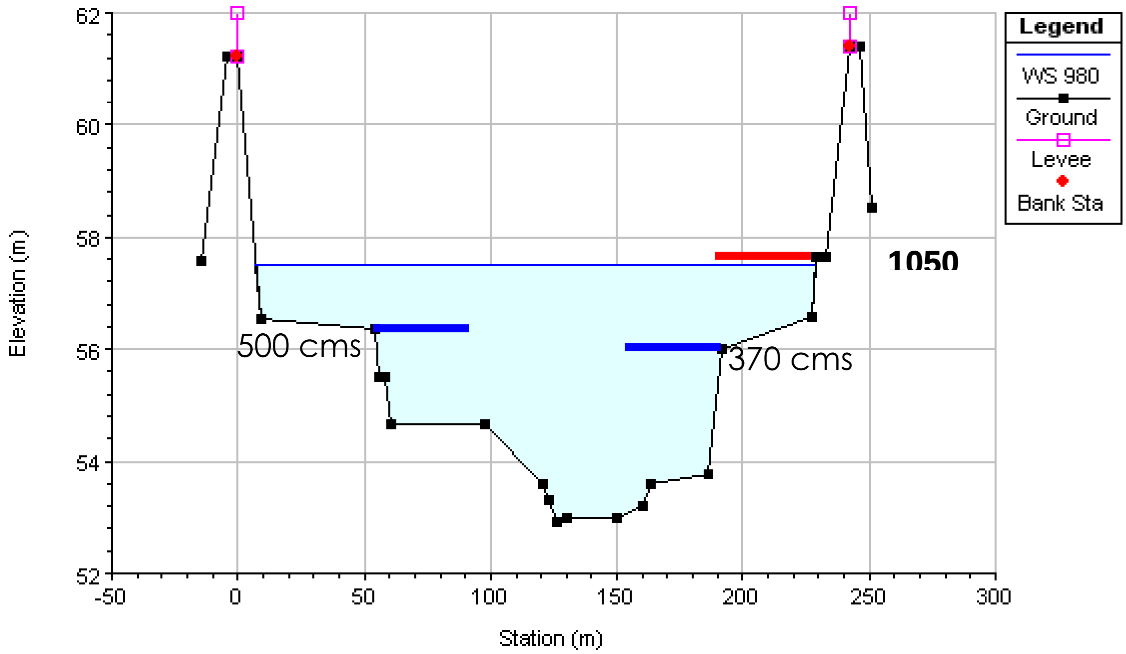

Figure H-5: Cross Section No. 16+400

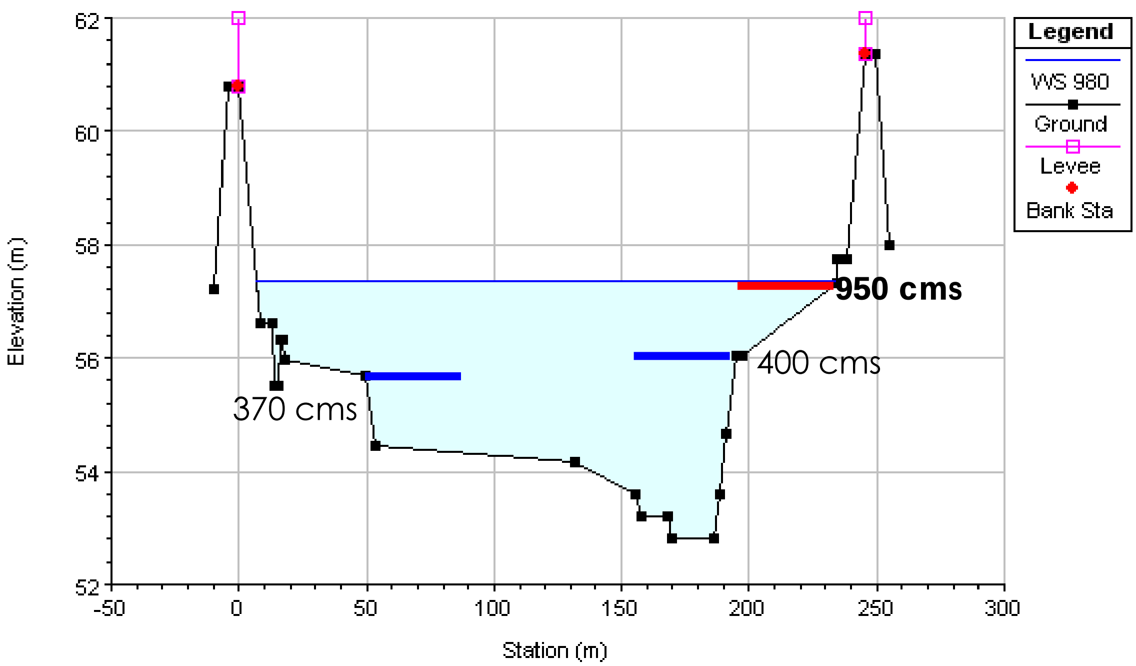

Figure H-6: Cross Section No. 16+200

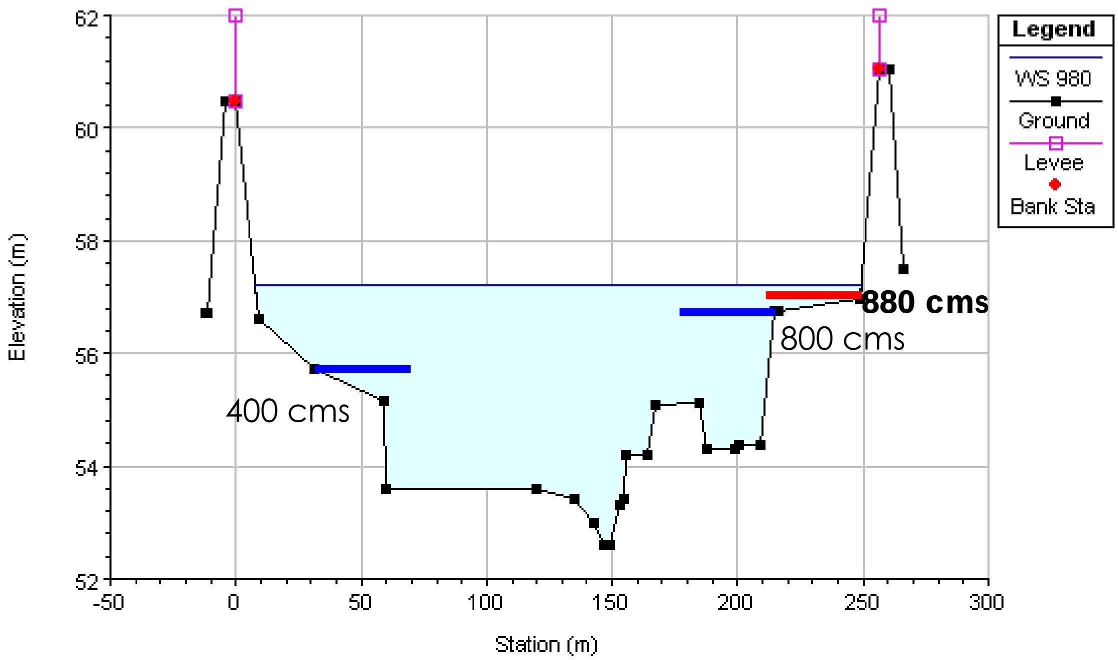

Figure H-7: Cross Section No. 16+000

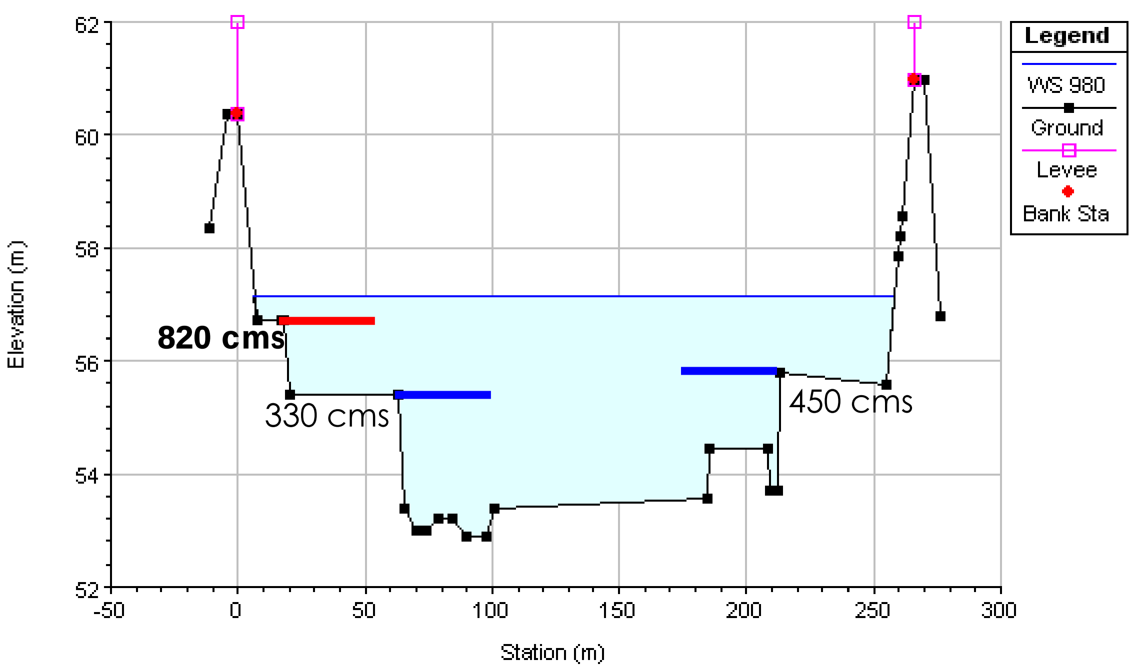

Figure H-8: Cross Section No. 15+800

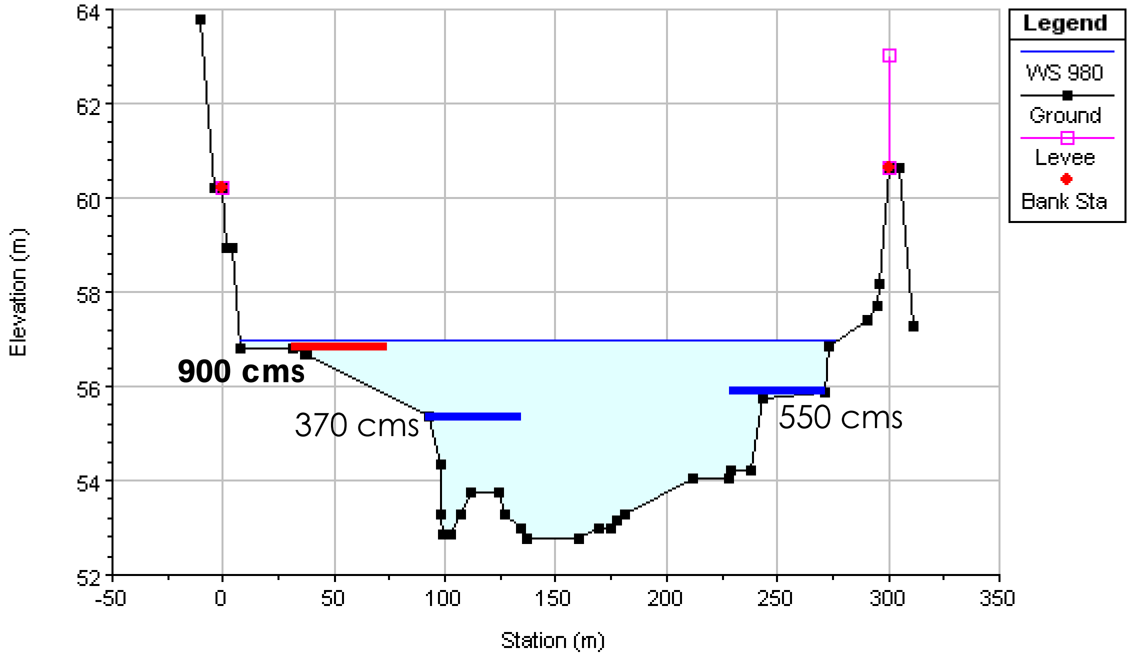

Figure H-9: Cross Section No. 15+600

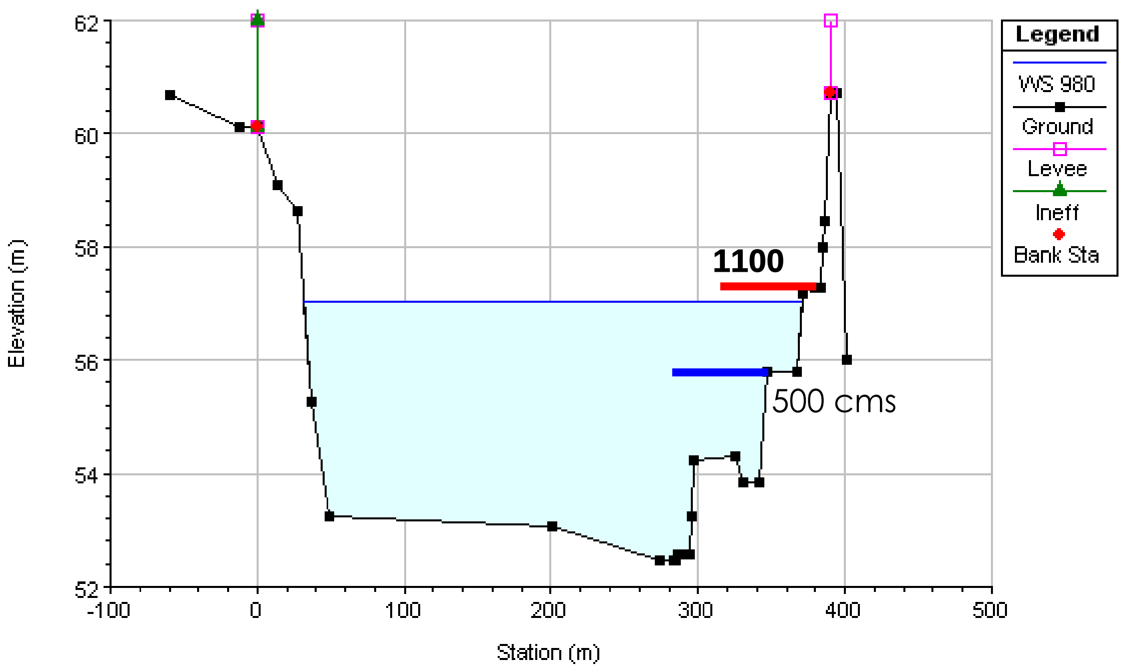

Figure H-10: Cross Section No. 15+523

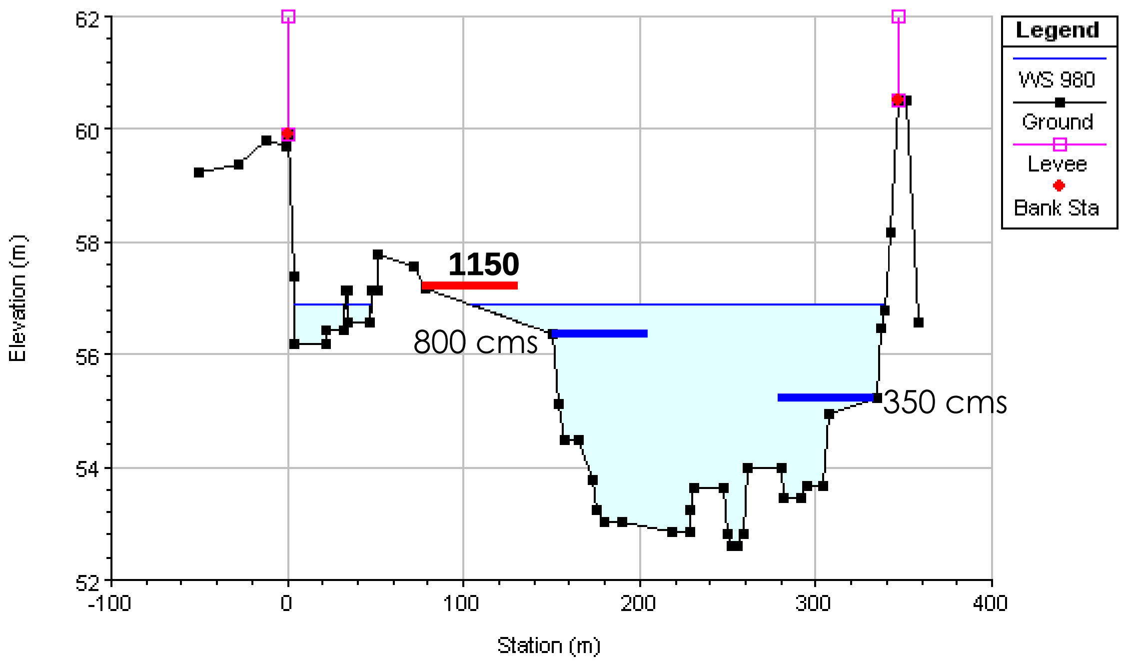

Figure H-11: Cross Section No. 15+400